APPENDIX A
SYMBOLS AND NOTATIONS

A–1. Symbols and notations

Symbols and notations are divided into two sections: ground motion chap 3 and app C) and buildings (chaps 4, 5, 6, and 7).

A–2. Ground motion (chapter 3 and appendix C)

A	= peak ground acceleration in cm/sec^2
α	= intercept of the log-recurrence line
β	= slope of the log-recurrence line
EPA	= effective peak acceleration
EPV	= effective peak velocity
EQ–I	= seismic ground motion having 50-percent probability of exceedance in 50 years
EQ–II	= seismic ground motion having 10-percent probability of exceedance in 100 years
DAF	= dynamic amplification factor
m_b	= body wave magnitude
M_L or M	= Richter or local magnitude
M_s	= surface wave magnitude
M_o	= seismic moment
M_m	= seismic moment magnitude
PGA	= peak ground acceleration
PGV	= peak ground velocity
PGD	= peak ground displacement
R_e	= effective distance
R_E	= epicentral distance
R_H	= hypocentral distance
SD	= relative displacement response spectrum
SV	= relative velocity response spectrum
SA	= absolute acceleration response spectrum
I_o	= modified Mercalli intensity at the epicentral area
I or MMI	= modified Mercalli intensity at the site
S_a	= response spectrum value for pseudo-acceleration
S_v	= response spectrum value for pseudo-velocity
S_d	= response spectrum value for displacement
T_R	= return period in years
$\ddot{x}(t)$	= corrected accelerogram record of ground motion
$\dot{x}(t)$	= computed ground velocity record
x(t)	= computed ground displacement record
t	= time in seconds
ω	= circular natural frequency in radians per second
k	= stiffness
c	= viscous damping
m	= system mass
T	= structural period in seconds
V	= coefficient of variation

A–3. Buildings (chaps 4, 5, 6, and 7)

A_G	= an effective peak ground acceleration to define S_a at a response period, T = 0
a_{xm}	= story lateral acceleration at level x for mode m
$(a_x)_{max}$	= maximum acceleration at level x, including effects of modal combinations
C_{bm}	= modal base shear coefficient for mode m. Equivalent to ZIKCS coefficient in Basic Design Manual, equation 3–1
subscript C	= denotes a force in terms of *capacity*
D	= dead load
subscript D	= denotes a force in terms of *demand*
E	= earthquake load
EC	= elastic capacity to resist the seismic effects, from equations 4–6, 4–7, and 4–8
EQ–I	= earthquake that has a 50-percent probability of being exceeded in 50 years
EQ–II	= earthquake that has a 10-percent probability of being exceeded in 100 years
F_{xm}	= story lateral force at level x for mode m
g	= acceleration due to gravity
K	= stiffness of a system in terms of force required for a unit of lateral displacement (K = F/δ) *Note:* not to be confused with the K used as a coefficient in the Basic Design Manual
K	= numerical coefficient as set forth in Basic Design Manual table 3–3
K*	= normalized stiffness of a system that is a function of the dynamic characteristics of the system
L	= live load
M	= mass of a system (M = W/g)

M^* = normalized mass of a system that is a function of the dynamic characteristics of the system

MDOF = Multi-degree-of-freedom system

M.F. = magnification factor to obtain floor response spectrum in equation 6–4

N = number of stories above the base to level n

n = the level that is uppermost in the main portion of the structure (generally the roof)

PF_{xm} = modal participation factor at level x for mode m, from equation 4–1

R_v = ratio of Basic Design Manual shear to modal analysis base shear, from equation 5–1

RSS = root-sum-squares, same as SRSS

S_a = spectral acceleration, as a ratio of the acceleration of gravity (g)

S_{am} = spectral acceleration for mode m

S_{dm} = spectral displacement for mode m

S_{fa} = spectral acceleration of a floor response spectrum

S_{fax} = spectral acceleration of floor response spectrum at level x

SDOF = single-degree-of-freedom system

SRSS = Square-root-of-the-sum-of-the-squares

S_1,S_2,S_3 = soil types for developing ATC–3–06 response spectra (NBS 510)

t = time in seconds

T_a = period of vibration of equipment or architectural appendage

T_m = period of vibration for mode m. T_1 designates the fundamental mode, T_2 designates the second mode, etc.

V_m = total lateral force for mode m

W = weight of a system or building

W_i/g = mass assigned to level i

W_p = weight of a portion of a structure, equipment, or architectural appendage

W_x = weight at or assigned to level x

α_m = modal base shear participation for mode m, from equation 4–2

β = damping as a percentage or ratio

δ = lateral displacement

δ_{xm} = lateral displacement at level x for mode m

Δ_{xm} = modal lateral interstory drifts for mode m within story x (e.g., the difference between δ_{xm} at story x = x + 1 and story x = x)

ϕ_{im} = amplitudes of mode m at levels i, from i = n to i = 1

ϕ_{xm} = amplitude of mode m at level x

θ = P-delta stability coefficient, as defined in paragraph 5–5d and ATC–3–06 (NBS 510)

APPENDIX B
REFERENCES

Government Publications.

Department of the Army.

TM 5–809–10	Seismic Design for Buildings
TM 5–838–2	Army Health Facility Design

Department of the Air Force.

AFM 88–3, Chapter 13	Seismic Design for Buildings

Department of the Navy.

NAVFAC P–355	Seismic Design for Buildings
NAVFAC P–355.1	Seismic Evaluation of Supports for Existing Electrical-Mechanical Equipment and Utilities

National Bureau of Standards (NBS).

National Technical Information Service, 5285 Port Royal Road, Springfield, VA, 22161

or

Superintendent of Documents, U.S. Government Printing Office, Washington, DC, 20402
Special Publication 510 (514 pages), Tentative Provisions for the Development of Seismic Regulations for Buildings (ATC–3–06), 1978

Nongovernment Publications.

National Fire Protection Association, Inc. (NFPA) Batterymarch Park, Quincy, MA, 02269

NFPA No. 13, Sprinkler Systems

NFPA No. 20, Centrifugal Fire Pumps

NFPA No. 76–A

NFPA P. 70, Article 700

Stanford University, The John A. Blume Earthquake Engineering Center, Stanford, CA, 94305

Technical Report No. 36, Computer Programs for Seismic Hazard Analysis—A User Manual (STASHA), G. A. Guidi, 1979

American Concrete Institute (ACI), Box 19150, Redford Station, Detroit MI, 48219

ACI 318–77, Building Code Requirements for Reinforced Concrete

Portland Cement Association (PCA), Old Orchard Road, Skokie, IL, 60076

Advanced Engineering Bulletin No. 20, Biaxial and Uniaxial Capacity of Rectangular Columns, 1967

APPENDIX C
GROUND MOTION BACKGROUND DATA

C-1. Earthquake Source and Earthquake Size Definition.

The actual release of earthquake energy along the fault plane in the crust of the earth is a very complex phenomenon. All the physical processes that occur just before, during and after a seismic event are still not completely understood, and considerable research is going on to better describe this phenomenon. However for engineering purposes, the above complex phenomenon is idealized, and figure C-1 gives the resulting simplified model representation of the earthquake source.

a. Earthquake location. Epicenter and Hypocenter are the two terms most commonly used to describe the source location of an event. Even though most of the seismic energy is released as the fault ruptures and that a substantial volume of the earth's crust (along the fault plane) is involved, it is generally assumed that there exists a discrete point where the rupture initiates. This point where the initial rupture of the rocks within the earth's crust begins is called the *hypocenter.* The point directly above the hypocenter on the earth's crust is called the *epicenter.* In recent times (since the beginning of seismographs), the location of the hypocenter and hence the epicenter is made by means of instruments. Before the advent of the instruments, the epicenter was located by means of finding the region of intense shaking. It is quite often that the field epicenter (region of intense shaking) and the instrumentally located epicenter do not coincide. See figure 3-22.

b. Earthquake size. Various empirical relationships are available to relate the size of the event with the rupture length and fault slip. The fault rupture length is the length of the fault that actually breaks on the surface of the earth. The fault slip is the relative displacement of the two plates with respect to each other at the fault plane. Figure C-2 shows different types of fault slips. Again, empirical relationships are available to relate earthquake size with slip length. To define the size of an earthquake, Charles Richter developed a Richter Magnitude scale. This scale is intended to be a rating given to an earthquake event, independent of the location of observation. The size was determined by means of a standard Wood-Anderson seismometer, with natural period of 0.8 seconds. Richter defined the Magnitude as the logarithm to the base ten of the ratio of the maximum amplitude on a seismogram written by a Wood-Anderson seismometer at a distance of 100 kms (62 miles) from the epicenter and the standard amplitude of one thousandth of a millimeter. Tables were constructed empirically to reduce from any given distance to 100 kms. Since the scale is logarithmic, an increase of one step on the magnitude scale increases the amplitude scale by a factor of 10. (See fig. C-3).

c. Other magnitude measures. In recent years, different types of instruments are used to obtain similar magnitude values which are referred to as local magnitude, M_L. The body wave magnitude m_b and the surface wave magnitude M_S are also used. In most studies, the local amplitude scale M_L is taken as a Richter magnitude. This assumption does introduce some errors in magnitude assignments. The local magnitude scale M_L can be related to the body wave magnitude m_b and the surface wave magnitude M_S by the following empirical relationships:

$$M_L = 1.34m_b - 1.71 \quad \text{(eq C-1)}$$

$$M_L = 2.20[m_S - 3.80]^{1/2} + 2.97 \quad \text{(eq C-2)}$$

Surface-wave magnitude M_s is usually based on the amplitude of 20 second waves recorded at distances of thousands of kilometers. The reason for preferring local magnitude is that for large earthquakes the surface-wave magnitude may increase as the physical size of the source region increases without a corresponding increase in the amplitude of ground motion in the period range affecting normal structures. This is well illustrated by the Kern County earthquake of 1952 which had a surface wave magnitude of 7.7 and a local magnitude of 7.2 and by the San Francisco earthquake of 1906 with a surface-wave magnitude of 8.25 and a local magnitude of 7.2 or less. It is generally believed that the local magnitude scale saturates in the range of 7 to 7.5. The largest measured value to date is 7.2.

d. Seismic moment. As more is known about the earthquake source mechanism and about the size of earthquake events, it is becoming increasingly clear that the existing magnitude scales are extremely inadequate to describe the overall size or the energy content of earthquake events. To overcome this deficiency, seismolo-

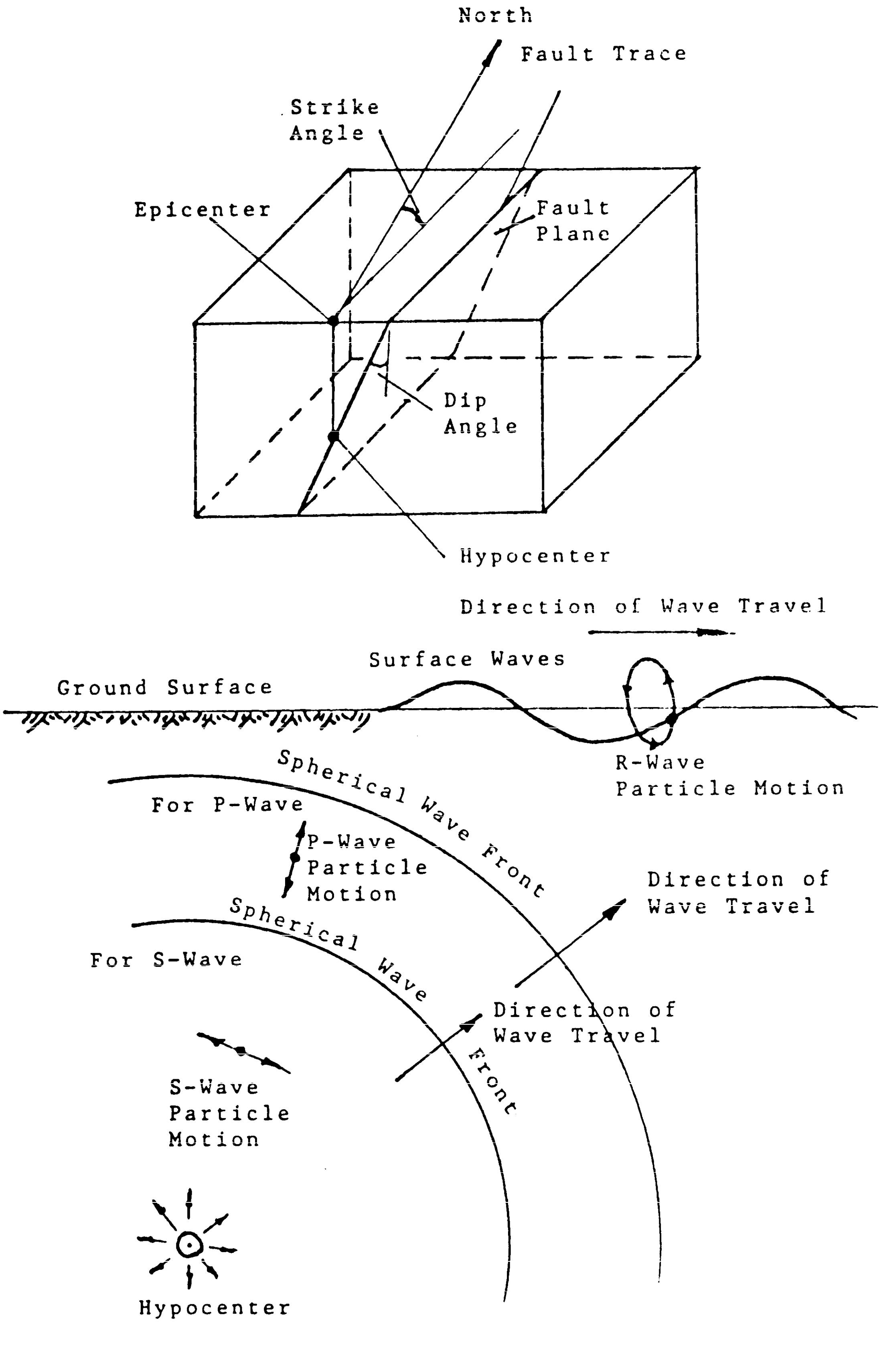

US Army Corps of Engineers

Figure C–1. Earthquake source model.

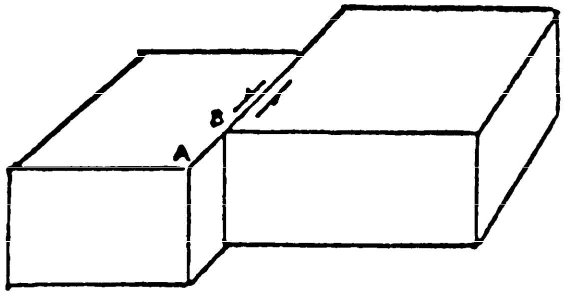

a. STRIKE-SLIP FAULT
(LEFT-SLIP FAULT)
AB=strike-slip= slip

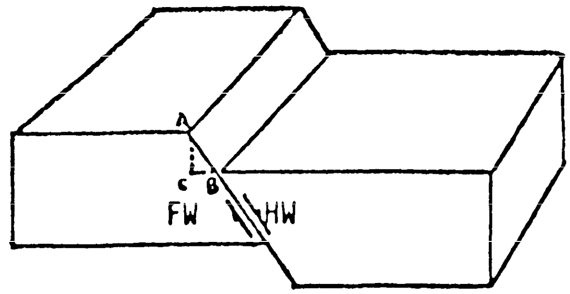

b. NORMAL-SLIP FAULT
AB = dip-slip= slip
AC = throw or vertical component
BC = heave or horiz. extension

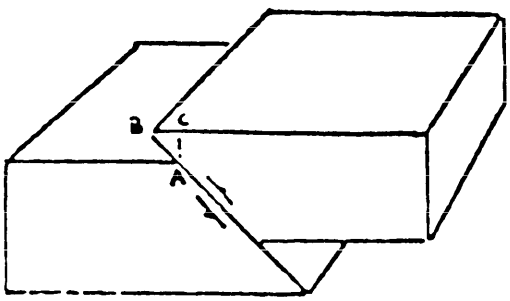

c. REVERSE-SLIP (THRUST) FAULT
AB = reverse-slip = slip
AC = throw or vertical component
BC = heave' = horiz. shortening

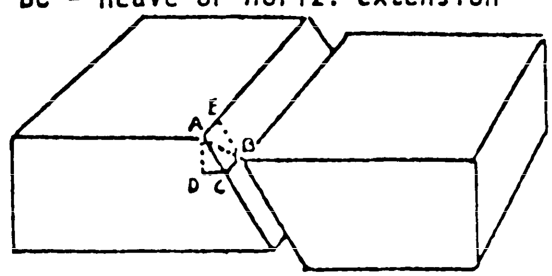

d. LEFT-OBLIQUE-SLIP FAULT

AB= oblique-slip = slip
AC = dip-slip component
AE = strike-slip component
AD = throw = vertical component
DC = heave = horiz. extension

US Army Corps of Engineers

Figure C–2. Types of fault slips.

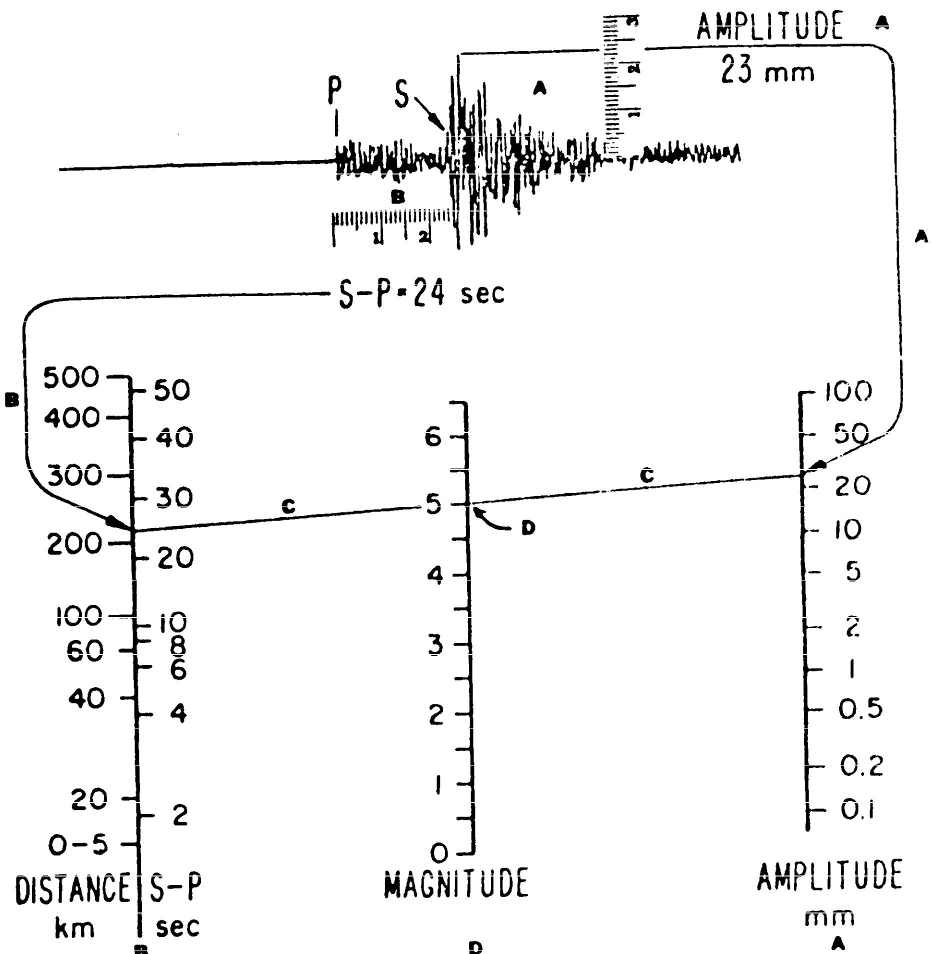

TO DETERMINE EARTHQUAKE MAGNITUDE WE CONNECT ON THE CHART

A. THE MAXIMUM AMPLITUDE RECORDED BY A STANDARD SEISMOMETER, AND
B. THE DISTANCE SEISMOMETER FROM THE EPICENTER OF THE EARTHQUAKE (OR DIFFERENCE IN ARRIVAL TIMES OF P AND S WAVES) BY
C. A STRAIGHT LINE,
D. READ THE MAGNITUDE, ON CENTER SCALE.

Reprinted from "Elementary Seismology,"
C. F. Richter, 1958, with permission from
W. H. Freeman and Company.

Figure C-3. The Richter Scale.

gists have introduced a new "physical" parameter called seismic moment, M_o, to describe the size of an earthquake. This parameter is related to the size of the fault rupture area, the average slip on the fault and the property in shear of the ruptured zone. Comparative values of the surface wave magnitudes and seismic moments of some famous earthquakes are given in table C–1.

Table C–1. Magnitude and seismic moment.

Earthquake	M_S	M_O
1960 Chili Earthquake	8.3 to 8.5	2.5×10^{30} dyne-cms
1964 Alaska Earthquake	8.3 to 8.4	7.5×10^{29} dyne-cms
1976 Tangshan Earthquake	7.8 to 8.0	1.0×10^{27} dyne-cms
1906 San Francisco Earthquake	8.2 to 8.3	1.0×10^{28} dyne-cms
1971 San Fernando Earthquake	6.4	1.0×10^{29} dyne-cms

US Army Corps of Engineers

In order to relate this new size parameter with the existing magnitude scales, a moment magnitude (M_m) is introduced. In the M_L range of 5.5 to 7.0, M_m corresponds to M_L. M_m is related to seismic moment M_o by the following empirical relationship.

$$M_m = \tfrac{2}{3}\log M_o - 10.7 \qquad \text{(eq C–3)}$$

M_o is defined as:

$$M_o = GAS \qquad \text{(eq C–4)}$$

where

G = average shear modulus over the rupture zone

A = fault rupture area

S = average slip on the fault during the earthquake

e. Intensity measures. Another means of describing the size of an earthquake at a given location is the intensity scale. The two intensity scales used in the United States are:

—The Rossi-Forel Scale (RF Scale)
—The Modified Mercalli Scale (MM Scale)

Where the Modified Mercalli Scale is the most common. A simplified version of this scale is given in Table C–2. Table C–3 gives the Rossi-Forel scale. The russian scale is very similar to the MM scale. The RF scale which was developed in the late 19th century was used in this century until 1930. Since then, use of the MM scale has become more common. Table C–4 shows the approximate relationship between the MM scale and the RF scale. It is important to note that all of the above scales are subjectively assigned by investigators after observing and reviewing the earthquake effects in a given region. The assignment of proper intensity value therefore requires a careful analysis of the affected region. Unless the guidelines for assigning intensities are properly and correctly followed, there could be an error in the assigned value.

f. Relations for magnitude and intensity. Empirical relationships are available in the literature to relate the magnitude of an earthquake and the epicentral intensity. The following show such relationships.

Gutenberg and Richter (1956) (Biblio 87),

$$M_L = 1 + \tfrac{2}{3}I_o \qquad \text{(eq C–5)}$$

Krinitzky and Chang (1975) (Biblio 92),

$$M_L = 2.1 + \tfrac{1}{2}I_o \qquad \text{(eq C–6)}$$

Chinnery and Rogers (1973) for Northeastern United States (Biblio 85)

$$M_L = 1.2 + 0.6I_o \qquad \text{(eq C–7)}$$

where M_L = Richter Magnitude or local magnitude

I_o = Modified Mercalli Intensity in the epicentral area

All such relationships, including those derived for specific sites where specific data are avail-

Table C-2. The Modified Mercalli intensity scale.

Mercalli's (1902) improved intensity scale served as the basis for the scale advanced by Wood and Nuemann (1931), known as the modified Mercalli scale and commonly abbreviated MM. The modified version is described below with some improvements by Richter (1958).

To eliminate many verbal repetitions in the original scale, the following convention has been adopted. Each effect is named at the level of intensity at which it first appears frequently and characteristically. Each effect may be found less strongly or more often at the next higher grade. A few effects are named at two successive levels to indicate a more gradual increase.

Masonry A, B, C, D. To avoid ambiguity of language, the quality of masonry, brick, or otherwise is specified by the following lettering (which has no connection with the conventional Class A, B, C construction).

Masonry A. Good workmanship, mortar, and design; reinforced, especially laterally, and bound together by using steel, concrete, etc.; designed to resist lateral forces.

Masonry B. Good workmanship and mortar; reinforced, but not designed in detail to resist lateral forces.

Masonry C. Ordinary workmanship and mortar; no extreme weaknesses like failing to tie in at corners, but neither reinforced nor designed against horizontal forces.

Masonry D. Weak materials, such as adobe; poor mortar; low standards of workmanship; weak horizontally.

Modified Mercalli Intensity Scale of 1931 (abriged and Rewritten by C. F. Richter).

I. Not felt. Marginal and long-period of large earthquakes.

II. Felt by persons at rest, on upper floors, or faborably placed.

III. Felt indoors. Hanging objects swing. Vibration like passing of light trucks. Duration estimated. May not be recognized as an earthquake.

IV. Hanging objects swing. Vibration like passing of heavy trucks or sensation of a jolt like a heavy ball striking the walls. Standing motor cars rock. Windows, dishes, doors rattle. Glasses clink. Crockery clashes. In the upper range of 4, wooden walls and frames crack.

V. Felt outdoors; direction estimated. Sleepers wakened. Liquids disturbed, some spilled. Small unstable objects displaced or upset. Doors swing, close, open. Shutters, pictures move. Pendulum clocks stop, start, change rate.

Table C-2. The Modified Mercalli intensity scale—continued.

VI. Felt by all. Many frightened and run outdoors. Persons walk unsteadily. Windows, dishes, glassware broken. Knickknacks, books, and so on, off shelves. Pictures off walls. Furniture moved or overturned. Weak plaster and masonry D cracked. Small bells ring (church, School). Trees, bushes shaken visibly or heard to rustle.

VII. Difficult to stand. Noticed by drivers of motor cars. Hanging objects quiver. Furniture broken. Damage to masonry D including cracks. Weak chimneys broken at roof line. Fall of plaster, loose bricks, stones, tiles, cornices, unbraced parapets, and architectural ornaments. Some cracks in masonry C. Waves on ponds; water turbid with mud. Small slides and caving in along sand or gravel banks. Large bells ring. Concrete irrigation ditches damaged.

VIII. Steering of motor cars affected. Damage to masonry C; partial collapse. Some damage to masonry B; none to masonry A. Fall of stucco and some masonry walls. Twisting, fall of chimneys, factory stacks, monuments, towers, elevated tanks. Frame houses moved on foundations if not bolted down; loose panel walls thrown out. Decayed piling broken off. Branches broken from trees. Changes in flow or temperature of springs and wells. Cracks in wet ground and on steep slopes.

IX. General panic. Masonry D destroyed; masonry C heavily damaged, sometimes with complete collapse; masonry B seriously damaged. General damage to foundations. Frames racked. Conspicuous cracks in ground. In alluviated areas, sand and mud ejected, earthquake fountains, sand craters.

X. Most masonry and frame structures destroyed with their foundations. Some well-built wooden structures and bridges destroyed. Serious damage to dame, dikes, embankments. Large landslides. Water thrown on bansk of canals, rivers, lakes, etc. Sand and mud shifted horizontally on beaches and flat land. Rails bent slightly.

XI. Rails bent greatly. Underground pipelines completely out of service.

XII. Damage nearly total. Large rock masses displaced. Lines of sight.

Reprinted from "Elementary Seismology," C. F. Richter, 1958, with permission from W. H. Freeman and Company.

Table C–3. The Rossi-Forel scale.

The most commonly used form of the Rossi-Forel (R.F.) scale reads as follows:

I. Microsiesmic shock. Recorded by a single seismograph or by seismographs of the same model, but not by several seismographs of different kinds: the shock felt by an experienced observer.

II. Extremely feeble shock. Recorded by several seismographs of different kinds; felt by a small number of persons at rest.

III. Very feeble shock. Felt by several persons at rest; strong enough for the direction or duration to be appreciable.

IV. Feeble shock. Felt by persons in motion; disturbance of movable objects, doors, windows, cracking of ceilings.

V. Shock of moderate intensity. Felt generally by everyone; disturbance of furnature, beds, etc., ringing of some bells.

VI. Fairly strong shock. general awakening of those asleep; general ringing of bells; oscillation of chandeliers; stopping of clocks; visible agitation of trees and shrubs; some startled persons leaving their dwellings.

VII. Strong shock. Overthrow of movable objects; fall of plaster; ringing of church bells; general panic, without damage to buildings.

VIII. Very strong shock. Fall of chimneys; cracks in the walls and buildings.

IX. Extremely strong shock. Partial or total destruction of some buildings.

X. Shock of extreme intensity. Great disaster; ruins; disturbance of the strata, fissures in the ground, rock falls from mountains.

Table C–4. The relation between Modified Mercalli intensity (MM) and Rossi-Forel intensity (RF).

MM	RF
I	I
II	I-II
III	III
IV	IV-V
V	V-VI
VI	VI-VII
VII	VIII
VIII	VIII+ to IX-
IX	IX+
X-XII	X

Reprinted from "Elementary Seismology," C. F. Richter, 1958, with permission from W. H. Freeman and Company.

able, are extremely approximate and the scatter of data about the predicted lines is large. Note that much of the scatter is due to the necessity of empirically converting site intensity data to the equivalent I_o value at the epicentral area; so as to normalize the site distance attenuation effects. Figure C–4 (taken from Krinitzky and Chang, Biblio 91) shows the above relationships along with the data behavior.

g. Recording instruments for ground motion. With the introduction of modern strong motion instruments, the size of the ground motion at a given location is often expressed by means of the instrumentally recorded ground motion parameter. The most commonly used instruments for engineering purposes are the strong motion accelerographs. These instruments record the acceleration time history of ground motion at a site. Figure 2–1 of paragraph 2–3*b* shows a typical accelerogram recorded by such an instrument. By proper analysis of this acceleration time history to account for instrument bias and base line correction, the resulting corrected acceleration record can be used by engineers. This corrected acceleration record can yield ground velocity and ground displacement by appropriate integrations, see figures 2–1, and 2–2 in paragraph 2–3*b*.

h. Relations for recorded ground motion and intensity. To relate the instrumentally recorded parameters such as acceleration, velocity and displacement with intensity parameters, empirical equations have been developed by various researchers. It should be cautioned again that such relationships are obtained from widely scattered and sparse data and should only be used with recognition of their inherently large prediction error. From studies related to earthquake damage estimation and earthquake insurance, it has been observed that the Modified Mercalli intensity scale is the easiest and most convenient with which to work. Most of the

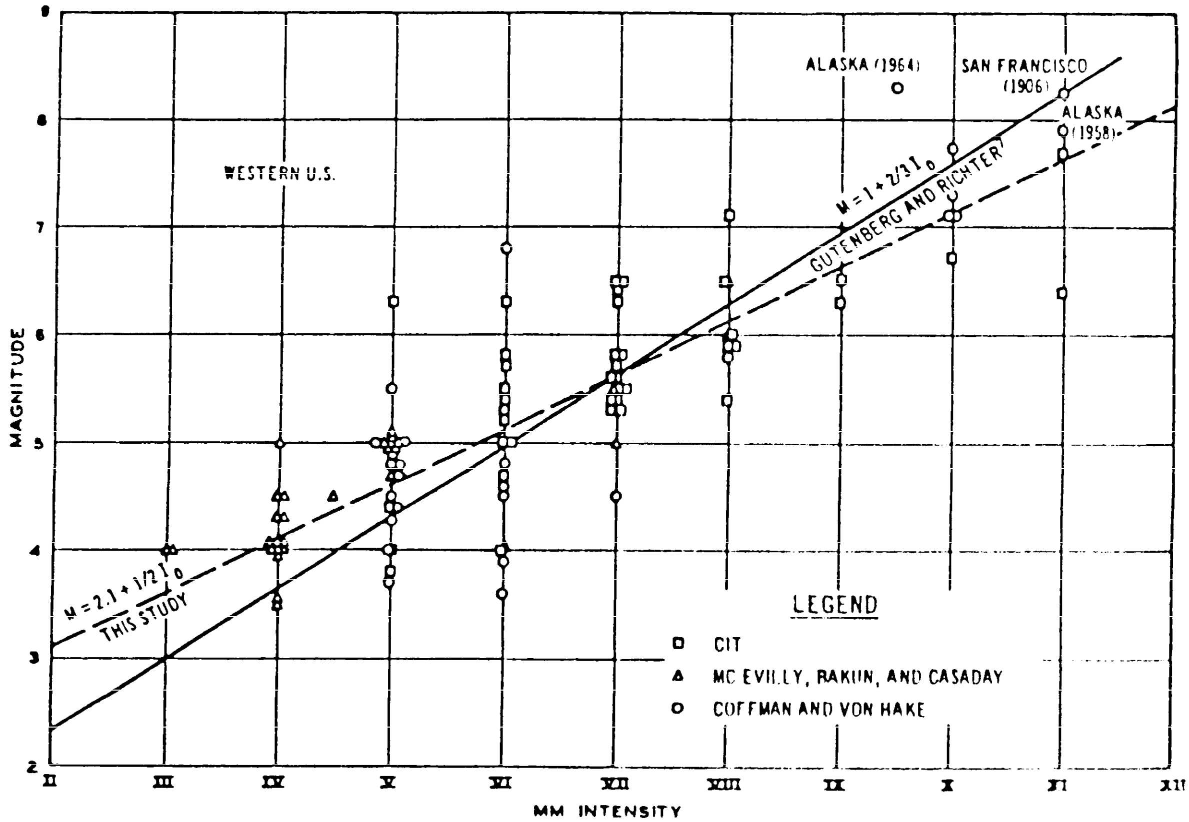

Reprinted from "Specifying Peak Motions for Design Earthquakes," Krinitzski, E. L. and Chang, F. K., Report No. 4 in the series, State-of-the-Art for Assessing Earthquake Hazards in the United States, U.S. Army Engineers Waterways Experiment Station, Misc. Paper S-73-1, 1975.

Figure C-4. Relation between earthquake magnitude and intensity.

available damage statistics are related to the MM intensity at a site. However, for the relatively recent instrumentally recorded data, the information on ground motion is usually in the form of a peak ground motion parameter such as the PGA, and many empirical relationships are available in the literature to relate the MM intensity with the PGA. Peak ground acceleration is an instrumentally recorded continuous variable whereas Modified Mercalli intensity is a subjectively assigned discrete integer variable. Thus, it should be expected that there will be a range or increment of continuous PGA values corresponding to a given intensity level. In the past, a number of researchers have developed PGA–MMI relationships. In each of the relationships given below, I is Modified Mercalli intensity and A is peak ground acceleration in cm/sec^2.

Gutenberg and Richter (1942) (Biblio 88) $\log A = -0.5 + 0.33I$ (eq C-8)

Hershberger (1956) (Biblio 89) $\log A = -0.9 + 0.43I$ (eq C-9)

Ambrasey (1974) (Biblio 84) $\log A = -0.16 + 0.36I$ (eq C-10)

Trifunac and Brady (1975) (Biblio 103) $\log A = 0.014 + 0.3I$ (eq C-11)

All the above relationships are log-linear in format. Recent work by McCann and Shah (Biblio 100) has shown that the assumption of a log-linear relationship between PGA and MMI may not be a reasonable one. Figure C-5 shows the following suggested relationship with two other relationships from above:

McCann and Shah (1979) (Biblio 100) $\log A = -0.024I^2 + 0.595I - 0.68$ (eq C-12)

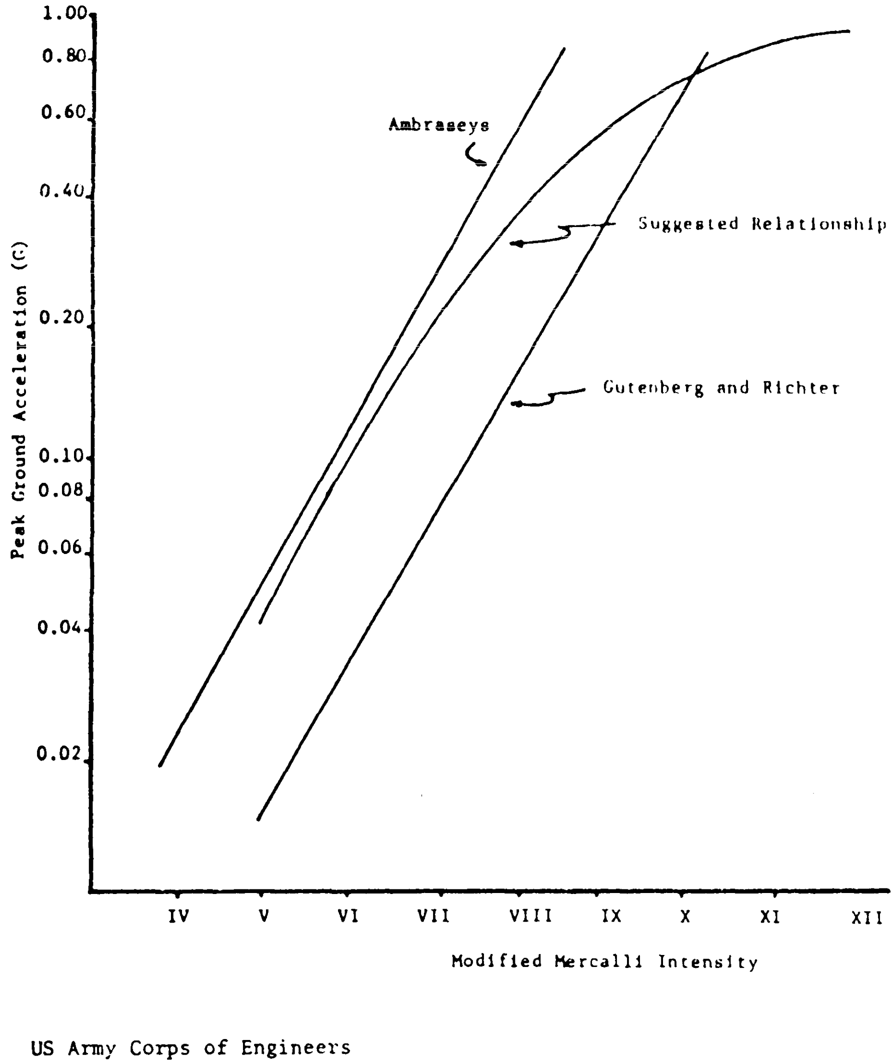

Figure C-5. McCann and Shah relationship.

In this relationship, it is assumed that a range of peak ground acceleration values are associated with each intensity level. Figure C-6 shows the PGA-MMI relation and the interval associated with each intensity. Table C-5 lists this range of PGA values associated with each MMI level.

C-2. Response Spectrum Representation of Seismic Ground Motion at Site.

Seismic ground motion may be roughly characterized as a set of time-varying harmonic vibrations having a fairly broad range of frequencies. Structures subjected to this input motion tend to amplify the harmonics near their own natural frequencies and filter or attenuate the others. The resulting structural response therefore, depends upon the frequency content of the harmonics in the ground motion and their relation to the dynamic frequency characteristics of the structure. This paragraph provides the definitions and discussions of the response spectrum representation of this inter-relationship between ground motion input and structural response.

a. Single degree-of-freedom system response. Figure C-7 shows the system and the definition for seismic input and response.

(1) *Response to General Input x(t).* For any given ground acceleration $\ddot{x}(t)$, the relative displacement response is

$$u(t) = -\frac{1}{\omega_D}\int_0^t \ddot{x}(\tau)e^{-\beta\omega(t-\tau)} \sin[\tau_D(t-\tau)]d\tau \qquad \text{(eq C-13)}$$

and for the case of zero damping this equation simplifies to

$$u(t) = -\frac{1}{\omega}\int_0^t \ddot{x}(\tau)\sin[\omega(t-\tau)]d\tau \qquad \text{(eq C-14)}$$

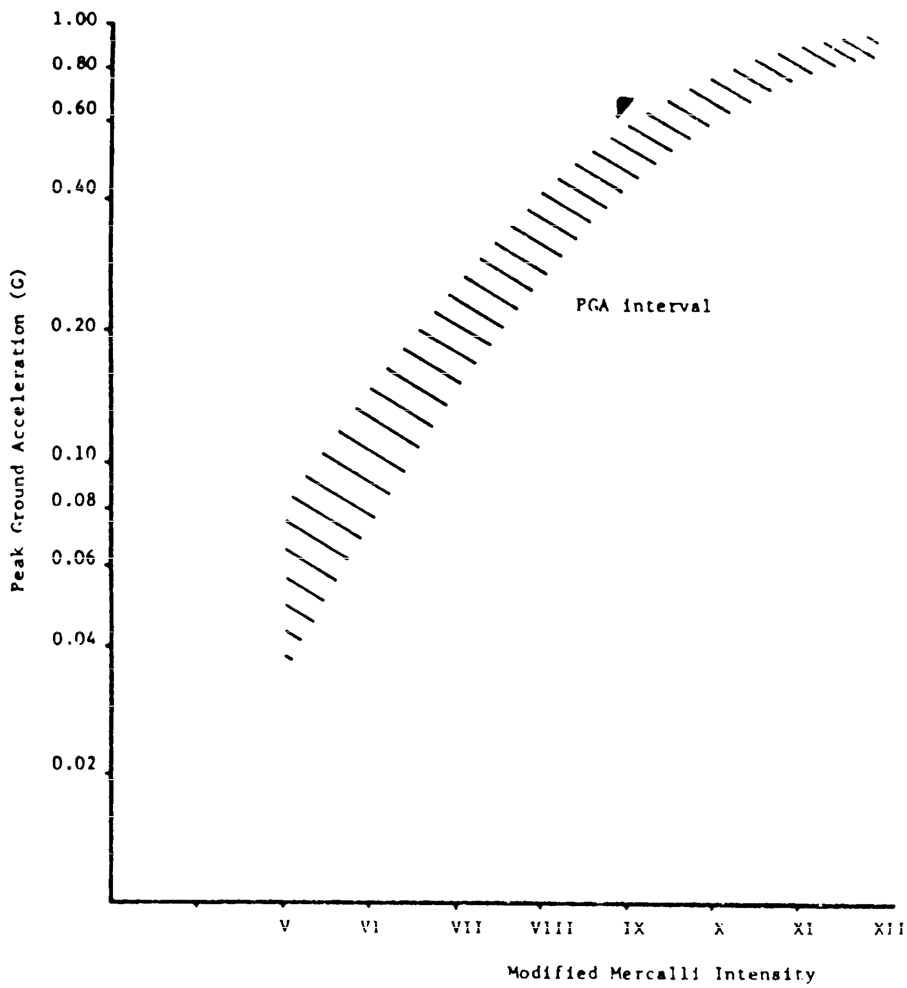

US Army Corps of Engineers

Figure C–6. The PGA-MMI relationship shown with the intervals associated with each intensity.

Table C-5. Relationship between MMI and PGA.

MMI	PGA(in g unit)
V	$0.03 < A < 0.08$
VI	$0.08 < A < 0.15$
VII	$0.15 < A < 0.25$
VIII	$0.25 < A < 0.45$
IX	$0.45 < A < 0.60$
X	$0.60 < A < 0.80$
XI	$0.80 < A < 0.90$
XII	$A > 0.90$

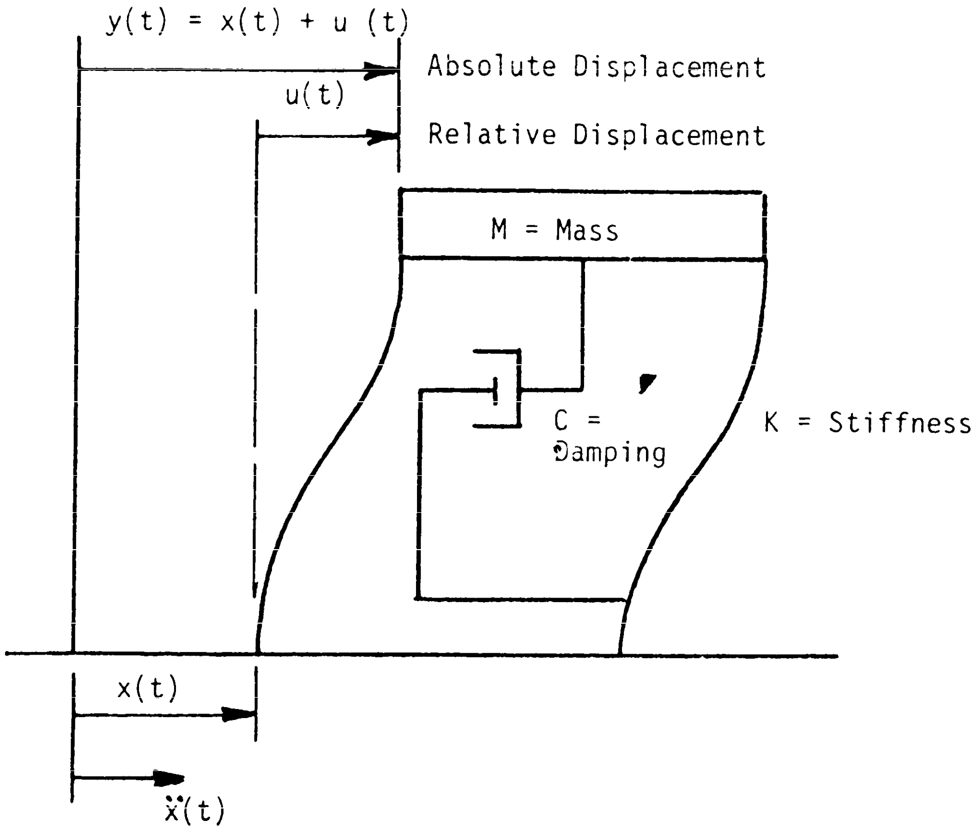

System Properties

$\omega = \sqrt{K/M}$ = undamped natural frequency

$\beta = \frac{C}{2M\omega}$ = fraction of critical damping

$\omega_D = \omega\sqrt{1-\beta^2}$ = damped natural frequency

Ground Motion

$x(t)$ = displacement

$\dot{x}(t) = \frac{dx}{dt}$ = velocity

$\ddot{x}(t) = \frac{d^2x}{dt^2}$ = acceleration

US Army Corps of Engineers

Figure C-7. Single degree of freedom system.

Relative velocities and accelerations are given by the time derivatives $\dot{u}(t)$ and $\ddot{u}(t)$ respectively. ω_D is damped natural frequency.

(2) Response to Sinusoidal Input. If the ground acceleration $\ddot{x}(t)$ were to be a single unit amplitude sinusoid at frequency Ω

$\ddot{x}(t) = \sin\Omega t$ then the corresponding response is given by $u(t) = [H(\omega)]\sin[\Omega t + \phi]$

where ϕ is a phase angle and

$$H(\omega) = \frac{1}{[(1-\Omega^2/\omega^2)^2 + 4(\beta\Omega/\omega^2)^2]^{1/2}} \quad \text{(eq C-15)}$$

is the system frequency response function which either amplifies or attenuates the response according to the frequency Ω/ω ratio, and the damping ratio β, see figure C–8. This function is most useful in the explanation of how predominant harmonics in ground motion, due to special soil conditions, can amplify the ordinates of the response spectrum.

b. Response spectra. For a given ground acceleration $\ddot{x}(t)$ such as shown in figure 2–4, and given damping, the absolute maximum values found from the complete time history solution of equation C–13 provide the response spectrum values at the system frequency ω or period $T = \frac{2\pi}{\omega}$. A response spectrum is traditionally presented as a curve connecting the maximum response values for a continuous range of frequency or period values, such as shown in figures 2–4 of paragraph 2–3c.

The different response spectra are defined as:

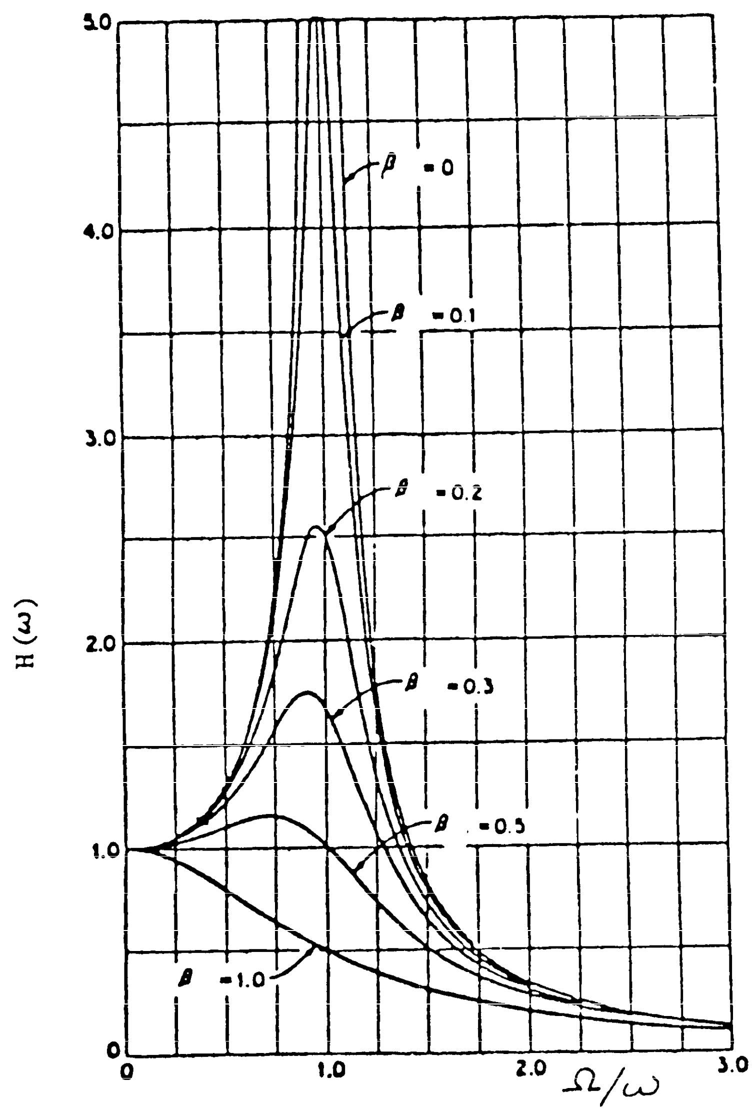

US Army Corps of Engineers

Figure C–8. Maximum dynamic load factor for sinusoidal load.

$SD = u(t)_{max}$ = Relative Displacement Response Spectrum

$SV = \dot{u}(t)_{max}$ = Relative Velocity Response Spectrum

$SA = \ddot{y}(t)$ max = $\ddot{u}(t) + \ddot{x}(t)$ max = Absolute Acceleration Response Spectrum

Then using the close approximation of $\omega = \omega_D$ for $\beta \leq 0.1$, the more commonly employed versions for engineering purposes are:

$$S_V = \omega\ (SD) = \text{Pseudovelocity Spectrum} \qquad \text{(eq C–16)}$$

$$S_a = \omega^2\ (SD) = \text{Pseudovelocity Spectrum.} \qquad \text{(eq C–19)}$$

For the common structural damping values, and the earthquake type of input motion, there is essential equality for the real and pseudo-values,

$$S_V \cong SV \qquad \text{(eq C–18)}$$

$$S_a \cong SA \qquad \text{(eq C–19)}$$

Of course, for long period structures, the velocity equality breaks down since S_V approaches zero, while SV approaches PGV. This is because relative displacement approaches the ground displacement value, and there is small motion of the mass. The relationships between SD, S_V, and S_a can be justified by the following physical behavior of the vibrating system. At maximum relative displacement SD, velocity is zero, and maximum spring force equals maximum inertia force,

$$k(SD) = m\ S_a$$

giving $\quad S_V = k/m(SD) = \omega^2(SD) \qquad$ (eq C–20)

Detailed discussions on response spectra and their computation from accelerograms are given in (Biblios 7,3,12). An example of a typical accelerogram spectrum is shown in figure 2–4. Also because of the relations $S_a = \omega\ S_V = \omega^2 S_d$, it is possible to represent spectra on tri-partite log paper, see figure 3–29 in paragraph 3–6*e*(1).

C–3. Methods of forecasting earthquake ground motion.

The following methods of ground motion specification are employed by engineers for the seismic resistant design of structures ranging from nuclear facilities to ordinary buildings. Herein the term "ground motion" is used in its general sense to include both the time history and response spectrum representations of earthquake effects. Also, all methods require an initial specification of the acceptable risk of exceeding the structural performance levels such as the damage threshold, functionality level, and condemnation threshold, in order to establish the corresponding level of ground motion severity.

a. Selected representative ground motion. Given the structure site, its soil column conditions, and the geological description of the effective earthquake sources and their corresponding travel paths to the site: a set of time histories (commonly three to five) is selected so as to have reasonably similar soil columns, source and travel path characteristics, distances, and magnitudes with these conditions at the site. The magnitude is selected according to the performance and reliability criteria for the structure. Both actual records and artificially generated time histories are both used for the selected set.

(1) This method has the advantages of providing a definite set of structural response time histories or response spectra. These results may be averaged to provide a single description of forecasted structure performance. The set of response spectra may be averaged (arithmetically or graphically) to provide the most representative response spectrum ordinates in the particular period range of the structural system. This method does not require the use of attenuation equations and spectral (DAF) shapes with their high variances of prediction error.

(2) The disadvantages are that it is often difficult to find the representative records that would correspond to the particular site condition; and the end results are based on an average representation of a very small sample. Much depends upon how sincerely the engineer believes that the selected small sample can actually forecast the future ground motion. Further description and discussion is given in (Biblio 102).

b. Analytical site-soil column response. This method uses a somewhat similar method to that of the selected method in C–3*a*. The main difference is that the selected time histories must be representative of bed rock motion. For a given magnitude, a set of rock site accelerograms is selected (or scaled) so as to best represent the forecasted duration, amplitude and spectrum shape of the site bed rock motion. Then with the data from the site soil boring investigations, a dynamic model of the site soil column is formulated. This model is subjected to the set of bed rock motions and the resulting set of site surface time histories is obtained. These histories or their averaged (and smoothed) spectra are used for the structural input. The principal advantage of this method is that it provides the best analytical representation of the effects of the site soil column on the surface response. The disadvantages are inherent in the selected specification of the limited set of bed rock time histories, and in the accuracy of the analytical model of the site soil column. The uncertainties due to a small data set to represent the future forecast are also present as in the method C-3*a*. (Biblios 93,98,99) give detailed discussions on this method. In the assignment of a particular weight, as will be discussed in paragraph C-3*f*, of preference for the spectral shape as provided by a site soil-column response analysis, the following items should be considered and assessed for validity and applicability:

(1) The time histories and scaling factor for bed-rock earthquake motion. Are the histories inclusive of duration and frequency content representative of the various possible sources and travel paths? Has the scaling factor (for PGA) been evaluated by a hazard analysis similar in quality to that used for surface ground motion?

(2) Soil-Column Model: Have adequate boring investigations and related tests been made to reasonably establish the dynamic model properties. Is there adequate geological information to supplement the boring data? Is the model appropriate for the site.

(3) Have a sufficient number of bed-rock time histories been used to establish a reasonably reliable statistical average and measure of dispersion of surface motion spectra.

c. Empirical forecasts from representative records. This method involves two basic steps: given the risk of exceedance, forecast a spectral scaling factor (PGA or EPA) corresponding to this risk; then apply this scaling factor to a response spectrum shape (DAF) representative of the general site soil column condition. The first step may be either "deterministic" such that the most severe magnitude event occurs on the source at the epicentral location nearest to the site: or may be probabilistic such that the union or combination of the probabilities of all the effective event magnitudes, sources, and epicentral locations is considered in the seismic hazard of the specified ground motion description (PGA) × (DAF). For a given magnitude of event M at a given source to site distance R, this method consists of:

(1) Attenuation of the spectral scaling parameter (such as PGA) to the site. These attenuation relations are derived from past data and vary according to the data used and the statistical model and fitting procedure (usually regression analysis). There is usually a large prediction error (50 to 100%) about the central or median predicted value.

(2) The PGA at the site is represenative of accelerogram peak records. This "instrumental" value is converted (by judgement) to an effective EPA value, which when used to scale the spectral (DAF) shape should produce a reliable structural response spectrum. With the "properly" formulated analytical model of the structure, this spectrum "should" provide a reliable estimate of the actual structural deformations that would result from the event or any one of the events included in the seismic hazard analysis (with stated risk of exceedance such as 10% in one-hundred years). This method is based on the statistical principle that the best prediction of the future is the average behavior of many past records. Despite the disadvantages listed below, it is a common practical way to forecasting and specifying ground motion. Its results may be modified by the results of the other methods given herein. The disadvantages are:

(a) The high prediction error in the attenuation equations for PGA.

(b) The high variability of the spectral shape DAF as obtained from the average of normalized spectra having roughly similar soil conditions. The method of normalizing the spectra to a common unity value of PGA contributes much to the high variability of the DAF shape.

d. Empirical forecasts of spectral ordinates. This method is a refinement of paragraph C-3*c*, where the response spectrum value S_a or S_v at a given period (rather than the zero period PGA value) is attenuated from source to site. The advantage is that the site spectrum is obtained directly in terms of: the source-to-site distance, the travel path geology, the event magnitude and the site soil conditions. It is not necessary to employ the highly variable empirical DAF spectral shape as needed by the method in C-3*c*. The disadvantage is that the attenuation relations for the spectrum ordinates are much more subject to prediction error than these relations for PGA. The available data for near-source spectra and corresponding spectra at various site distances is from only a few recent events (such as 1971 San Fernando and 1980 Imperial Valley). The data is therefore both sparse and very sensitive to the geological conditions of the region where the records were obtained.

e. Mathematical or theoretical modeling of the seismic event. This method models the source fracture size and sequence of rupture impulses. These impulses are then propagated by wave mechanics through a model of the source to site path. This allows inclusion of all that is both theoretically and empirically known about source mechanics and site response (included are directivity and magnitude effects). Disadvantages are lack of data and knowledge concerning the faulting mechanism and the travel path geology.

f. Summary. For any actual site hazard study requiring specified ground motion description, the most popular methods are those in C–3*b* and C–3*c*. When both are used for a particular project, the individual results should be reviewed for consistency and resolution of significant differences. Of course any knowledge available from results of the other methods can contribute to this consistency and resolution process for the final ground motion specification. In actual practice, when there are two or more sources of spectral shapes, the smoothing and averaging process is done by judgement rather than by any formal statistical method, see figure C–9.

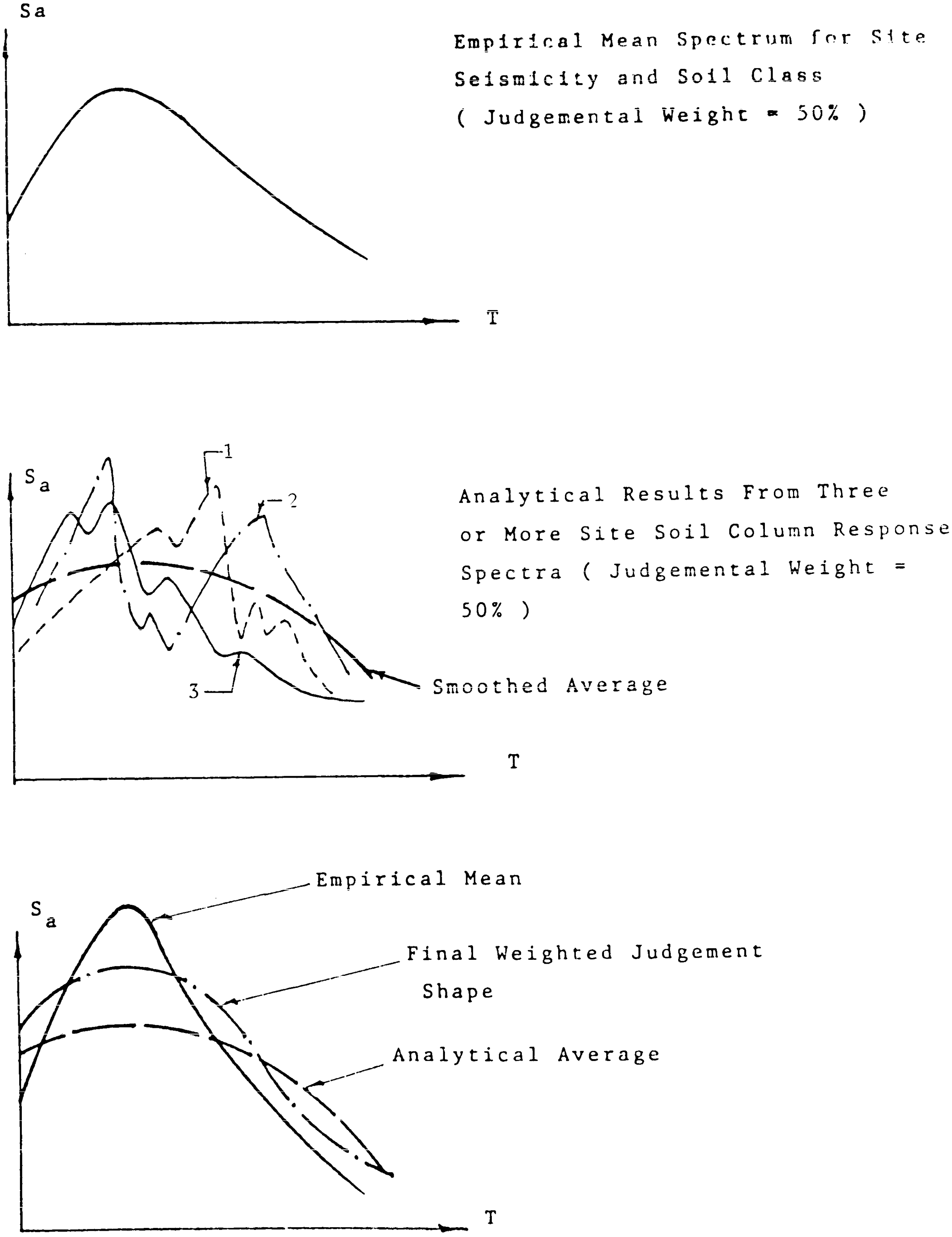

US Army Corps of Engineers

Figure C-9. Judgemental averaging of empirical and analytical site spectra.

C–4. Emperical relations for seismicity and fault activity.

The following tables and figure are given to provide supplementary information concerning empirical relationships between fault length, fault displacement, and earthquake magnitude, Biblio (101) and degree of fault activity in terms of slip rate, Biblio (100).

Table C–6. Magnitude-displacement relation.

Equations of Best Straight-Line Fit for Magnitude Versus Log Displacement: M = a + b Log D

Fault	No.	a	b	Standard Deviation	Correlation Coefficient
North America	24	6.745	0.995	0.595	0.840
Rest of world	51	6.821	1.120	0.549	0.643
Worldwide	75	6.750	1.197	0.541	0.791
A normal-slip	20	6.827	1.050	0.449	0.777
B reverse-slip	11	7.002	0.986	0.469	0.744
C normal-oblique-slip	8	6.750	1.260	0.395	0.672
D reverse-oblique-slip	6	6.917	-0.150	0.421	-0.063
E strike-slip	30	6.717	1.214	0.639	0.814
A + C	28	6.757	1.226	0.431	0.774
B + D	17	6.846	1.023	0.506	0.674
C + D + E	44	6.705	1.206	0.586	0.794
C + D	14	6.692	1.165	0.451	0.568
B + E	41	6.767	1.200	0.606	0.811
A + C + E	58	6.737	1.221	0.549	0.806
B + D + E	47	6.742	1.188	0.597	0.795

Reprinted from "Fault and Earthquake Magnitude," Slemmons, D. B., State-of-the-Art for Assessing Earthquake Hazards in the United States, Report No. 6, Miscellaneous Paper S-73-1, U.S. Army Engineer Waterways Experiment Station, 1977.

Table C-7. Displacement-fault length relation.

Equations of Best Straight-Line Fit for Log Displacement
Versus Log Length: Log D = a + b Log L

Fault	No.	a	b	Standard Deviation	Correlation Coefficient
North America	26	-4.720	1.036	0.632	0.737
Rest of world	48	-1.654	0.444	0.320	0.589
Worldwide	74	-3.185	0.747	0.515	0.645
A normal-slip	20	-4.375	1.014	0.567	0.620
B reverse-slip	9	-2.123	0.568	0.226	0.832
C normal-oblique-slip	8	-0.107	0.128	0.279	0.183
D reverse-oblique-slip	6	1.242	-0.220	0.154	-0.487
E strike-slip	31	-3.571	0.805	0.541	0.703
A + C	28	-2.898	0.705	0.351	0.685
B + D	15	-1.665	0.462	0.276	0.700
C + D + E	45	-2.924	0.684	0.516	0.624
C + D	14	0.033	0.081	0.265	0.130
B + E	40	-3.469	0.797	0.506	0.722
A + C + E	59	-3.239	0.756	0.474	0.680
B + D + E	46	-3.119	0.728	0.501	0.682

Reprinted from "Fault and Earthquake Magnitude," Slemmons, D. B., State-of-the-Art for Assessing Earthquake Hazards in the United States, Report No. 6, Miscellaneous Paper S-73-1, U.S. Army Engineer Waterways Experiment Station, 1977.

Table C–8. Magnitude-fault length relation.

Equations of Best Straight-Line Fit for Magnitude Versus Log Fault Length: $M = a + b \text{ Log } L$

Fault	No.	a	b	Standard Deviation	Correlation Coefficient
North America	26	-0.146	1.504	0.628	0.815
Rest of world	49	2.971	0.920	0.500	0.680
Worldwide	75	1.606	1.182	0.603	0.724
A normal-slip	18	1.845	1.151	0.521	0.575
B reverse-slip	9	4.145	0.717	0.167	0.932
C normal-oblique-slip	10	3.117	0.913	0.497	0.604
D reverse-oblique-slip	7	4.398	0.568	0.340	0.522
E strike-slip	31	0.597	1.351	0.694	0.775
A + C	28	2.042	1.121	0.490	0.666
B + D	16	3.355	0.847	0.320	0.833
C + D + E	48	1.149	1.262	0.650	0.737
C + D	17	2.992	0.918	0.437	0.652
B + E	40	1.042	1.277	0.664	0.773
A + C + E	59	1.204	1.260	0.639	0.724
B + D + E	47	1.357	1.217	0.638	0.758

Reprinted from "Fault and Earthquake Magnitude," Slemmons, D. B., State-of-the-Art for Assessing Earthquake Hazards in the United States, Report No. 6, Miscellaneous Paper S-73-1, U.S. Army Engineer Waterways Experiment Station, 1977.

Table C–9. Magnitude-length times displacement relation.

Equations of Best Straight-Line Fit for Magnitude Versus
Log Length Times Displacement: M = a + b Log LD

Fault	No.	a	b	Standard Deviation	Correlation Coefficient
North America	24	3.510	0.701	0.503	0.889
Rest of world	46	4.158	0.610	0.464	0.731
Worldwide	70	3.740	0.680	0.489	0.828
A normal-slip	18	4.551	0.530	0.421	0.750
B reverse-slip	9	5.310	0.423	0.213	0.886
C normal-oblique-slip	8	3.281	0.785	0.325	0.793
D reverse-oblique-slip	6	3.706	0.678	0.353	0.550
E strike-slip	29	3.220	0.759	0.567	0.859
A + C	26	3.691	0.707	0.388	0.792
B + D	15	4.478	0.550	0.327	0.834
C + D + E	43	3.238	0.766	0.510	0.850
C + D	14	3.168	0.802	0.340	0.784
B + E	38	3.424	0.728	0.536	0.859
A + C + E	55	3.393	0.745	0.503	0.837
B + D + E	44	3.441	0.726	0.515	0.853

Reprinted from "Fault and Earthquake Magnitude," Slemmons, D. B., State-of-the-Art for Assessing Earthquake Hazards in the United States, Report No. 6, Miscellaneous Paper S-73-1, U.S. Army Engineer Waterways Experiment Station, 1977.

Table C–10. Magnitude-length times squared displacement relation.

Equations of Best Straight-Line Fit for Magnitude Versus Log Length Times Square of Displacement: $M = a + b \text{ Log } LD^2$

Fault	No.	a	b	Standard Deviation	Correlation Coefficient
North America	24	4.808	0.420	0.526	0.878
Rest of world	46	4.967	0.417	0.473	0.719
Worldwide	70	4.865	0.427	0.496	0.823
A normal-slip	18	5.568	0.299	0.427	0.742
B reverse-slip	9	5.865	0.289	0.242	0.850
C normal-oblique-slip	8	4.103	0.573	0.309	0.815
D reverse-oblique-slip	6	4.290	0.522	0.373	0.468
E strike-slip	29	4.491	0.480	0.574	0.855
A + C	26	4.752	0.459	0.384	0.796
B + D	15	5.162	0.382	0.350	0.808
C + D + E	43	4.473	0.489	0.513	0.848
C + D	14	3.985	0.590	0.340	0.785
B + E	38	4.597	0.468	0.535	0.859
A + C + E	55	4.582	0.477	0.499	0.840
B + D + E	44	4.587	0.469	0.516	0.852

Reprinted from "Fault and Earthquake Magnitude," Slemmons, D. B., State-of-the-Art for Assessing Earthquake Hazards in the United States, Report No. 6, Miscellaneous Paper S-73-1, U.S. Army Engineer Waterways Experiment Station, 1977.

Table C–11. Degree of fault activity.

FAULT	SLIP RATE (CM/YEAR)	CALCULATED CUMULATIVE SLIP (M)				MAX SLIP /EVENT (METERS)	RECURRENCE INTERVAL (YRS.)
		10K yrs	35K yrs	100K yrs	500K yrs		
Fairweather, Ak.	5.8	680	2030	5800	29000	10	170
San Andreas, Ca.	3.7	370	1295	3700	18500	10	270
Hayward, Ca.	.6	60	210	600	3000	2	300
Coyote Creek, Ca.	.3	30	105	300	1500	1.5	500
Lower Rhine Graben, Ger.	.023	2.3	8.5	23	115	.5	2000
Upper Rhine Graben, Ger.	.005	.5	1.75	5	25	.3	6000
Cleveland Hill, Ca.	.0006	.06	.21	.60	3	.24	30000
Rawhide Flat West, Ca.	.00025	.025	.087	.25	1.25	.08	32000
Negro Jack Point, Ca.	.00007	.007	.025	.07	.35	.02	29000

US Army Corps of Engineers

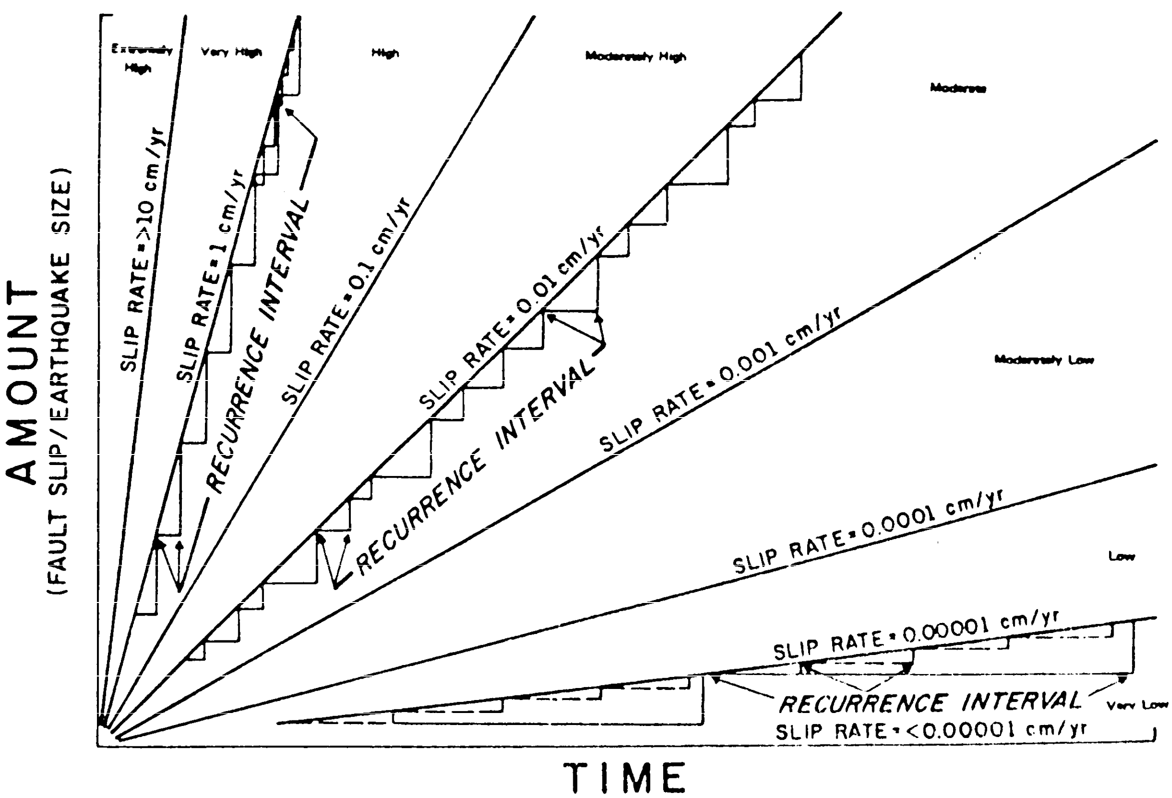

US Army Corps of Engineers

Figure C–10. Relative degree of fault activity.

APPENDIX D
DESIGN EXAMPLES—GROUND MOTION

D–1. Purpose and Objectives.

The purpose of this appendix is to provide examples of the assumptions, procedures, and calculations required for each step of the probabilistic hazard analysis for site specific ground motion. Example 1 is a simplified version that shows hand calculations for all steps; it is intended to provide a direct understanding of how each successive value is obtained. Examples 2 and 3 represent the more detailed, actual types of hazard analyses necessitating the use of a computer program. Example 2 covers steps I and II and detail; and example 3 provides additional examples of steps I and II and then shows steps III and IV leading to the description of hazard as the complementary cumulative distribution function or hazard curve for site PGA.

D–2. Introduction for Simplified Example 1.

The purpose of this example is to show a simple, by-hand set of calculations for each of the steps I through IV for a site hazard analysis. A point is to be determined on the hazard curve (fig 3–39), for P [PGA < PGA_j] with PGA_j = 0.20g, for an exposure time of t = 50 years. Then assuming that the complete hazard curve has been determined from a set of similarly calculated values of PGA_j, a selected response spectrum shape is scaled to illustrate step V, and provide an EQ-I site specific spectrum.

a. Step I. Identification and Modeling of Seismic Sources (para 3–4*b*). The building site is located in a region containing two distinct sources of seismicity; a line source 1, and an area source 2. Source 1 has been identified by the surface trace and subsurface geological structure of a strike-slip fault along with a history of earthquake reports and records associated with this fault. Source 2 is a general area within which a history of earthquake reports have occured; there may be faults with this area, however there is no surface evidence of their location. Figure D-1 shows the line and area models of sources 1 and 2, the estimated epicentral locations of past earthquakes along with the listings of historical records of earthquakes assigned to each source.

b. Step II. Evaluation of source seismicity and recurrence relations (para 3–4c). As shown in figure D–1, the line source 1 has a period of t_1 = 150 years of reported seismic events and records along its assigned length L_1 = 30 kilometers. The older reports in terms of intensity have been converted to equivalent magnitude values M, and the more recent events have directly measured magnitudes. Based on the fault length, along with its depth and slip activity, a maximum magnitude of M = 7.5 is assigned for this source. Area source 2 has a period of t_2 = 300 years of reported history. All events except the last one are in terms of MMI intensity I_o, and the last event has a measured magnitude. The MMI values are converted to equivalent local magnitude values by use of the Gutenberg-Richter equation C–5 given in appendix C. The geological structure within source 2 is judged to be capable of a maximum magnitude of M = 6.5. The recurrence relation for source 1 is developed by linear regression analysis as follows. The eight recorded events are ranked according to descending magnitude values such that the number N of events having magnitudes equal to greater than a given ranked magnitude is the ranked order number. These data are shown in figure D–2 along with the corresponding logarithm values ln N. A plot of ln N versus M in figure D–3 shows that a single straight line can represent the source 1. recurrence relation

$$\ln N_1 = \alpha_1 + \beta_1 M$$

Letting y = ln N_1 and x = M, the linear regression analysis calculations for the least-squared-error line

$$y = \alpha_1 + \beta_1 \chi$$

are shown in figure D–2, along with the normalization required to give

$$\ln N_i = \alpha_i + \beta_1 M = 1.29 - 1.32M$$

for a one kilometer, one year basis. A similar processing of the source 2 data provided the recurrence relation

$$\ln N_2 = 5.81 - 0.95M$$

for the 300 year time period and the 400 square kilometer area. Normalization then gave

$$\ln N'_2 = \alpha'_2 + \beta_2 M = -5.89 - 0.95M$$

for a one square kilometer, one year basis.

c. Step III. Probabilistic Forecasting Model (para 3–4d). The Poisson occurrence model is assumed to forecast the probabilities of magnitude levels for both sources 1 and 2. Referring to equation 3–14 of paragraph 3–4d; given a length increment ΔL and the future time period t for source 1, the probability of no events greater

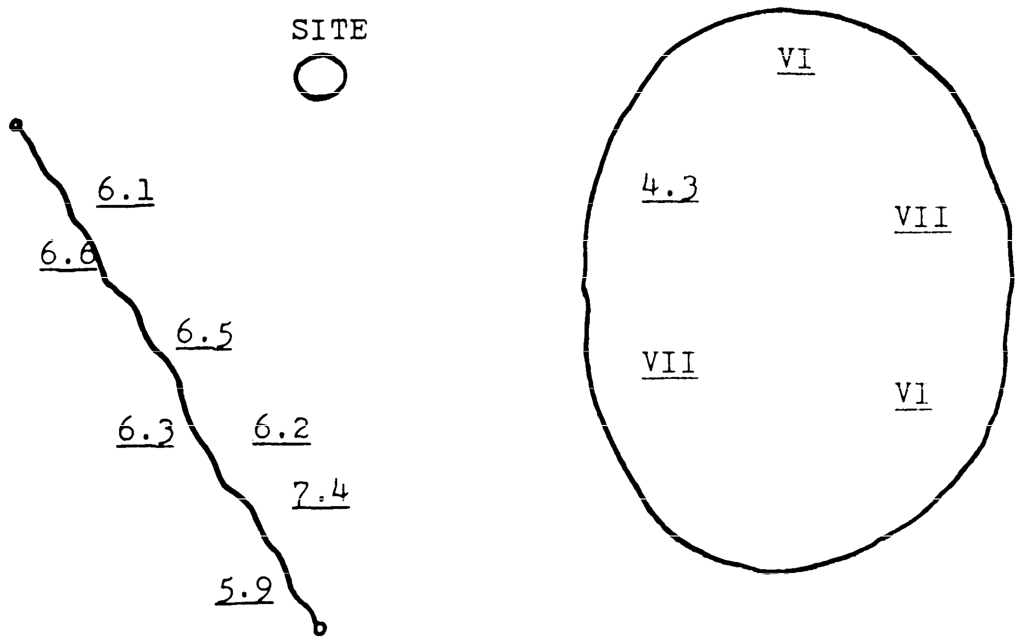

LINE SOURCE 1.
Length=30 km
150 Years of Record

Date	M
1830	6.5
1852	6.1
1871	6.6
1890	6.2
1911	5.9
1920	6.3
1946	7.4
1980	5.7

AREA SOURCE 2.
Area=400 sq km
300 Years of Record

Date	I_o	M*
1682	VII	5.7
1765	VI	5.0
1812	VI	5.0
1920	VII	5.7
1982	V	4.3

* $M=1.0+(2/3)I_o$, (eq C-5)

US Army Corps of Engineers

Figure D-1. Source models and records for sources 1 and 2.

LINE SOURCE 1.

$L_1 = 30$ km, $T_1 = 150$ years, $M_{max} = 7.5$

N_1	$\ln N_1 = y$	$M = x$	$(y-\bar{y})$	$(x-\bar{x})$	$(x-\bar{x})^2$	$(y-\bar{y})(x-\bar{x})$
1	0	7.4	−1.33	1.06	1.12	−1.41
2	0.69	6.6	−0.64	0.26	0.07	−0.15
3	1.10	6.5	−0.23	0.16	0.03	−0.04
4	1.39	6.3	0.06	−0.04	0	0
5	1.61	6.2	0.28	−0.14	0.02	−0.04
6	1.79	6.1	0.46	−0.24	0.06	−0.11
7	1.95	5.9	0.62	−0.44	0.19	−0.27
8	2.08	5.7	0.75	−0.64	0.41	−0.48
Σ =	10.61	50.7		Σ =	1.90	−2.50

$$\bar{y} = \frac{10.61}{8} = 1.33, \quad \bar{x} = \frac{50.7}{8} = 6.34$$

$$\beta_1 = \frac{\Sigma(y-\bar{y})(x-\bar{x})}{\Sigma(x-\bar{x})^2} = \frac{-2.50}{1.90} = -1.32$$

$$\alpha_1 = \bar{y} - \beta_1\bar{x} = 1.33 - (-1.32)(6.34) = 9.70$$

$$\ln N_1 = \alpha_1 + \beta_1 M = 9.70 - 1.32M$$

Normalizing to a 1 km, 1 year Basis, using (eq 3-5);

$$\alpha_1' = \alpha_1 - \ln(L_1T_1) = 9.70 - \ln(4500) = 1.29$$

$$\ln N_1'(m) = \alpha_1' + \beta_1 m = 1.29 - 1.32\,m$$

for $m \leq 7.5$

US Army Corps of Engineers

Figure D-2. Recurrence relation calculations for source 1.

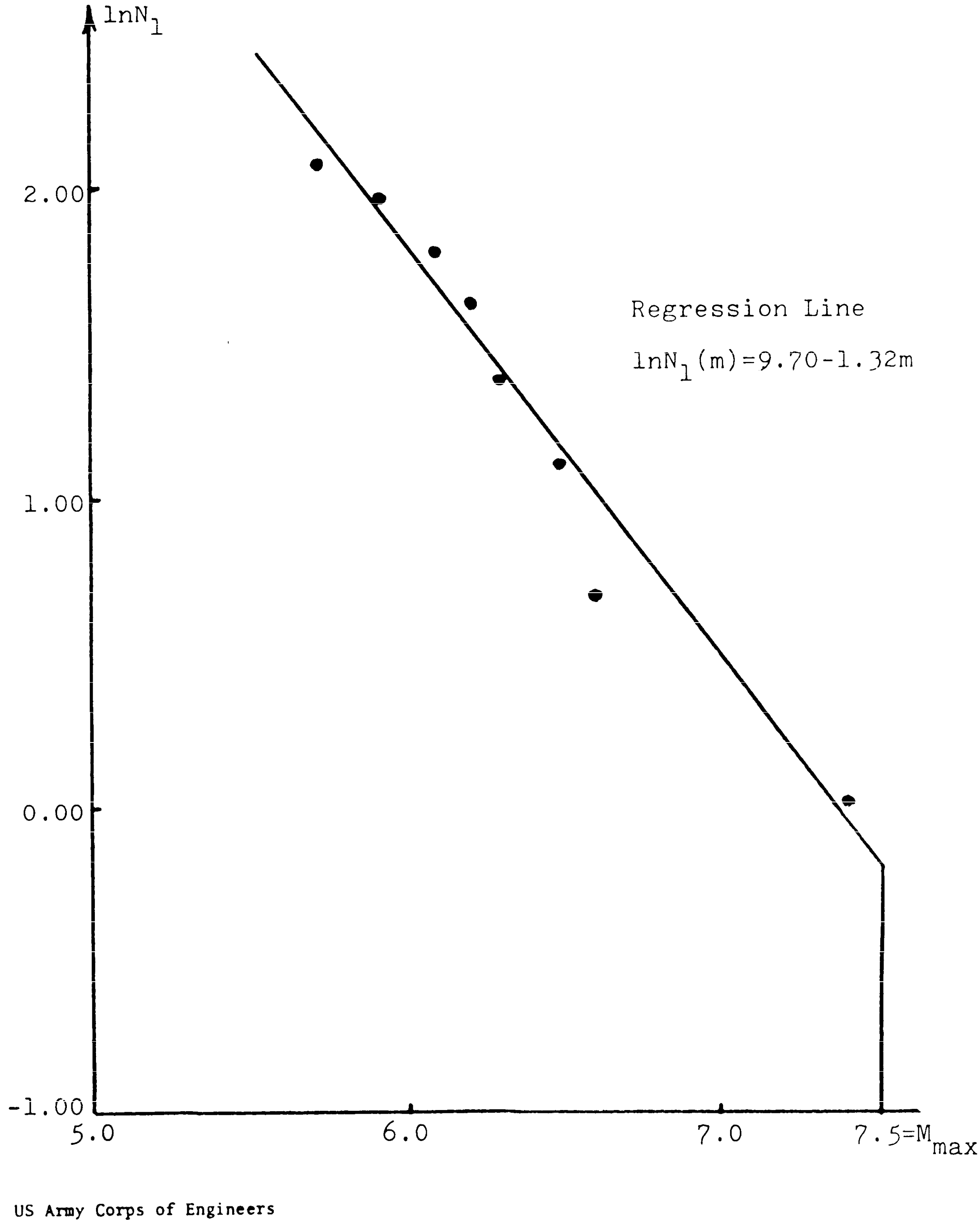

Figure D-3. Recurrence data plot for source 2.

than $M_1 = m$ is

$P[M_1 \leq m] = P(o,m,t) = \exp[-N'_1(m)\,\Delta L\,t]$

where $N'_1(m) = \alpha'_1 + \beta_1 m$.

Similarly given an area increment ΔA and t for source 2,

$P[M_2 \leq m] = P(o,m,t) = \exp[-N'_2(m)\,\Delta A\,t]$

where $N'_2(m) = \alpha'_2 + \beta_2 m$

The value of magnitude m to be employed in these equations is that which can produce the attenuated value of PGA = 0.20g at the building site when the earthquake event occurs at the center of the increments ΔL and ΔA of sources 1 and 2 respectively. In order to determine these magnitudes it is necessary to divide the sources into elements, measure the element-to-site distance R, and then use the attenuation relation in Step IV. Figure D–4 shows the element modeling of the sources.

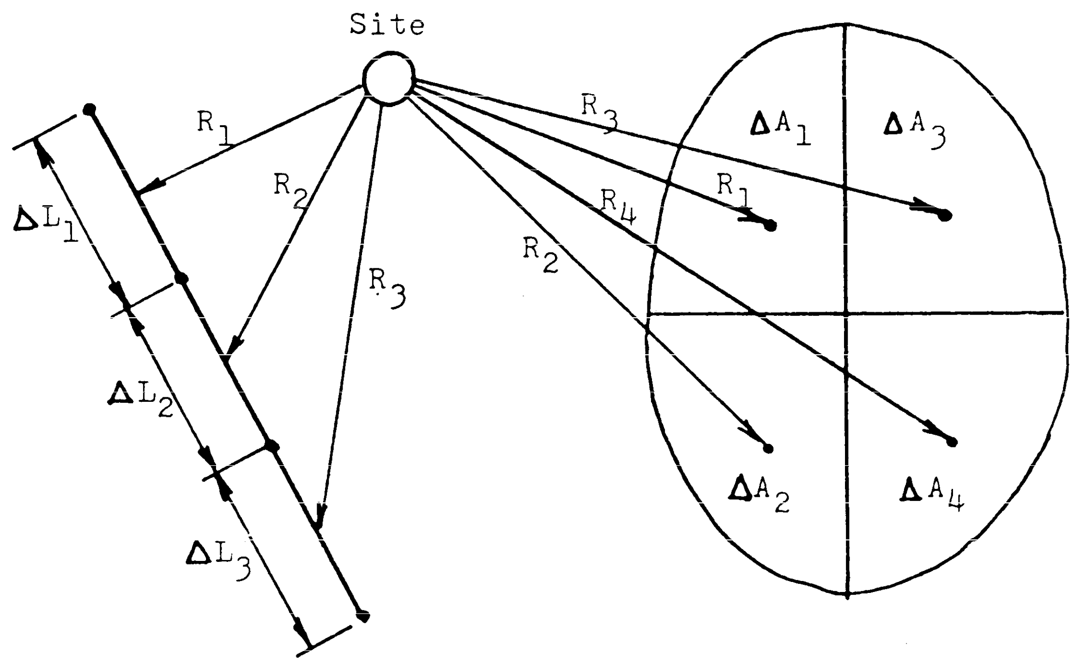

LINE SOURCE 1.
L=30 km
n=3 Elements
ΔL=10 km
Transmission Path A

AREA SOURCE 2.
A=400 sq km
n=4 Elements
ΔA=100 sq km
Transmission Path B

For the given PGA_j=0.20g ,the OASES attenuation curves in figure 3-23 provide the magnitudes m_i for each of the measured element to site distances R_i.

SOURCE 1.

i	R_i km	m_i
1	15	6.5
2	18	6.7
3	24	7.2

SOURCE 2.

i	R_i km	m_i
1	22	5.0
2	28	5.3
3	32	5.7
4	37	6.1

US Army Corps of Engineers

Figure D–4. Source location and element properties.

d. Step IV Selection of the Attenuation Relation (para 3-5). The OASES relationship given by equation 3-21 and as shown in figure 3-23 has been judged to be appropriate for the source depth, travel path, and site soil characteristics. With the measured source element-to-site distances R given in figure D-4, and the given objective PGA = 0.20g = 196cm per second squared, the corresponding magnitude values can be found by interpolation between the curves of figure 3-23. The results are tabulated in figure D-4.

e. Combination of element and source probabilities. With the magnitudes m necessary to produce PGA = 0.20g at the site, the normalized recurrence relations are used to evaluate the corresponding rate values of $N'_1(m)$ and $N'_2(m)$ for use in the Poisson probability equations; these rates are tabulated in figure D-5.

The total hazard P [PGA > 0.20g] is calculated by 1 − P [PGA ≤ 0.20g], where P [PGA ≤ 0.20g] is the total probability of no exceedence of 0.20g at the site. This total probability is the probability of the intersection or mutual occurence of the occurences of ($M \leq m_i$) at all of the elements ΔL_i and ΔA_i of sources 1 and 2 respectively. In order to evaluate this intersection probability, an independent point source model is assumed for elements ΔL_i and ΔA_i. Accordingly, for the given level of PGA = 0.20g and the future time t = 50 years, the elements ΔL_i and ΔA_i are considered as point sources with seismicity rate $N'_1(m_i)\ \Delta L\ t$ and $N'_2(m_i)\ \Delta A\ t$ respectively. Here for each element the m_i is the magnitude level necessary to produce 0.20g at the site. Having the normalized rates $N'_1(m_i)$ and $N'_2(m_i)$ from the recurrence relations, the individual element probabilities of no magnitudes m_i capable of exceeding 0.20g at the site are:

$$P\,[M_1 \leq m_i] = \exp\,[-N'_1\,(m_i\,\Delta L\,t]$$

for elements ΔL_i on source 1 and

$$P\,[M_2 \leq m_i] = \exp\,[-N'_2\,(m_1)\,\Delta A\,t$$

for elements ΔA_i on source 2. Since each point source is assumed to be independent of the occurences of events on the other point sources, the intersection probability P [PGA ≤ 0.20g] for each source 1 and 2 is found by the product of the individual element probabilities for each source: P [PGA ≤ 0.20g] due to source 1 is the product of all of the (i = 1, 2, 3) element probabilities $\exp\,[-N'_1\,(m_i)\,\Delta L\,t]$ and equals (because exponents are added), $\exp\,[-\Sigma N'_1\,(m_i)\,\Delta L\,t]$. Similarly P[PGA ≤ 0.20g] due to source 2 is $\exp\,[-\Sigma N'_2\,(m_i)\,\Delta A\,t]$. Finally since each source is independent of events that may occur on the other source, the total probability at the site is

$$P[PGA \leq 0.20g] = \underset{\text{Source 1}}{P[PGA \leq 0.20g]}\ \ \underset{\text{Source 2}}{P[PGA \leq 0.20g]}$$

and hazard P[PGA>0.20g] is 1 − P [PGA≤0.20g].

The complete set of calculations is shown in figure D-5.

f. Construction of the site hazard curve. The calculations as performed for PGA_j = 0.20g, are repeated to evaluate P [PGA > PGA_j] for successive incremented values of PGA_j such as (0.10g, 0.15g, 0.25g, and 0.30g). The site hazard curve is drawn through the plot of the calculated hazard values verses their respective PGA_j values, as shown in figure D-6.

Since this curve is for the exposure time of t = 50 years which corresponds to the exposure time for EQ-I, the spectral scaling value PGA_I for this level of ground motion can be taken directly from the curve at the 50 percent hazard value. The curve gives PGA_I = 0.23g.

g. Step V Site Specific Response Spectrum for EQ-I. The soil conditions correspond to those for the soil class 1 as defined in paragraph 3-6*f*(3). It is therefore judged that the Kiremidjian and Shah mean DAF shape in figure 3-35, for the soil class = 1, damping = 5% is appropriate for the site. Having the scaling PGA_I = 0.23g, the EQ-I acceleration response spectrum S_{aI} is found by multiplying the selected DAF shape by 0.23g. This S_{aI} is shown in figure D-6. It should also be mentioned that the ATC 3-06 response spectrum shape (para 3-8) for the soil type S_2, as scaled by the PGA_I = 0.23g, would have been suitable for this site.

D-3. Introduction for Computer Examples 2 and 3.

It is assumed that computer programs for seismic hazard analysis such as the Stanford Seismic Hazard Analysis = STASHA, are available for use. A complete flow chart describing the seismic hazard methodology is presented. This will be followed by numerical examples describing the separate stages of the model. It is important to note that computer programs must be available to conduct the probabilistic hazard analysis as outlined in paragraphs 3-3 through 3-5. Figure D-7 shows the general flow chart for seismic hazard analysis. Figure D-8 shows further subtasks within each of the three stages outlined in figure D-7. In most of the available computer programs, the plotting programs are usually system dependent. In the examples, it will be assumed that stage I, the raw data, has

Source 1. $\Delta L = 10$ km, $t = 50$ years

$$\ln N_1'(m) = 1.29 - 1.32\,m$$

Elem. i	m_i	$\ln N_1'(m)$	$N_1'(m) \times 10^4$	$N_1'(m) \cdot \Delta L \cdot t$
1	6.5	−7.29	6.82	0.341
2	6.7	−7.55	5.26	0.263
3	7.2	−8.21	2.72	0.136

$$\sum N_1'(m) \cdot \Delta L \cdot t = 0.740$$

$P[PGA \leq 0.20g]$ due to source 1.

$$= \exp\left[-\sum N_1'(m) \cdot \Delta L \cdot t\right] = \exp[-0.740] = \underline{\underline{0.477}}$$

Source 2. $\Delta A = 100$ sq km, $t = 50$ years

$$\ln N_2'(m) = -5.89 - 0.95\,m$$

Elem i	m_i	$\ln N_2'(m)$	$N_2'(m) \times 10^5$	$N_2'(m) \cdot \Delta A\, t$
1	5.0	−10.64	2.39	0.120
2	5.3	−10.93	1.79	0.090
3	5.7	−11.31	1.22	0.061
4	6.1	−11.68	0.85	0.043

$$\sum N_2'(m) \cdot \Delta A \cdot t = 0.314$$

$P[PGA \leq 0.20g]$ due to source 2.

$$= \exp\left[-\sum N_2'(m) \cdot \Delta A \cdot t\right] = \exp[-0.314] = \underline{\underline{0.731}}$$

$P[PGA \leq 0.20g]$ due to both sources

$$= (0.477)(0.731) = 0.349$$

$$\text{Hazard} = P[PGA > 0.20g] = 1 - 0.349 = \underline{\underline{0.651}}$$

US Army Corps of Engineers

Figure D–5. Probability calculations for event combinations giving the hazard P [PGA > 0.20g].

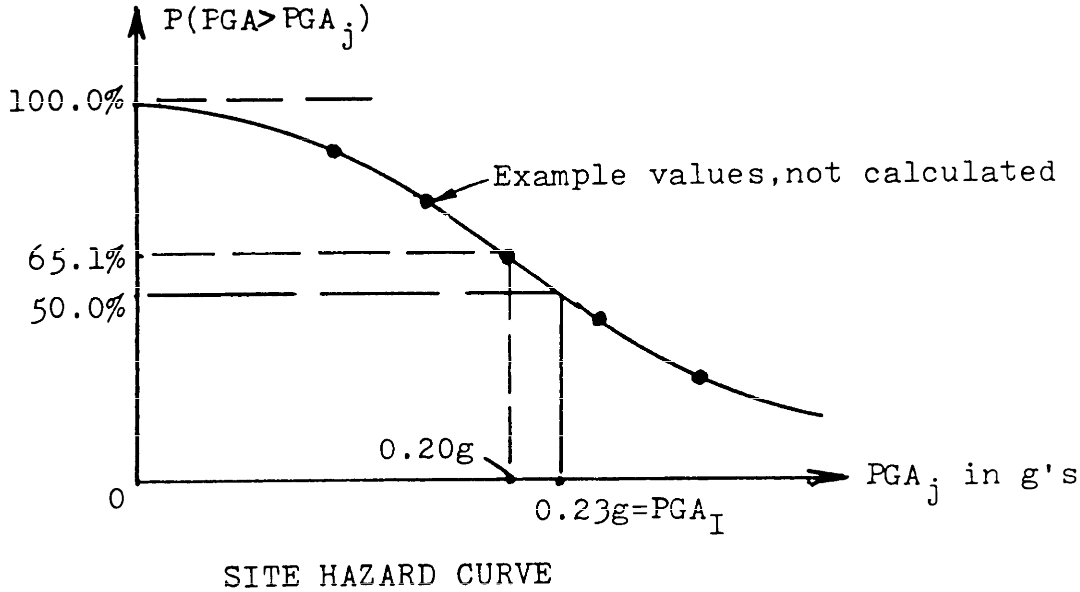

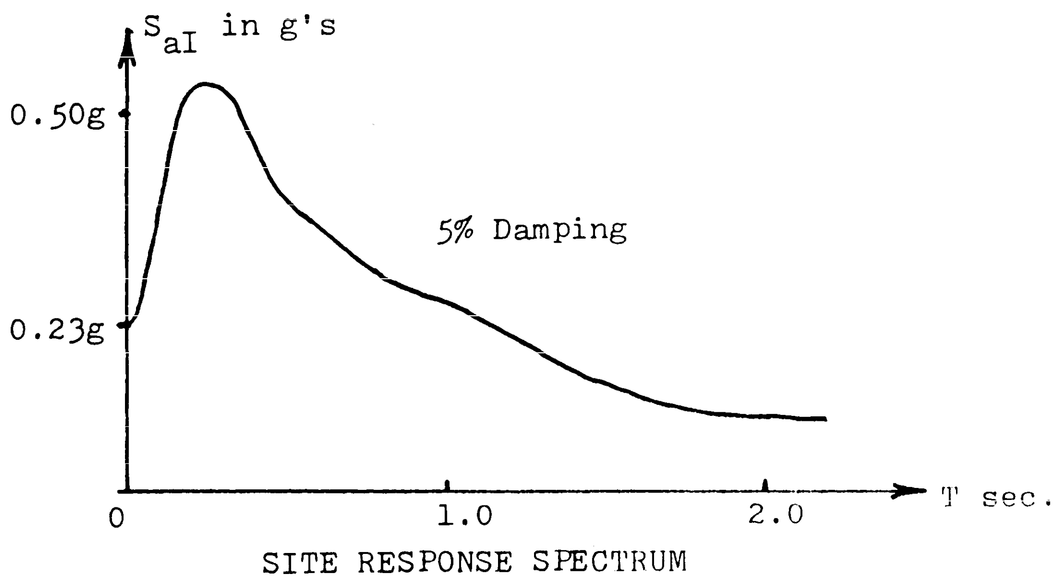

US Army Corps of Engineers

Figure D-6. Site hazard curve and scaled site spectrum for EQ-I.

already been treated and that the seismic sources of stage II have been identified; these correspond to step I of the hazard analysis. The next section will give an example of how one determines the recurrence relationship for the identified seismic sources; step II of the hazard analysis.

D-4. Example 2.

Figure D-9 shows a listing of earthquakes for a region between 1850 and 1967. There were 18 events with magnitudes between 3 and 5.5. The data base is for a 125 year time period. The format in which the data is read is given in section 6.3 of STASHA. A log-linear recurrence relationship of the form needs to be fitted to these data (Step II). The analyst does not wish to normalize with respect to the source length (or area) or the time period over which the data was available; (See para 3-4 for normalization). A magnitude increment of 0.2 is used to compute the cumulative histogram. It is assumed in this example that a single log-linear line will suffice to describe the source seismicity. An upper cutoff magnitude of 6.5 (which is obtained from geological considerations) is given for the source; (see para 3-3). Figure D-10 shows the output of the computer program which gives the recurrence relationship. The following nomenclature is used in figure D-10.

NBRC	=	Number of earthquake records used in the analysis.
AREA	=	Area or length of the seismic source under consideration. (In this example, it is shown as zero since normalization of α is not needed)
RMBK	=	Breakoff magnitude
X-Mean	=	Mean of the independent variable (Richter magnitude in this case)
Y-Mean	=	Mean of the dependent variable (number of earthquakes, log-scale)
XVAR	=	Variance of independent variable.
YVAR	=	Variance of dependent variable.
COVARXY	=	Covariance for X and Y.
VAR(LNNM)	=	Variance of the log to the base e of the cumulative number of occurrences.
STDV(LNNM)	=	Standard deviation of (LNNM).
CONF. VALUE	=	Value of t-student's distribution for the fitted line.
UPCNF	=	Value of upper confidence interval for a given RM.
DNCNF	=	Value of lower confidence interval for a given RM.

Figure D-11 shows the fitted recurrence line together with the data points and the confidence interval. Note that the regression line is extended beyond the last data point in order to intercept the cutoff magnitude line. In the above example, the RMBK, the breakpoint for the Richter magnitude was defined as zero; (See fig D-10). This indicates that only one single line was used to relate ln N(m) to m. Close examination of figure D-11 shows that the regression line does not fit well to the data. For example, for the magnitude range between 4 and 5, the fitted line underestimates the cumulative number of occurrences, and beyound the 5.0 magnitude the fitted line overestimates the cumulative number of occurrences. Thus, it seems reasonable to try a bi-linear fit with RMBK at 4.2. Figure D-12 shows the new output format and figure D-13 shows the bilinear fit. The resulting recurrence lines provide the mean number or rate of events equal to or above Richter magnitude m. This rate is used in the Poisson model (para 3-4) to estimate the probability of future activity for a given source (Step III).

D-5. Example 3.

In this example, the seismic hazard at a site in terms of probabilistic peak ground acceleration will be obtained. Figure D-14 shows a seismic region with two line sources and one area source. Occurrence data for each of the sources are given in figure D-15. The seismic sources were modelled after correlating past events to major fault systems and the tectonic features identified within the region (Step I). The future seismic exposure (PGA) for "CITY2" (see fig D-14) for a time period of 50 years is required. For this purpose, the following assumptions are made:

a. Past earthquake events (as recorded for the region) have been classified as shallow with hypocenters between 0 and 15km.

b. The average depth of the three seismic sources has been set equal to 10 km (0.087 degrees for the particular geographic location).

c. The length in degrees of the two line sources are, respectively:

Line Source 1 = 0.871°

Line Source 2 = 0.764°

These lengths have been obtained in the following manner:

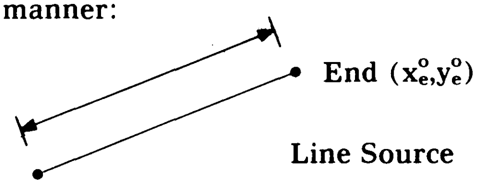

Origin (x_o^o, y_o^o) $L = \sqrt{(x_e^o - x_o^o)^2 + (y_e^o - y_o^o)^2}$

d. The radius (in degrees) of the area source is

$$R = 0.749°$$

and is defined as the distance from the centroid of the epicenters associated to the source to the most distant epicenter in the source.

e. From regression analysis the following recurrence coefficients have been obtained (Step II).

Line Source 1 (bi-linear recurrence relationship)

ALPHA1 = 2.58, BETA1 = -1.09, ALPHA2 = 24.00, BETA = -4.55

Cutoff magnitude = 6.8, breakpoint magnitude = 6.45

Line Source 2 (bi-linear recurrence relationship)

ALPHA1 = 3.17, BETA1 = -0.74, ALPHA2 = 79.15, BETA2 = -12.4

Cutoff magnitude = 7.8, breakpoint magnitude = 6.50

Area Source 1 (bi-linear recurrence relationship)

ALPHA1 = 0.14, BETA1 = -0.07, ALPHA2 = 79.90, BETA2 = -13.04

Cutoff magnitude = 6.5, breakpoint magnitude = 6.15

All alpha values have been normalized with respect to time t = 50 years and the length (in degrees) or area of source, and the resulting recurrence rates are used in the Poisson probability model (Step III).

f. The attenuation parameters b_1, b_2, b_3, and c in eq. 3–21 for PGA are as follows (Step IV):

b_1 = 0.00429937

b_2 = 0.800

b_3 = 2.000

c = 0.3673769

g. Coordinates for sources and site.

Line Source 1:	X-coordinate of origin = 30.50° (longitude)
	Y-coordinate of origin = 31.97° (latitude)
	X-coordinate or end = 30.92° (longitude)
	Y-coordinate or end = 32.62° (latitude)
Line Source 2:	X-coordinate of origin = 30.51° (longitude)
	Y-coordinate of origin = 31.75° (latitude)
	X-coordinate of end = 31.30° (longitude)
	Y-coordinate of end = 31.00° (latitude)
Area Source 1:	X-coordinate of center = 32.39° (longitude)
	Y-coordinate of center = 31.078° (latitude)
Site (City2):	X-coordinate = 32.00° (longitude)

h. The input data format is given in section 7–2 of STASHA. Figure D–16 shows the listing of the output program ACC.LINE.AREA (STASHA, 1979). The output contains the input parameters plus the probabilities of exceedance and non-exceedance for each discrete value of the ground parameter of interest (PGA discretized at 0.05g intervals) under the heading "Probability Distribution of Peak Ground Acceleration". Figure D–17 shows a plot of the complementary cumulative distribution function or hazard curve for the City 2. From figure D–16,

$$P(A < 0.10g) = 0.7512$$

Thus, for city 2, there is an approximately 75% chance of exceeding 0.10g at least once during the next 50 years, or 25% chance of not exceeding 0.10g during the same time period. Hence,

$$P(\text{zero exceedance of } 0.10g \text{ in } 50 \text{ years}) = 0.25$$

(1) From the binomial probability law, it is known that for independent trials with probability of success p at each trail, the probability of r successes in n trials is given by

$$P_n(r) = \binom{n}{r} p^r (1-p)^{n-r}$$

where $r = 0, 1, 2, \ldots, n$ and $\binom{n}{r} = \dfrac{n!}{r!\,(n-r)!}$

(2) Let each trial be a one-year duration for which we are observing the level of peak ground acceleration. Define success as that event when the peak ground acceleration for a given trial

(year) exceeds 0.10g. Thus, the probability of zero successes in 50 years is the same as the probability of zero successes in 50 trials. Hence,

$$P_{50}(o) = \binom{50}{o} p^{o} (1\text{-}p)^{50} = (1\text{-}p)^{50}$$

Then having

$$P_{50} = 0.25 = (1\text{-}p)^{50}$$

giving

$$p = 0.027$$

Therefore, for CITY2, there is a 2.7 percent chance that in any given year, a peak ground acceleration of 0.10g will be exceeded. The corresponding Return Period RP in "CITY2" for a peak ground acceleration of 0.10g is

$$1/0.027 = 37 \text{ years}$$

(3) Similarly, using the complementary cumulative distribution function computed for "CITY2", a table of peak ground acceleration and return period can be developed and plotted to obtain a curve referred to as an Acceleration Z one Graph (AZG). Table D–1 and figure D–18 show the values of Return Period versus PGA and the AZG for "CITY2." Using this figure D–18, the PGA_I for EQ-I would be approximately 0.12g (corresponding to a 72-year return period); and the PGA_{II} value for EQ-II would be 0.145g (corresponding to a 950 year return period). These PGA values for EQ-I and EQ-II are not very different in this example because the example site has relatively low seismicity and the three sources have low maximum magnitudes.

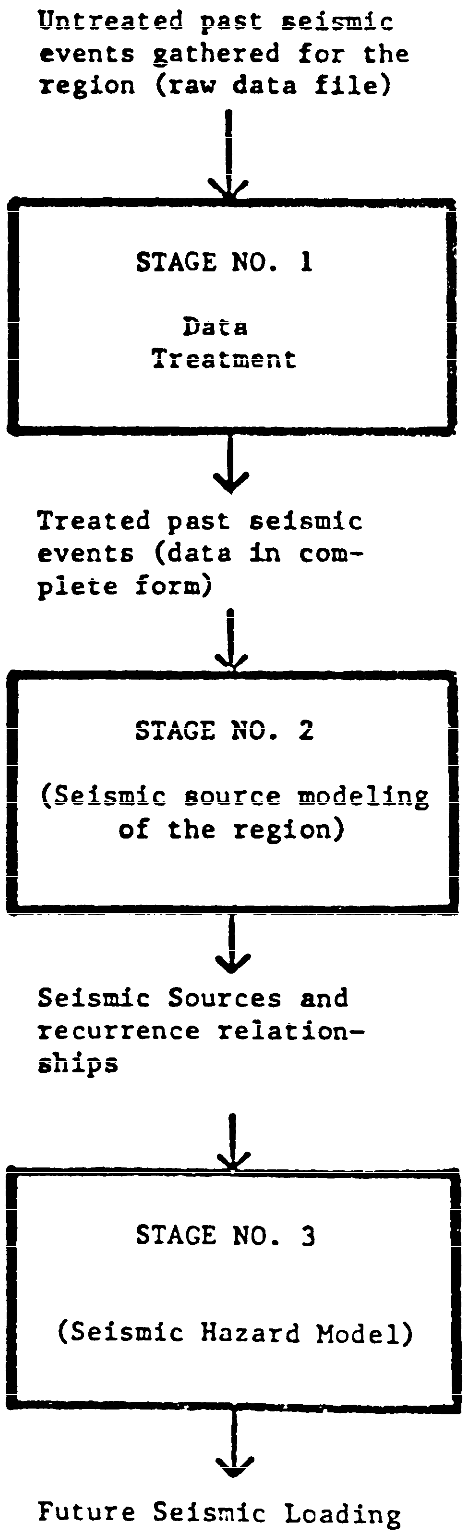

US Army Corps of Engineers

Figure D–7. Scheme of present seismic hazard methodology.

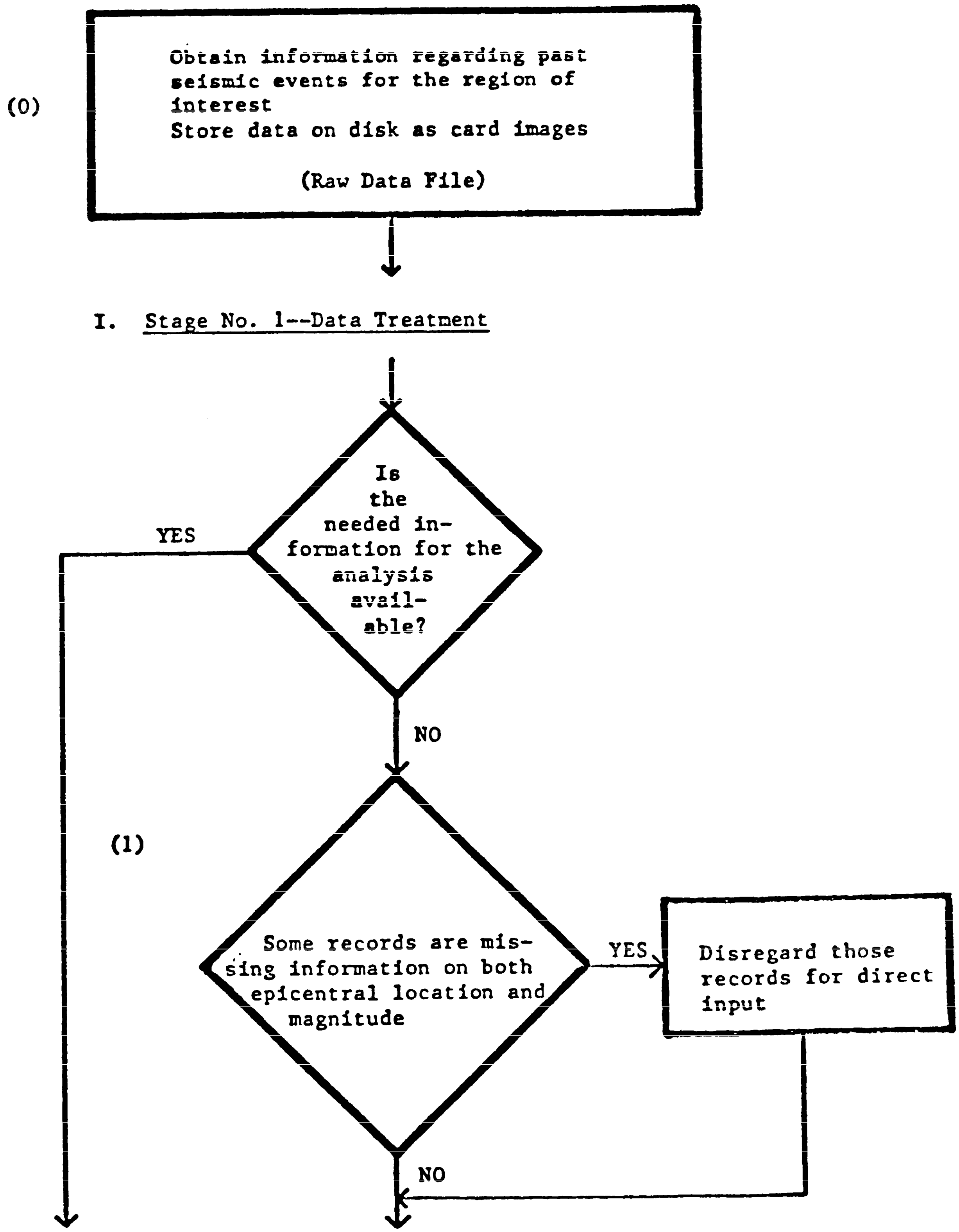

US Army Corps of Engineers

Figure D–8. General flow chart for seismic hazard analysis.

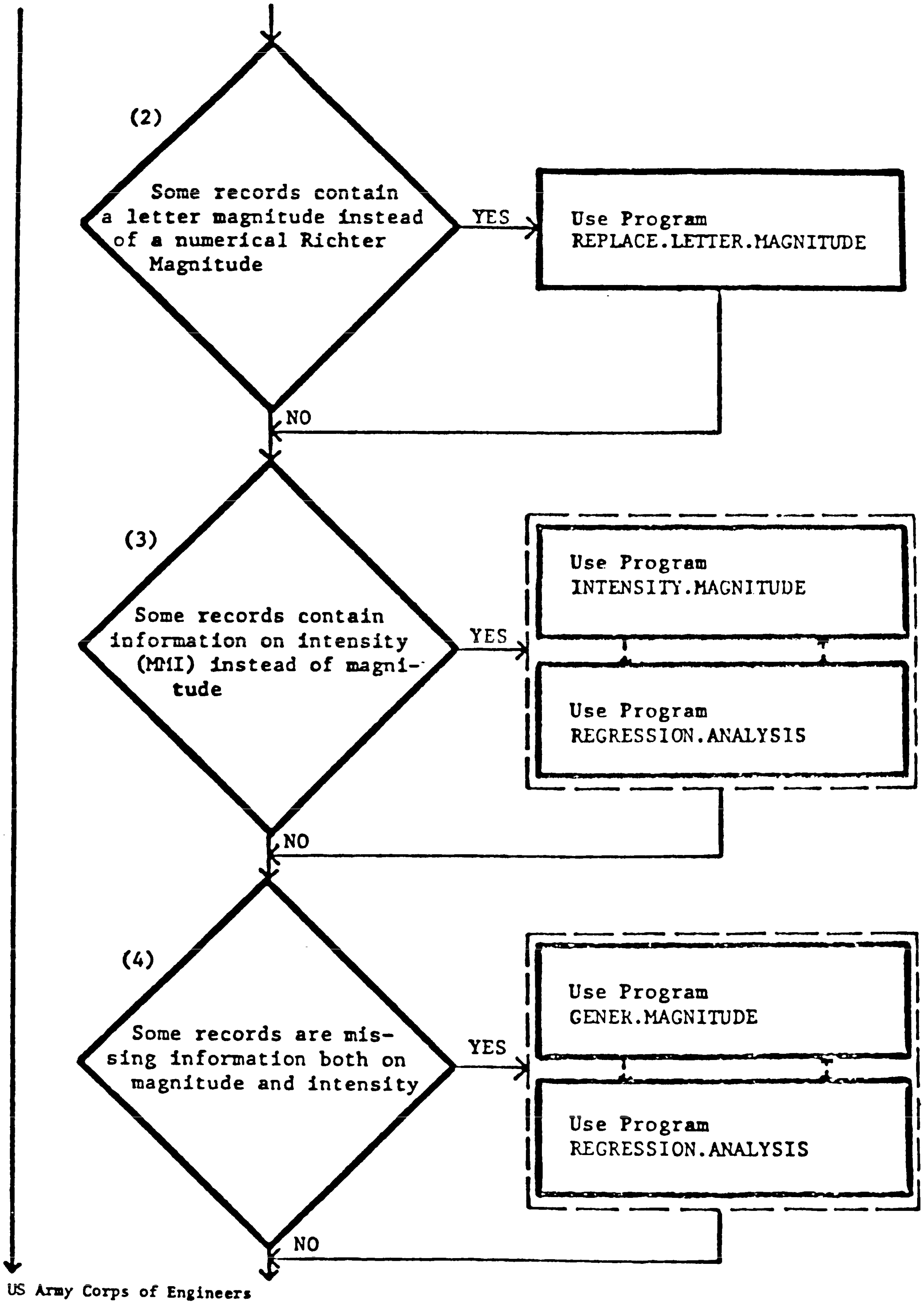

Figure D–8. General Flow Chart for Seismic Hazard Analysis—continued.

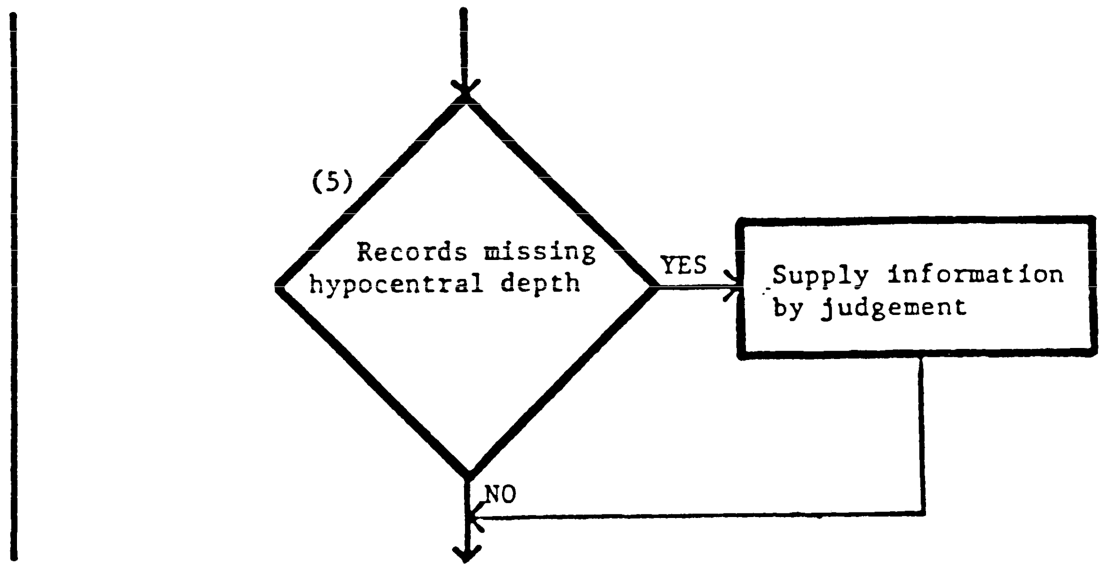

II. Stage No. 2--Seismic Modeling of the Region

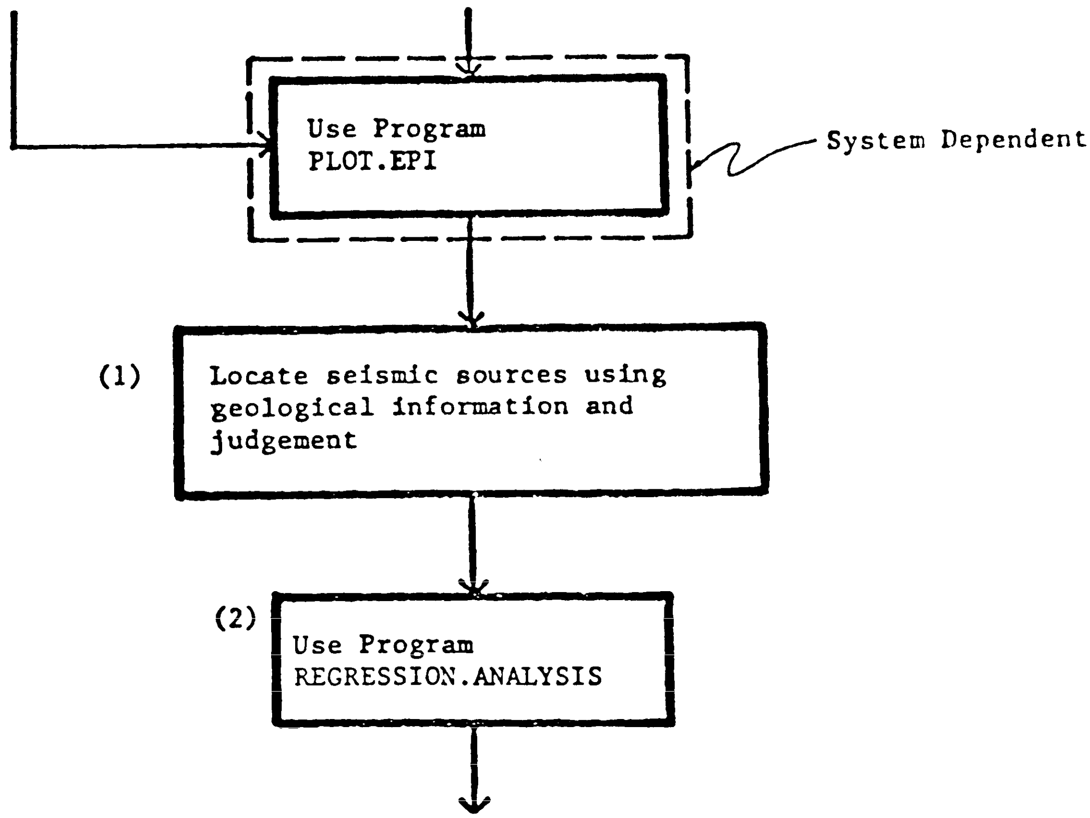

III. Stage No. 3--Seismic Hazard Model

US Army Corps of Engineers

Figure D–8. General Flow Chart for Seismic Hazard Analysis—continued.

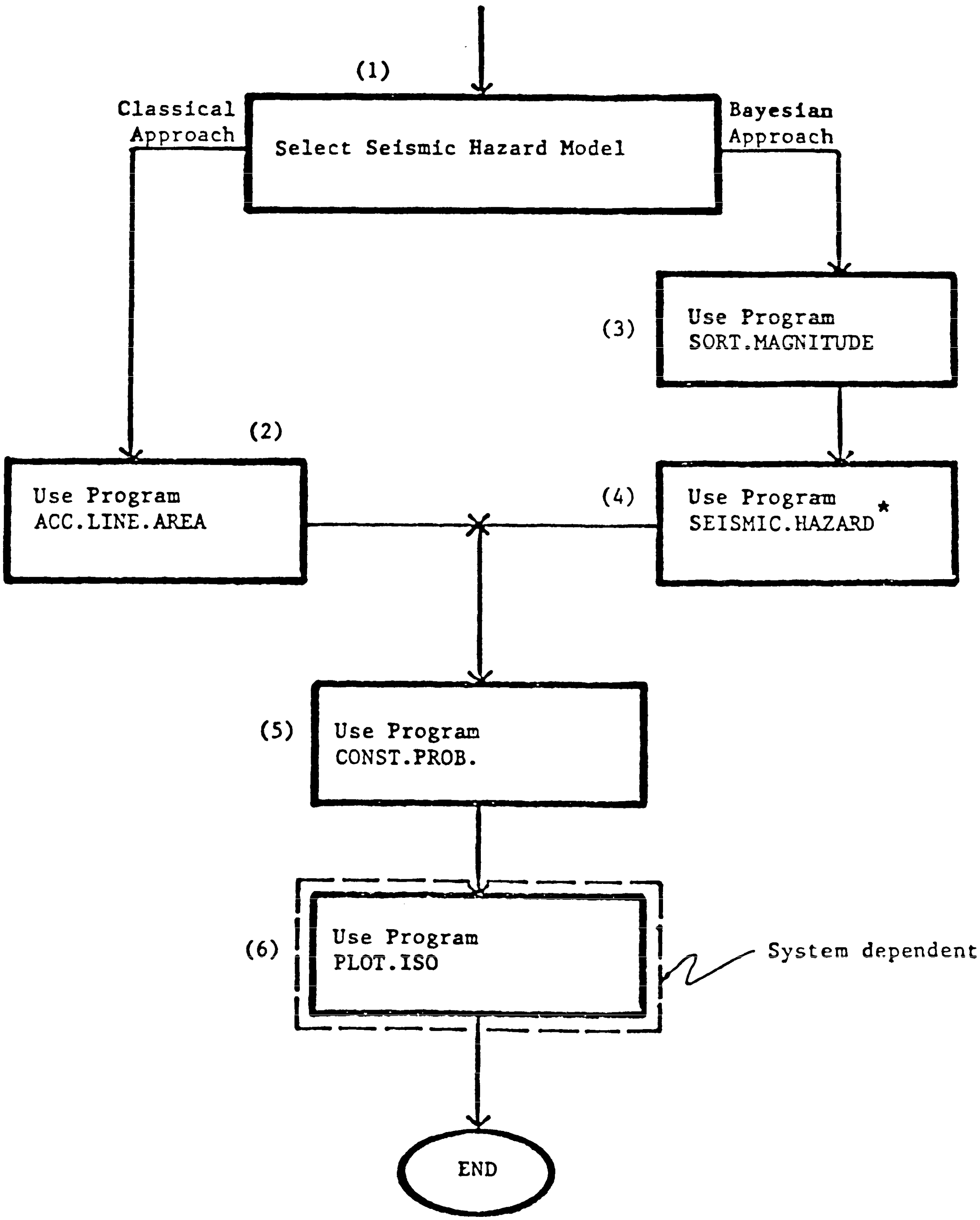

US Army Corps of Engineers

Figure D–8. General Flow Chart for Seismic Hazard Analysis—continued.

SOURCE	DAY	MONTH	YEAR	HOUR	MINUTE	LATITUDE	LONGITUDE	CLASS	MMI	RADIUS	DEPTH	MS	MB	MR1	MR2	SYMBOL
A.GRAN	17	12	1650	12	30	36.500N	07.400E		6.5					4.61	4.61	I
A.GRAN	17	06	1908	00	24	36.500N	07.500E		7.5					5.25	5.25	I
A.GRAN	04	08	1908	02	11	36.400N	06.600E	D	8.0					5.10	5.10	
A.GRAN	03	12	1928	05	30	36.400N	07.200E	D						5.00	5.00	
A.GRAN	10	02	1937	18	16	36.400N	07.500E	D	9.0					5.40	5.40	
A.GRAN	06	08	1947	09	46	36.300N	06.667E	D	8.5					5.30	5.30	
A.GRAN	27	10	1947	10	29	37.600N	08.500E	D	5.5						5.40	L
A.GRAN	22	11	1950	02	43	36.100N	07.200E	E	5.0						4.10	L
A.GRAN	01	04	1952	04	21	36.500N	07.300E	E	6.0					4.50	4.50	
A.GRAN	12	04	1952	16	23	36 500N	07.300E	E	5.5					4.20	4.20	
A.GRAN	23	05	1956	06	37	36.400N	07.300E	E	7.5						5.00	L
A.GRAN	26	06	1956	01	50	36.000N	08.100E	E	7.0						4.15	L
A.GRAN	02	09	1955	12	26	36.500N	07.400E	F	5.0						3.55	L
A.GRAN	14	11	1959	16	10	36.400N	07.500E	F	4.5						3.05	L
A.GRAN	05	03	1960	04	18	36.600N	07.100E	F	5.5						4.00	L
A.GRAN	02	12	1961	12	40	36.500N	08.200E							5.50	5.50	
A.GRAN	14	03	1963	12	25	36.200N	06.100E	E	7.0						4.40	L
A.GRAN	14	04	1967	23	44	36 500N	07.800E	E						4.30	4.30	

US Army Corps of Engineers

Figure D-9. Earthquake listing for example 2.

```
REGRESSION ANALYSIS
LINEAR-LN SCALE     NRC     AREA        RMOK
SAMPLE PROBLEM 1     18     0.0        4.200

NUMBER OF RECORDS INCLUDED     18
AREA                 0.0
TIME (YEARS)       125.00
MINIMUM MAGNITUDE                  3.00
MAGNITUDE INCREMENT FOR CDF        0.20
EARTHQUAKE MAGNITUDES
     4.60      5.20      5.10      5.00      5.40      5.30      5.40      4.10      4.50      4.20      5.00      4.10
     3.50      3.00      4.00      5.50      4.40      4.30
      RM          INTERVAL          CUMULATIVE FREQUENCY
    INTERVAL      FREQUENCY         OCCURRENCES ABOVE RM

   3.00 - 3.19       1                  18.          3.00
   3.20 - 3.39       0                  17.          3.20
   3.40 - 3.59       1                  17.          3.40
   3.60 - 3.79       0                  16.          3.60
   3.80 - 3.99       0                  16.          3.80
   4.00 - 4.19       3                  16.          4.00
   4.20 - 4.39       2                  13.          4.20
   4.40 - 4.59       2                  11.          4.40
   4.60 - 4.79       1                   9.          4.60
   4.80 - 4.99       0                   8.          4.80
   5.00 - 5.19       3                   8.          5.00
   5.20 - 5.39       2                   5.          5.20
   5.40 - 5.59       3                   3.          5.40
TWO STRAIGHT LINES WILL BE USED TO FIT THE DATA
BREAK POINT MAGNITUDE    4.20
    7 POINTS IN THE FIRST LINE
    7 POINTS IN THE SECOND LINE
INTERCEPT AND SLOPE OF LINE    1
 STATISTICS FORM REGRESSION LINE SEGMENT =  1
X-MEAN=    3.57999     Y-MEAN=    2.77707     XVAR=    0.16003     YVAR=    0.00918
COVARXY=   -0.03307     COEFF. OF VAR.=    0.74502     VAR(LNNM)=    0.00328     STDV(LNNM)=    0.05723

ALPHA  3.521115
BETA  -0.206679
INTERCPT AT 3.          5.        6.        7.
        18.19374  12.03300   9.70686   7.95946
INTERCEPT AND SLOPE OF LINE    2
 STATISTICS FORM REGRESSION LINE SEGMENT =  2
X-MEAN=    4.79999     Y-MEAN=    2.00306     XVAR=    0.16003     YVAR=    0.21342
COVARXY=   -0.17410     COEFF. OF VAR.=    0.88750     VAR(LNNM)=    0.03361     STDV(LNNM)=    0.18334

ALPHA  7.225738
BETA  -1.037904
INTERCPT AT 3.          5.        6.        7.
        52.56635   5.96714   2.01046   0.67737
INTERSECTION POINT
MAGNITUDE      4.20
LN OF N        2.65
```

US Army Corps of Engineers

Figure D–10. Output for recurrence relationship, example 2.

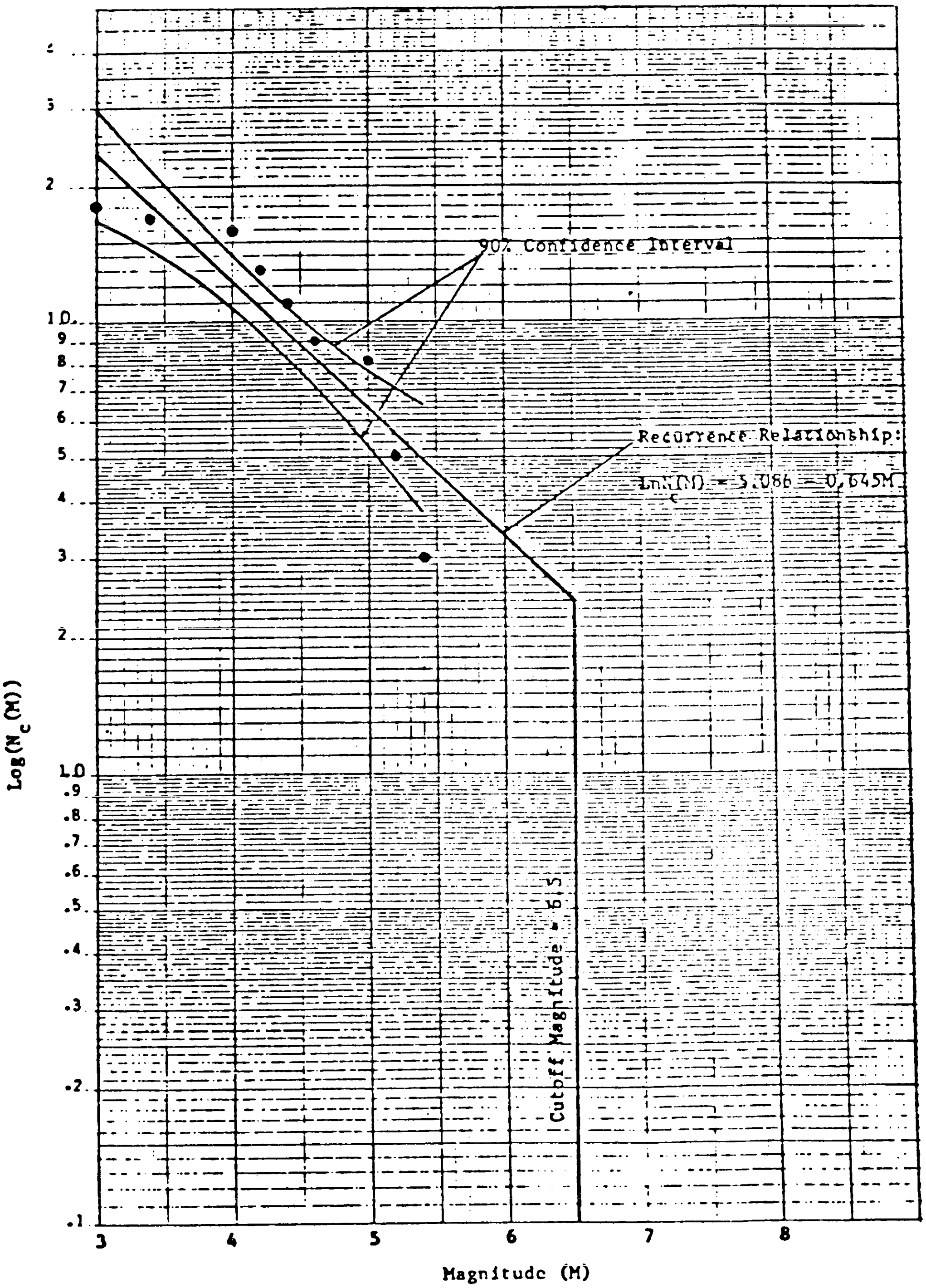

US Army Corps of Engineers

Figure D–11. Recurrence relationship for example 2.

```
REGRESSION ANALYSIS
LINEAR-LN SCALE      NBRC    AREA      RMDK
SAMPLE PROBLEM 1      18     0.0       0.0

NUMBER OF RECORDS INCLUDED    18
AREA              0.0
TIME (YEARS)     125.00
MINIMUM MAGNITUDE                  3.00
MAGNITUDE INCREMENT FOR CDF        0.20
EARTHQUAKE MAGNITUDES
      4.60      5.20      5.10      5.00      5.40      5.30      5.40      4.10      4.50      4.20      5.00      4.10
      3.50      3.00      4.00      5.50      4.40      4.30
      RM           INTERVAL          CUMULATIVE FREQUENCY
    INTERVAL       FREQUENCY         OCCURRENCES ABOVE RM

   3.00 - 3.19       1                    18.        3.00
   3.20 - 3.39       0                    17.        3.20
   3.40 - 3.59       1                    17.        3.40
   3.60 - 3.79       0                    16.        3.60
   3.80 - 3.99       0                    16.        3.80
   4.00 - 4.19       3                    16.        4.00
   4.20 - 4.39       2                    13.        4.20
   4.40 - 4.59       2                    11.        4.40
   4.60 - 4.79       1                     9.        4.60
   4.80 - 4.99       0                     8.        4.80
   5.00 - 5.19       3                     8.        5.00
   5.20 - 5.39       2                     5.        5.20
   5.40 - 5.59       3                     3.        5.40
INTERCEPT AND SLOPE OF LINE     1
 STATISTICS FORM REGRESSION LINE SEGMENT =  1
X-MEAN=    4.19999     Y-MEAN=    2.37704     XVAR=     0.56004     YVAR=    0.27831
COVARXY=   -0.36135     COEFF. OF VAR.=    0.83776     VAR(LNNM)=    0.05336     STDV(LNNM)=    0.23100

ALPHA  5.036937
BETA  -0.645227
INTERCPT AT 3.        5.       6.        7.
       23.36659   6.42923   3.37241   1.76898
   90 %  CONFIDENCE INTERVALS

 CONF. VALUE=    2.20098      ERROR INDIC.=     0

X =         3.000      3.200      3.400      3.600      3.800      4.000      4.200      4.400      4.600      4.800
UPCNF=     30.502     25.987     22.190     19.009     16.363     14.103     12.404     10.957      9.765      8.764
DNCNF=     17.930     16.231     14.605     13.243     11.885     10.592      9.356      8.183      7.093      6.105
X =         5.000      5.200      5.400
UPCNF=      7.903      7.150      6.493
DNCNF=      5.230      4.466      3.805
```

US Army Corps of Engineers

Figure D-12. Output for bilinear recurrence relationship, example 2.

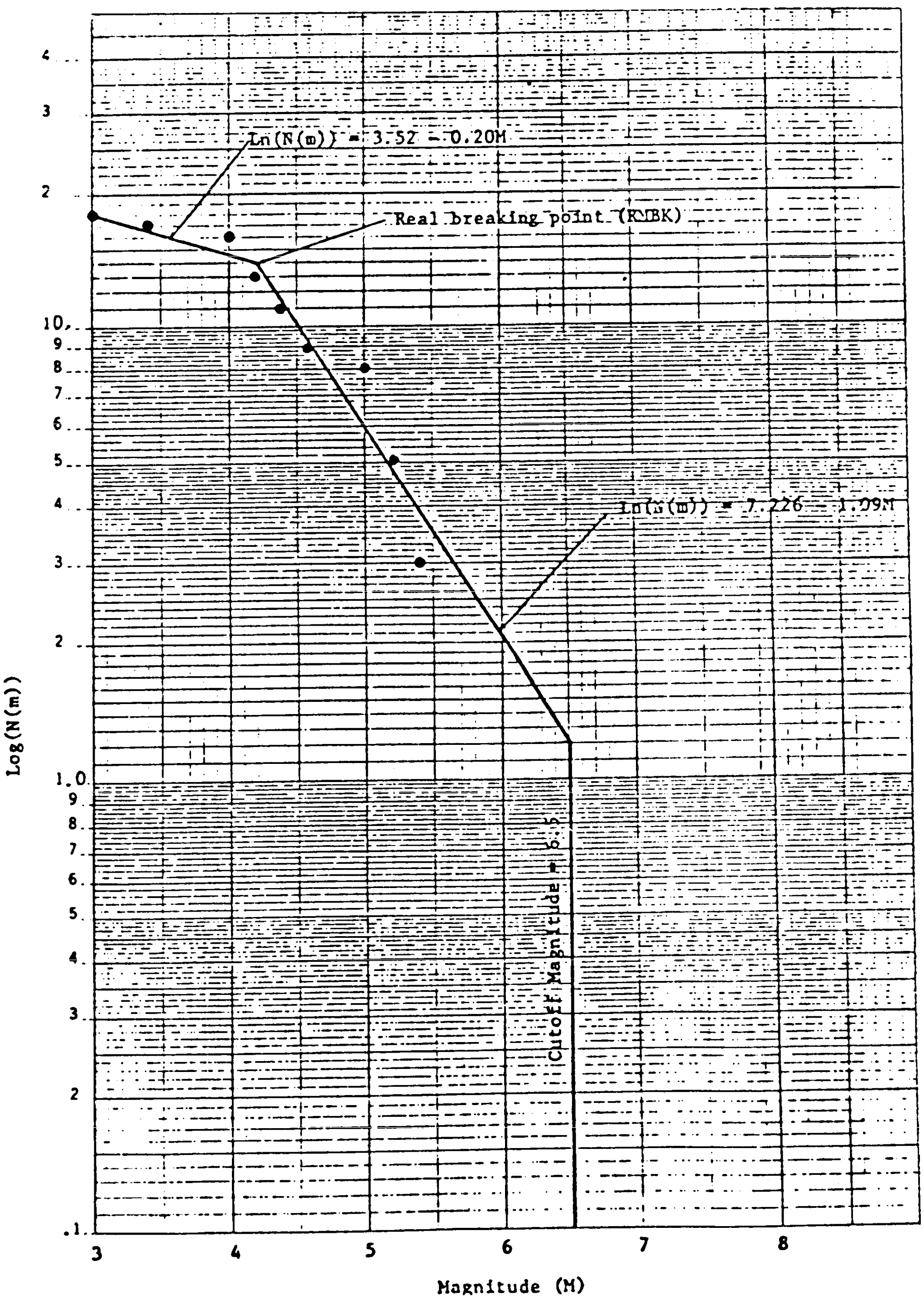

Figure D-13. Bilinear recurrence relationship for example 2.

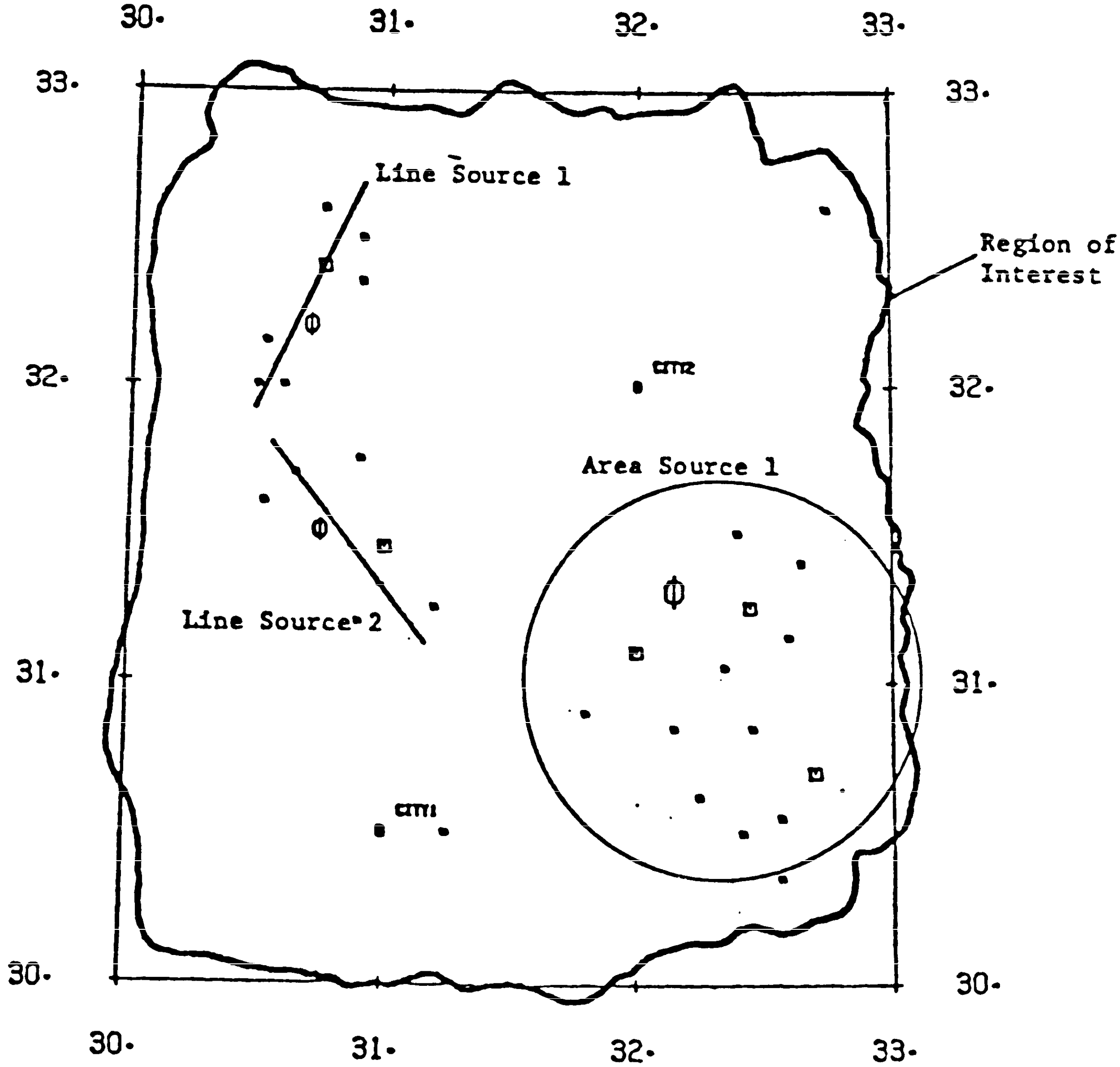

o Magnitude 4+
o Magnitude 5+
Ø Magnitude 6+
Ø Magnitude 7+

Plot of epicenters (sample problem)

US Army Corps of Engineers

Figure D–14. Seismic sources for region of example 3.

EARTHQUAKE DATA SORTED BY SOURCES

SOURCE	DAY	MONTH	YEAR	HOUR	MINUTE	LATITUDE	LONGITUDE	CLASS	MMI	RADIUS	DEPTH	MS	MB	MR1	MR2	SYMBOL
LINE SOURCE 1 (8 RECORDS)																
A.GRAN	02	03	1900	07	00	32.600N	30.750E							3.50	3.50	
A.GRAN	03	05	1902	05	00	32.500N	30.900E							3.75	3.75	
A.GRAN	05	03	1905	01	00	32.350N	30.900E							4.75	4.75	
A.GRAN	05	03	1912	02	00	32.000N	30.500E							3.25	3.25	
A.GRAN	08	01	1920	02	30	32.200N	30.700E							6.00	6.00	
A.GRAN	04	03	1965	09	30	32.000N	30.600E							4.65	4.65	
A.GRAN	03	08	1973	08	30	32.400N	30.750E							5.00	5.00	
A.GRAN	06	04	1976	05	00	32.150N	30.530E							3.25	3.25	
LINE SOURCE 2 (9 RECORDS)																
A.GRAN	04	09	1916	01	00	31.600N	30.530E							3.50	3.50	
A.GRAN	06	08	1921	09	10	31.700N	30.650E							4.50	4.50	
A.GRAN	04	01	1935	15	30	31.450N	31.000E							5.55	5.55	
A.GRAN	10	08	1937	01	15	31.200N	30.900E							3.60	3.60	
A.GRAN	04	12	1940	03	00	31.250N	31.200E							4.10	4.10	
A.GRAN	12	01	1972	11	05	31.750N	30.900E							4.65	4.65	
A.GRAN	11	05	1975	01	15	31.500N	30.750E							6.30	6.30	
A.GRAN	01	03	1976	08	12	30.500N	31.250E							3.50	3.50	
A.GRAN	01	07	1978	03	15	30.500N	32.420E							4.25	4.25	
AREA SOURCE 1 (15 RECORDS)																
A.GRAN	17	02	1923	08	00	31.050N	32.350E							4.35	4.35	
A.GRAN	16	01	1925	14	00	30.700N	32.700E							5.60	5.60	
A.GRAN	30	11	1925	12	15	31.500N	32.400E							3.50	3.50	
A.GRAN	14	02	1948	01	00	31.250N	32.450E							5.60	5.60	
A.GRAN	13	04	1950	13	30	31.150N	32.600E							3.80	3.80	
A.GRAN	18	11	1951	02	15	31.300N	32.150E							7.00	7.00	
A.GRAN	15	06	1954	06	35	31.100N	32.000E							5.60	5.60	
A.GRAN	02	12	1958	06	15	30.900N	31.800E							3.00	3.00	
A.GRAN	18	01	1960	04	18	30.620N	32.250E							4.85	4.85	
A.GRAN	01	01	1968	13	14	30.550N	32.570E							3.40	3.40	
A.GRAN	04	10	1969	02	00	30.850N	32.150E							3.15	3.15	
A.GRAN	03	12	1970	10	12	30.350N	32.570E							3.00	3.00	
A.GRAN	17	03	1972	13	05	30.850N	32.460E							4.50	4.50	
A.GRAN	08	11	1973	15	00	32.600N	32.750E							3.50	3.50	
A.GRAN	16	10	1976	10	00	31.400N	32.650E							3.65	3.65	

US Army Corps of Engineers

Figure D–15. Earthquake listing for sources in example 3.

```
PROGRAM ACC.LINE.AREA (SAMPLE PROBLEM)
ATTENUATION CONSTANTS

B1=  0.4299370D-03   B2=  0.8000000D+00   B3=  0.2000000D+01   B4=  0.3673769D+00
DELTAL =  0.5000000D-01   DELTAC =  0.5000000D-01

TIME PERIODS
     50.00
ACCELERATIONS
      0.05      0.10      0.15      0.20      0.25      0.30      0.35      0.40      0.45      0.50
      0.55      0.60      0.65      0.70      0.75      0.80
LINE SOURCES
************

LINE SOURCE 1
  ALPHA1           BETA1            XL1            XL2            YL1            YL2            HL
  0.25600D+01  -0.10900D+01   0.30500D+02   0.30920D+02   0.31970D+02   0.32620D+02   0.87000D-01
SECOND REGRESSION CONSTANTS
  ALPHAL2          BETAL2           MR
  0.24000D+02  -0.45500D+01   0.64500D+01   0.68000D+01
LINE SOURCE 2
  ALPHA1           BETA1            XL1            XL2            YL1            YL2            HL
  0.31700D+01  -0.74000D+00   0.30510D+02   0.31300D+02   0.31750D+02   0.31000D+02   0.87000D-01
SECOND REGRESSION CONSTANTS
  ALPHAL2          BETAL2           MR
  0.79150D+02  -0.12400D+02   0.65000D+01   0.76000D+01


AREA SOURCES
************

AREA SOURCE 1
  ALPHA1           BETA1            X0             Y0             R              HA
  0.14000D+00  -0.70000D-01   0.32390D+02   0.31078D+02   0.74900D+00   0.87000D-01
SECOND REGRESSION CONSTANTS
  ALPHA2           BETA2            MR
  0.79900D+02  -0.13040D+02   0.61500D+01   0.65000D+01
********** P R O B A B I L I T Y   D I S T R I B U T I O N   O F   P E A K   G R O U N D   A C C E L E R A T I O N
***


SITE OF INTEREST (CITY 2)
GEOMETRIC CONSTANTS

NL=    2    NA =     1    NXMAX=     1    NYMAX=    1    NT=    1

SITE LOCATION
X=     32.000     Y=     32.060
TIME PERIOD =  50.00 YRS
PGA =       0.0500   0.1000   0.1500   0.2000   0.2500   0.3000   0.3500   0.4000   0.4500   0.5000
P(Y>Y0)     1.0000   0.7512   0.0043   0.0      0.0      0.0      0.0      0.0      0.0      0.0
P(Y<Y0)     0.0030   0.2488   0.9957   1.0000   1.0000   1.0000   1.0000   1.0000   1.0000   1.0000
PGA =       0.5500   0.6000   0.6500   0.7000   0.7500   0.8000
P(Y>Y0)     0.0      0.0      0.0      0.0      0.0      0.0
P(Y<Y0)     1.0000   1.0000   1.0000   1.0000   1.0000   1.0000
```

US Army Corps of Engineers

Figure D–16. Output for recurrence relationships and site PGA probability distribution for example 3.

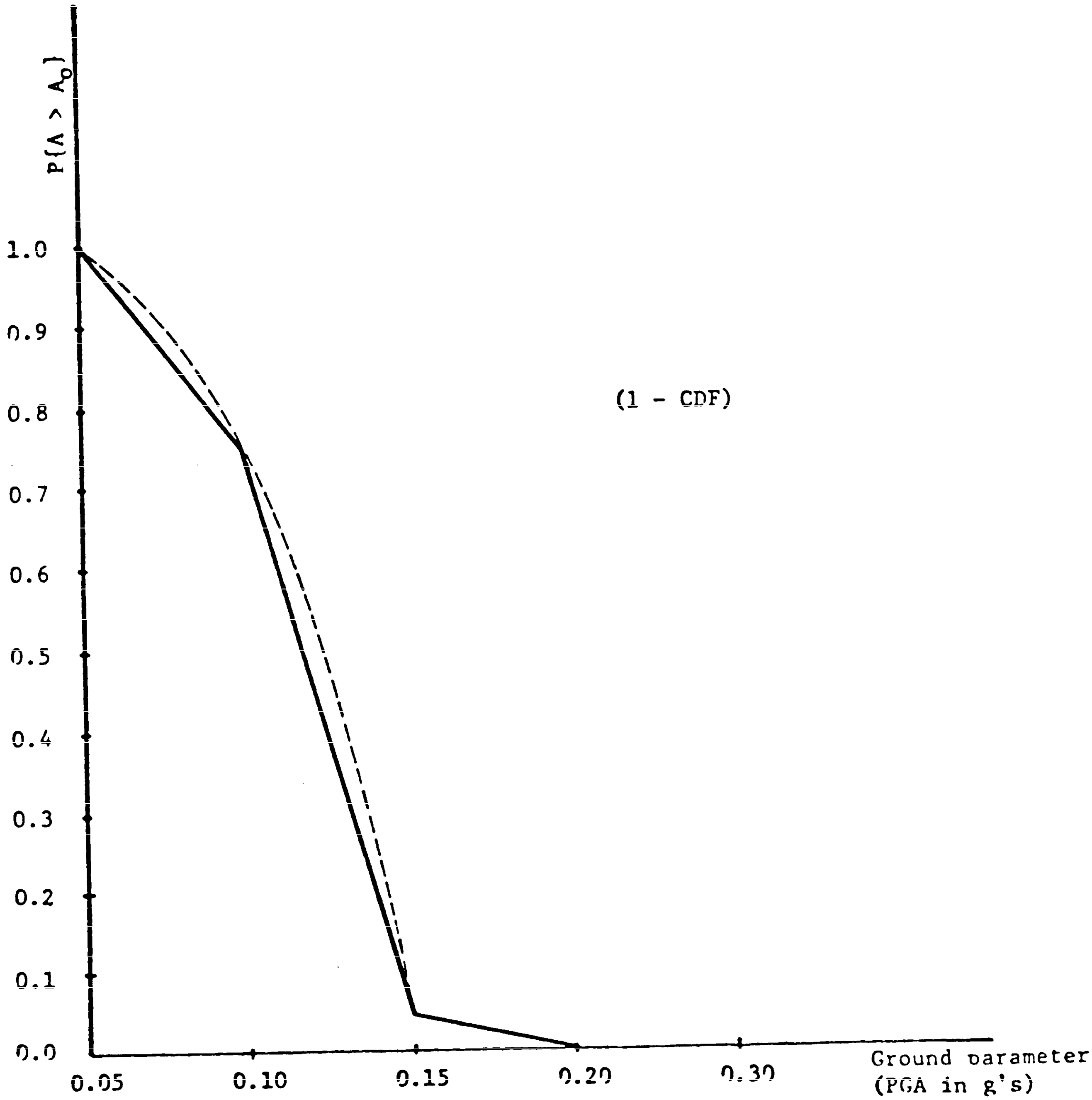

US Army Corps of Engineers

Figure D-17. Complementary cumulative distribution function for example 3.

Table D–1. Return period vs. PGA for CITY 2.

PGA in g units	Return Period in Years
0.06	18
0.075	23
0.100	37
0.110	63
0.120	87
0.130	141
0.140	358
0.150	10000

US Army Corps of Engineers

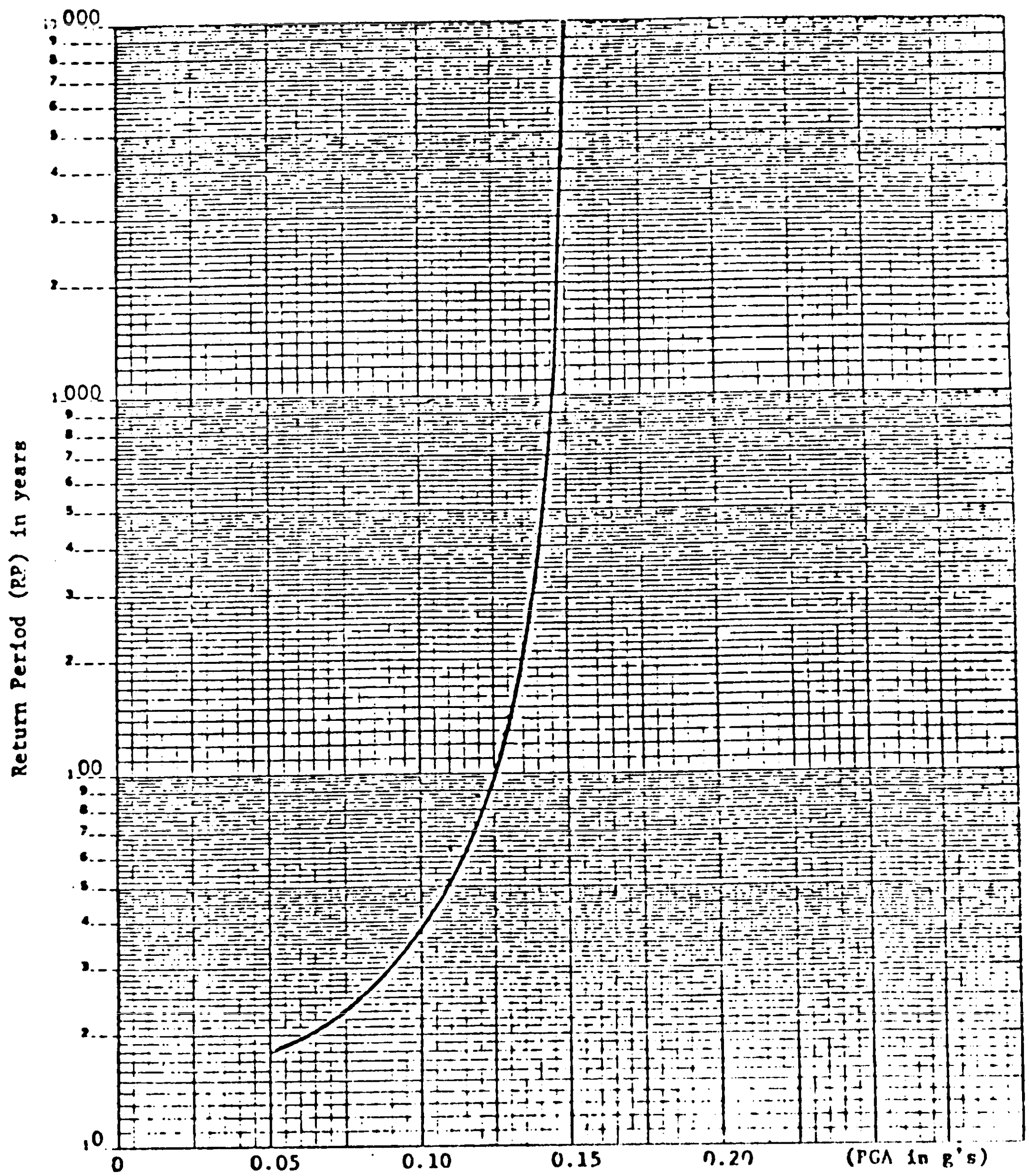

US Army Corps of Engineers

Figure D-18. Acceleration zone graph (AZG) for CITY 2.

APPENDIX E
DESIGN EXAMPLES—STRUCTURES

E–1. Purpose and scope.

This appendix gives illustrative examples for designing and analyzing various types of lateral systems in accordance with the criteria and procedures of chapters 4 and 5 of this manual.

E–2. Use of appendix.

The design examples are purely advisory; they are not intended to place super-restrictions on the manual. This appendix is not a handbook for the inexperienced designer. Neither the manual or the manual supplemented by the appendices can replace good engineering judgment in specific situations. Designers are urged to study the entire manual.

Table E–1. Design Examples—Structures

Fig. No.	*Example No. and Description*
E–1	E–1 Sample modal analyses.
E–2	E–2 Box system. A 2-story building with bearing walls in concrete using a series of interior, vertical-load-carrying columns and girder bents.
E–3	E–3 Steel ductile moment-resisting space frame and steel braced frame. A 3-story building with transverse ductile moment-resisting frames and longitudinal frames with K-bracing.
E–4	E–4 Concrete ductile moment-resisting space frame. A 7-story building with a complete ductile moment-resisting space frame in concrete without shear walls.

DESIGN EXAMPLE: E-1

SAMPLE MODAL ANALYSES:

Purpose. This example is presented to illustrate the method of obtaining story forces, accelerations, and displacements from given building characteristics and ground motion response spectra. The results are shown in a format similar to the sample format used in the equivalent static force procedure of the Basic Design Manual, table 4-4. Thus, a comparison of static force procedures and dynamic analysis procedures can be made. The data in this example serve as a back-up for the examples given in paragraph 2-5c of this manual. The results are graphically displayed in figures 2-9 and 2-10 of this manual.

Description of Structure. The data on sheets 3 through 6 are based on the characteristics of a 7-story reinforced concrete moment-resisting space frame building. Sheet 7 represents a 30-story building. The model for this building was developed by expanding the 7-story building characteristics. Each story mass (w/g) of the 30-story building lumped mass model was assumed to represent 4 stories similar to those of the 7-story building (i.e., the indicated story plus one-and-one-half stories above and below). This was done only for illustrative purposes to demonstrate the influences of higher modes of vibration for taller buildings with longer periods of vibration (refer to para 2-5c(3)).

Response Spectrum. The modal analyses were performed on the basis of the 5-percent damped response spectrum shown in figure 2-8 of this manual.

Masses, Mode Shapes, and Periods. Story masses were obtained from the calculated story weights of the building. A mathematical model of the building was developed from the section properties of the structural system. The building was modeled as a series of two-dimensional frames. A computer program that analyzes two-dimensional framing systems was used to determine the periods and mode shapes of the first three modes of vibration. In this computer program, each mode is normalized for $\Sigma(w/g)\phi^2 = 1.0$. The mode shapes are shown in figure 2-6 of this manual. In figure 2-6, the modes are normalized to a value of 1/2-inch at the top story.

US Army Corps of Engineers

Example E-1 1 of 7 Sample Modal Analyses

Figure E-1. Sample modal analysis.

Modal Analysis to Determine Total Base Shear and Story Accelerations. Sheet 3 illustrates a hand-calculation procedure to determine the total base shear and the story accelerations using mass, mode shape, period, and response spectrum data. Equations 4-1 and 4-2 are used to determine the participation factors. The spectral acceleration (S_a) for the period (T) of each mode is determined from the response spectrum. The story accelerations (a) are determined from equation 6-1 and the base shears (V) are determined from equation 4-4. The sum of the participation factors (P.F. and α) add up to 1.08 and 0.986, respectively. These values being close to the value of 1.0 indicate that most of the model participation is included in the three modes considered in this example (refer to paras 4-3c(1)(b) and 5-4c(2)). The story accelerations and the base shears are combined by the square-root-of-the-sum-of-the-squares (SRSS) on the last column of the table. The modal base shears are 2408 kips, 632 kips, and 200 kips for the first, second, and third modes, respectively. These are used on the following sheets to determine story forces. The SRSS base shear is 2498 kips.

Story Forces, Accelerations, and Displacements. Sheets 4, 5, and 6 are set up in a manner very similar to the Basic Design Manual, table 4-4. In the static lateral force procedure, wh/Σwh is used to distribute the force on the assumption of a straight line mode shape. In the dynamic analysis, the more representational $w\phi/\Sigma w\phi$ is used to distribute the forces for each mode. Story shears and overturning moments are determined in the same manner for each method. Modal story accelerations are determined by dividing the story force by the story weight. These are essentially the same values as shown on sheet 3 (slight differences are due to rounding off). The SRSS of the accelerations of sheet 3 are roughly estimated in the static procedure by the bracketed quantity in equation 3-9 of the Basic Design Manual and are listed in the last column of table 4-4 in that manual. Modal story displacements (δ) are calculated from the accelerations and the period (equations 4-5 and 6-1 of this manual). Modal interstory drifts ($\Delta\delta$) are calculated by taking the differences between the δ values of adjacent stories. The values shown on sheets 4, 5, and 6 of this design example are summarized in table 5-3 and are plotted with the SRSS combination in figure 2-10.

Thirty-Story Example. Sheet 7 shows the model analysis for base shears and story accelerations for the 30-story example. This parallels the 7-story example on sheet 3. Parallel tables for sheets 4, 5, and 6 are not shown, but the results are summarized in figure 2-9.

US Army Corps of Engineers

Example E-1	2 of 7	Sample Modal Analyses

Figure E-1. Sample modal analysis—continued.

7 STORY REINFORCED CONCRETE FRAME BUILDING

Mathematical Model - Gross Concrete Sections, Spandrel Beams increased 50% for Slab participation.
Periods (T) and Mode Shapes (ϕ) have been calculated by a two-dimensional computer program.
Spectral Accelerations for 3 modes obtained from Response Spectrum

GIVEN: Masses (w/g), ϕ's, T's, S_a's.
REQ'D: Story Accelerations (a) and Base Shear Forces (V)

LEVEL	$\frac{w}{g}$ $\left(\frac{k\text{-}s^2}{ft}\right)$	MODE 1 ϕ_1	$\frac{w}{g}\phi_1$	$\frac{w}{g}\phi_1^2$	a_1 (g)	MODE 2 ϕ_2	$\frac{w}{g}\phi_2$	$\frac{w}{g}\phi_2^2$	a_2 (g)	MODE 3 ϕ_3	$\frac{w}{g}\phi_3$	$\frac{w}{g}\phi_3^2$	a_3 (g)	SRSS a_x (g)
Roof	43.78	.0794	3.48	.276	0.362	.0747	3.27	0.244	-0.235	.0684	2.99	0.205	0.120	0.448
7	45.34	.0745	3.38	.252	0.340	.0411	1.86	0.076	-0.129	-.0040	-.18	0.001	-0.007	0.364
6	45.34	.0666	3.02	.201	0.304	-.0042	-.19	0.001	0.013	-.0644	-2.92	0.188	-0.113	0.325
5	45.34	.0558	2.53	.141	0.254	-.0471	-2.14	0.101	0.148	-.0630	-2.86	0.180	-0.111	0.314
4	45.34	.0425	1.93	.082	0.194	-.0718	-3.26	0.234	0.226	-.0023	-.10	0.000	-0.004	0.298
3	45.34	.0279	1.27	.035	0.127	-.0697	-3.16	0.220	0.219	.0604	2.74	0.166	0.106	0.275
2	56.83	.0149	0.85	.013	0.068	-.0467	-2.65	0.124	0.147	.0677	3.85	0.261	0.119	0.201
1	—	0	0	0	0	0	0	0	0	0	0	0	0	0
Σ	327.31		16.46	1.000			-6.27	1.000			3.52	1.001		
PF_{roof}	(Eq. 4-1)	$\frac{16.46}{1.000}(.0794) = 1.31$				$\frac{-6.27}{1.000}(.0747) = -0.47$				$\frac{3.52}{1.001}(.0684) = 0.24$				$\Sigma = 1.08$
α	(Eq. 4-2)	$\frac{(16.46)^2}{(327.31)(1.000)} = 0.828$				$\frac{(-6.27)^2}{(327.31)(1.000)} = 0.120$				$\frac{(3.52)^2}{(327.31)(1.001)} = 0.038$				$\Sigma = .986$
T		0.880 sec.				0.288 sec.				0.164 sec.				
S_a		0.276 g				0.500 g				0.500 g				
a_{roof}	(Eq. 6-1)	(1.31)(0.276) = 0.362 g				(-0.47)(0.500) = -0.235 g				(0.24)(0.500) = 0.120 g				0.448
V	(Eq. 4-4)	(.828)(.276)(10,539) = 2,408 kips				(0.12)(.500)(10,539) = 632 kips				(.038)(.500)(10,539) = 200 kips				2498 k
V/W		0.229				0.060				0.019				0.237

$W = \Sigma\left(\frac{w}{g}\right) \times g = 327.31 \times 32.2 = 10{,}539$ kips Building Weight

$A_G = 0.20\,g$ Site PGA

$\beta = .05$ Damping Factor

MODAL ANALYSIS TO DETERMINE TOTAL BASE SHEAR & STORY ACCELERATIONS

US Army Corps of Engineers

Example E-1   3 of 7   Sample Modal Analyses

Figure E-1. Sample modal analysis—continued.

SEVEN STORY BLDG. - TRANSVERSE DIRECTION

1ST MODE FORCES $T_1 = 0.880$ sec.

MODAL BASE SHEAR $V_1 = 2408^K$

(1) STORY	(2) ϕ	(3) h FT.	(4) Δh FT.	(5) w KIPS	(6) $\frac{w\phi}{\Sigma w\phi}$	(7) F KIPS $(V_1)\times(6)$	(8) V KIPS $\Sigma(7)$	(9) ΔOTM K-FT $(4)\times(8)$	(10) OTM K-FT $\Sigma(9)$	(11) ACCEL. g $(7)\div(5)$	δ^* FT.	$\Delta\delta$ FT
ROOF	.0794	65.7		1410	0.211	508			0	0.360	.228	
			8.7				508	4420				.014
7	.0745	57.0		1460	0.205	494			4420	0.338	.214	
			8.7				1002	8717				.022
6	.0666	48.3		1460	0.184	443			13,137	0.303	.192	
			8.7				1445	12,572				.031
5	.0558	39.6		1460	0.154	371			25,709	0.254	.161	
			8.7				1816	15,799				.039
4	.0425	30.9		1460	0.117	282			41,508	0.193	.122	
			8.7				2098	18,253				.042
3	.0279	22.2		1460	0.077	185			59,761	0.127	.080	
			8.7				2283	19,862				.037
2	.0149	13.5		1830	0.052	125			79,623	0.068	.043	
			13.5				2408	32,508				.043
GROUND	0	0		.0	0	0			112,131	0	0	
				Σ	1.000	2408^K		112,131				

$$* \quad \delta_x = \frac{g}{4\pi^2} \times T^2 \times F/w = .632 \times \text{Accel.}$$

US Army Corps of Engineers

Example E-1 4 of 7 Sample Modal Analyses

Figure E-1. Sample modal analysis—continued.

SEVEN STORY BLDG. - TRANSVERSE DIRECTION

2ND MODE FORCES $T_2 = .288$ sec.

MODAL BASE SHEAR $V_2 = 632$ KIPS

(1) STORY	(2) ϕ	(3) h FT.	(4) Δh FT	(5) w KIPS	(6) $\frac{w\phi}{\Sigma w\phi}$	(7) F KIPS $(V_2)\times(6)$	(8) V KIPS $\Sigma(7)$	(9) ΔOTM K-FT $(4)\times(8)$	(10) OTM K-FT $\Sigma(9)$	(11) ACCEL. g (7)÷(5)	δ* FT	$\Delta\delta$ FT
ROOF	.0747	65.7		1410	-.322	-330			0	-.234	-.016	
			8.7				-330	-2871				.007
7	.0411	57.0		1460	-.297	-188			-2871	-.129	-.009	
			8.7				-518	-4507				.010
6	-.0042	48.3		1460	.030	19			-7378	.013	.001	
			8.7				-499	-4341				.009
5	-.0471	39.6		1460	.341	216			-11,719	.148	.010	
			8.7				-283	-2462				.005
4	-.0718	30.9		1460	.520	329			-14,181	.225	.015	
			8.7				46	400				.000
3	-.0697	22.2		1460	.504	319			-13,781	.219	.015	
			8.7				365	3176				.005
2	-.0467	13.5		1830	.423	267			-10,605	.146	.010	
			13.5				632	8532				.010
GROUND	0	0							-2073	0	0	
				Σ	.999	632*		-2073				

$$^{*}\ \delta_{x2} = \frac{g}{4\pi^2} \times T^2 \times F/w = .068 \times \text{Accel.}$$

US Army Corps of Engineers

Example E-1 5 of 7 Sample Modal Analyses

Figure E-1. Sample modal analysis—continued.

SEVEN STORY BLDG. - TRANSVERSE DIRECTION

3RD MODE FORCES $T_3 = .164$ SEC.

MODAL BASE SHEAR $V_3 = 200$ KIPS

(1) STORY	(2) ϕ	(3) h FT	(4) Δh FT	(5) w KIPS	(6) $\frac{w\phi}{\Sigma w\phi}$	(7) F KIPS $(V_3)\times(6)$	(8) V KIPS $\Sigma(7)$	(9) ΔOTM K-FT $(4)\times(8)$	(10) OTM K-FT $\Sigma(9)$	(11) ACCEL. g $(7)\div(5)$	δ* FT.	$\Delta\delta$ FT
ROOF	.0684	65.7		1410	0.849	170			0	.121	.003	
			8.7				170	1479				.003
7	-.0040	57.0		1460	-0.051	-10			1479	-.007	.000	
			8.7				160	1392				.003
6	-.0644	48.3		1460	-0.830	-166			2871	-.114	-.003	
			8.7				-6	-52				.000
5	-.0630	39.6		1460	-0.813	-163			2819	-.112	-.003	
			8.7				-169	-1470				.003
4	-.0023	30.9		1460	-0.028	-6			1349	-.004	.000	
			8.7				-175	-1523				.002
3	.0604	22.2		1460	0.778	156			-174	.107	.002	
			8.7				-19	-165				.001
2	.0677	13.5		1830	1.094	219			-339	.120	.003	
			13.5				200	2700				.003
GROUND	0	0							2361	0	0	
				Σ	0.999	200		2361				

$$* \ \delta_{x3} = \frac{g}{4\pi^2} \times T^2 \times F/w = .022 \times \text{Accel.}$$

US Army Corps of Engineers

Figure E-1. Sample modal analysis—continued.

30 STORY REINFORCED CONCRETE FRAME BUILDING

Mathematical Model - Gross Concrete Sections, Spandrel Beams increased 50% for Slab participation, Masses of Every four stories lumped into one.

Periods (T) and Mode Shapes (ϕ) are based on the results of a two-dimensional computer program.

Spectral Accelerations for 3 modes obtained from Resp. Spectrum.

GIVEN: Masses ($\frac{w}{g}$), ϕ's, T's, S_a's

REQ'D: Story Accelerations (a) and Base Shear Forces (V)

* LEVEL	w/g $\left(\frac{k \cdot s^2}{ft.}\right)$	MODE 1 ϕ_1	$\frac{w}{g}\phi_1$	$\frac{w}{g}\phi_1^2$	a_1 (g)	MODE 2 ϕ_2	$\frac{w}{g}\phi_2$	$\frac{w}{g}\phi_2^2$	a_2 (g)	MODE 3 ϕ_3	$\frac{w}{g}\phi_3$	$\frac{w}{g}\phi_3^2$	a_3 (g)	SRSS a_x (g)
29	179.8	.0794	14.28	1.134	.104	.0747	13.43	1.003	-.106	.0684	12.30	.841	.094	.176
25	181.4	.0745	13.51	1.007	.098	.0411	7.46	.307	-.058	-.0040	-.73	.003	-.006	.114
21	181.4	.0666	12.08	.805	.087	-.0042	-.76	.003	.006	-.0644	-11.68	.752	-.089	.125
17	181.4	.0558	10.12	.565	.073	-.0471	-8.54	.402	.067	-.0630	-11.43	.720	-.087	.132
13	181.4	.0425	7.71	.328	.056	-.0718	-13.02	.935	.102	-.0023	-.42	.001	-.003	.116
9	181.4	.0279	5.06	.141	.037	-.0697	-12.64	.881	.099	.0604	10.96	.662	.083	.134
5	192.9	.0149	2.87	.043	.020	-.0467	-9.01	.421	.066	.0677	13.06	.884	.093	.116
GROUND	—	0	0	0	0	0	0	0	0	0	0	0	0	
Σ	1279.7		6563	4.023			-23.08	3.952			12.06	3.863		
PF_{ROOF}	(Eq. 4-1)	$\frac{65.63}{4.023}(.0794) = 1.30$				$\frac{-23.08}{3.952}(.0747) = -.44$				$\frac{12.06}{3.863}(.0684) = .21$				$\Sigma = 1.07$
α	(Eq. 4-2)	$\frac{(65.63)^2}{(1279.7)(4.023)} = 0.837$				$\frac{(23.08)^2}{(1279.7)(3.952)} = 0.105$				$\frac{(12.06)^2}{(1279.7)(3.863)} = 0.029$				$\Sigma = .971$
T		3.00 sec				1.00 sec.				0.56 sec				
S_a		0.080 g				0.240 g				0.445 g				
a_{ROOF}	(Eq. 6-1)	(1.30)(.080) = 0.104 g				(-.44)(.240) = -0.106 g				(.21)(.445) = 0.094 g				.176
V	(Eq. 4-4)	(.837)(.080)(41206) = 2759^k				(.105)(.24)(41206) = 1038^k				(.029)(.445)(41206) = 532^k				2995^k
V/W		.067				.025				.013				.073

* Story 29 represents the roof, 29, 28 and one-half the 27th story. Stories 5 through 25 represent the indicated story plus 1½ stories above & below.

US Army Corps of Engineers

Example E-1   7 of 7   Sample Modal Analyses

Figure E–1. Sample modal analysis—continued.

DESIGN EXAMPLE: E-2

BUILDING WITH A BOX SYSTEM:

Description of Structure. A 2-story hospital building with bearing walls in concrete, using a series of interior, vertical-load-carrying column and girder bents. The structural concept is illustrated in the Basic Design Manual, Design Example A-1.

Initial Trial Structure. The building in Design Example A-1 of the Basic Design Manual was designed for Z = 1.0 and I = 1.0 with a base shear coefficient V/W = ZIKCS = 0.186. In order to utilize the same structure in this example, the following conditions are assumed:

Seismic Zone 3, Z = 3/4
Hospital building, I = 1.5
Box building, K = 1.33
Soil factor, based on T_S = 2.5 sec
Building period T < 0.3 sec
CS = 0.133
ZIKCS = 0.20

The base shear, V, for this example is 0.20W, which is close enough to that design base shear in the building in Design Example A-1 so that building will be used for the initial trial design.

Seismic Design Criteria. The building is to be designed in accordance with the dynamic analysis procedures of this manual. The following conditions apply:

Building classification: Essential facility
Ground motion spectra: ATC 3-06 spectra with $A_a = A_v = 0.30g$
Soil profile coefficient: Type S_3

Design Procedure.

US Army Corps of Engineers

Example E-2 1 of 23 Box System

Figure E-2. Building with a box system.

INTRODUCTION

THE SITE RESPONSE SPECTRA ARE DEVELOPED IN ACCORDANCE WITH THE PROCEDURE DESCRIBED IN CHAPTER 3. THE GOVERNING EQUATIONS AND SPECTRA FOR EQ-I AND EQ-II ARE SHOWN ON SHEETS 3 & 4, INCLUDING THE EFFECTS OF SITE SEVERITY, SOIL TYPE, AND STRUCTURAL DAMPING.

THE STRUCTURE OF EXAMPLE A-1 IN THE BASIC DESIGN MANUAL IS ASSUMED TO BE THE INITIAL TRIAL DESIGN AS DESCRIBED IN PARAGRAPH 5-3a OF THIS MANUAL. SINCE THE PERIOD OF VIBRATION IS SHORT, APPROXIMATELY .1 -.2 SECONDS, THE SPECTRAL ACCELERATION FOR EQ-I IS .28g. THIS Sa VALUE IS TWICE THE ZICS VALUE OF .14g WHICH WAS USED FOR THE TRIAL DESIGN, THEREFORE THE ANALYSIS FOR EQ-I WILL PROCEED WITHOUT MODIFYING THE STRUCTURE.

THE EXAMPLE STRUCTURE IS A BOX BUILDING WITH CONCRETE SHEAR WALLS IN BOTH THE TRANSVERSE AND LONGITUDINAL DIRECTIONS. THE METAL DECK ROOF SYSTEM FORMS A FLEXIBLE DIAPHRAGM WHILE THE METAL DECK WITH CONCRETE FILL FORMS A RIGID DIAPHRAGM AT THE SECOND FLOOR LEVEL.

IN ORDER TO PERFORM THE DYNAMIC MODAL ANALYSIS, BOTH THE ROOF AND 2ND FLOOR DIAPHRAGMS ARE ASSUMED TO BE RIGID. THE TRANSVERSE AND LONGITUDINAL ANALYSES ARE PERFORMED FOR THE BUILDING AS A WHOLE ASSUMING STRAIGHT LINE 1ST MODE SHAPES IN EACH DIRECTION. ONCE THE STORY SHEARS ARE DETERMINED, DISTRIBUTION TO INDIVIDUAL WALLS IS MADE CONSIDERING DIAPHRAGM FLEXIBILITY AND ANY ADDITIONAL CONTRIBUTION DUE TO TORSION.

US Army Corps of Engineers

Example E-2 | 2 of 23 | Box System

Figure E-2. Building with a box system—continued.

DETERMINATION OF SITE RESPONSE SPECTRA

SITE SEVERITY

FIGURES 3-40 TO 3-43 SHOW THE A_a AND A_v VALUES FOR AN ATC 3-06 SPECTRUM. SCALE FACTORS FOR EQ-I AND EQ-II ARE OBTAINED BY INTERPOLATION BETWEEN VALUES IN TABLE 3-4. VALUES USED IN THIS EXAMPLE ARE AS FOLLOWS:

	ATC 3-06	EQ - I	EQ - II
A_a	0.30g	0.14g	0.35g
A_v	0.30g	0.14g	0.35g

SOIL PROFILE COEFFICIENT, S_i

ASSUME SOIL PROFILE TYPE S_3

FROM TABLE 3-6, $S_i = 1.5$

DAMPING ADJUSTMENT FACTORS

DAMPING VALUES FROM TABLE 4-1, DAMPING FACTORS FROM TABLE 3-7

	DAMPING	DAMPING FACTOR
EQ - I	5%	1.0
EQ - II	10%	0.8

GOVERNING EQUATIONS (EQ. 3-27, 3-29)

EQ-I : $S_a = 1.22\,A_v S_i / T = 1.22(.14)1.5/T = .2562/T \leq 2(A_a) = .28$

EQ-II : $S_a = .8(1.22)(.35)1.5/T = .5124/T \leq .8(2.0)(.35) = .56$.

US Army Corps of Engineers

Example E-2 3 of 23 Box System

Figure E-2. Building with a box system—continued.

DESIGN RESPONSE SPECTRA FOR EQ-I AND EQ-II

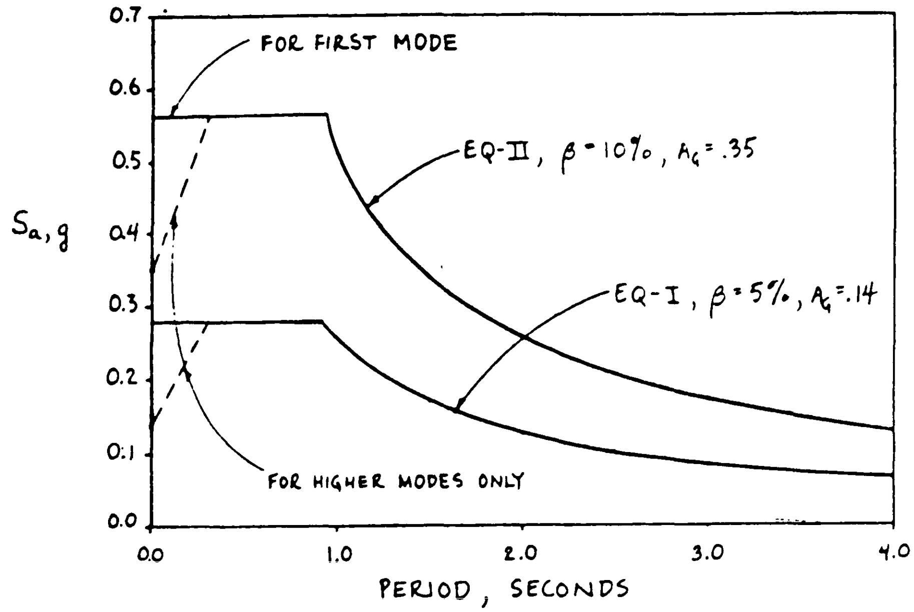

	β		PERIOD							
			0.0	.3-.915	1.0	1.5	2.0	2.5	3.0	4.0
EQ-I	5%	S_a, g	.14	.28	.256	.171	.128	.102	.085	.064
EQ-II	10%	S_a, g	.35	.56	.512	.342	.256	.205	.171	.128

US Army Corps of Engineers

Example E-2 4 of 23 Box System

Figure E-2. Building with a box system—continued.

EQ - I

SPECTRAL ACCELERATION FOR FIRST MODE, S_{a1}

PERIOD $T = .05h/\sqrt{D}$

TRANSVERSE (N-S) $T = .05(23)/\sqrt{48} = .166$ SEC

LONGITUDINAL (E-W) $T = .05(22)/\sqrt{192} = .079$ SEC

$\underline{S_{a1} = .28g}$ FROM EQ-I SPECTRUM FOR BOTH E-W AND N-S

MODE SHAPES, ϕ_{x1}

ASSUME A STRAIGHT LINE 1ST MODE SHAPE $\begin{Bmatrix} \phi_{21} \\ \phi_{11} \end{Bmatrix} = \begin{Bmatrix} 1.0 \\ .5 \end{Bmatrix}$

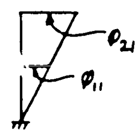

FIRST MODE BASE SHEAR, V_1 (SEE PAR. 4-3c FOR APPLICABLE EQUATIONS)

LEVEL	W_x, k	m_x, $\frac{k\text{-}sec^2}{ft}$	ϕ_{x1}	$m_x\phi_{x1}$	$m_x\phi_{x1}^2$	PF_{x1}	a_{x1}, g	F_{x1}, k	V_{x1}, k
2	534	16.6	1.0	16.6	16.6	1.336	.374	200.0	200.0
1	1080	33.5	.5	16.8	8.4	.668	.187	202.0	402.0
Σ	1614	50.1		33.4	25.0			402.0	

$\alpha_1 = \dfrac{(33.4)^2}{(50.1)(25.0)} = .891$ 1ST MODE BASE SHEAR PARTICIPATION FACTOR (EQ. 4-2)

$C_{b1} = \alpha_1 S_{a1} = .891(.28) = .249$ 1ST MODE BASE SHEAR COEFFICIENT

$V_1 = \alpha_1 S_{a1} W = C_{b1} W = \underline{402\ k}$ 1ST MODE BASE SHEAR (EQ. 4-4)

US Army Corps of Engineers

Example E-2 | 5 of 23 | Box System

Figure E-2. Building with a box system—continued.

DISTRIBUTION OF SEISMIC FORCES

SEISMIC FORCES FROM ROOF DIAPHRAGM TO WALLS BELOW

DIRECT SHEAR : THE ROOF SHEAR IS DISTRIBUTED BY TRIBUTARY AREA ($^W/_{\Sigma W}$) SINCE THE DIAPHRAGM IS FLEXIBLE.

TORSIONAL SHEAR: NO TORSION ASSUMED.

SEISMIC FORCES FROM 2ND FLOOR TO WALLS BELOW

DIRECT SHEAR : THE 2ND STORY SHEAR IS DISTRIBUTED ACCORDING TO THE RELATIVE RIGIDITIES OF THE WALLS BELOW ($^R/_{\Sigma R}$).

TORSIONAL SHEAR: THE TORSIONAL MOMENT, M_T, IS THE LARGER OF THE "CALCULATED" TORSION OR THE "ACCIDENTAL" TORSION DUE TO EITHER THE E-W OR N-S EARTHQUAKE. THE "ACCIDENTAL" TORSION IS COMPUTED USING THE ECCENTRICITIES WHICH RESULT BY MOVING THE CENTER OF MASS 5% OF THE MAXIMUM BUILDING DIMENSION TO EITHER SIDE OF ITS CALCULATED POSITION. THE TORSIONAL MOMENT IS RESISTED BY BOTH N-S AND E-W WALLS ACCORDING TO THEIR RIGIDITIES AND DISTANCE FROM THE CENTER OF RIGIDITY. THE TORSIONAL SHEARS ARE ADDED ALGEBRAICALLY TO THE DIRECT SHEARS.

US Army Corps of Engineers

Example E-2	6 of 23	Box System

Figure E-2. Building with a box system—continued.

EQ-I : DISTRIBUTION OF SEISMIC FORCES FROM ROOF TO WALLS BELOW

TOTAL SHEAR BELOW ROOF $F_{x(NS)} = 200$ k
$F_{x(EW)} = 200$ k

TORSIONAL MOMENT $M_T = 0$

EQ-I	WALL	DIRECT SHEAR			TORSIONAL SHEAR				DIRECT SHEAR + TORSION
		W, kips	R	DIRECT SHEAR	d	Rd^2	M_T	$\frac{Rd^2}{\Sigma Rd^2} \cdot \frac{M_T}{d}$	
N-S	1	94	26.3	35.2					35.2
	3	169	38.1	63.3					63.3
	5	169	38.1	63.3					63.3
	7	102	55.5	38.2					38.2
		534		200.0					200.0
	A	267	35.6	0					
	C	267	35.6	0					
		534							
E-W	1	94	26.3	0					
	3	169	38.1	0					
	5	169	38.1	0					
	7	102	55.5	0					
		534							
	A	267	35.6	100.0					100.0
	C	267	35.6	100.0					100.0
		534		200.0					200.0

NO TORSION ASSUMED.

Figure E-2. Building with a box system—continued.

EQ-I: 2ND FLOOR PLAN SHOWING DIRECT SHEAR AND TORSIONAL SHEAR FORCES (SEE SHEET 10 FOR WALL ELEVATIONS)

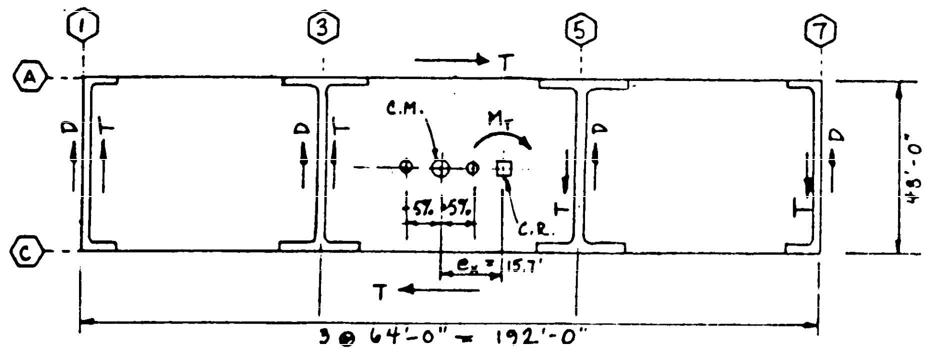

NOTES: C.M. = CENTER OF MASS

C.R. = CENTER OF RIGIDITY

D = DIRECT SHEAR FORCE ($D = R/\Sigma R \; V_x$)

T = TORSIONAL SHEAR FORCE ($T = Rd^2/\Sigma Rd^2 \cdot M_T/d$)

M_T = TORSIONAL MOMENT

NORTH-SOUTH DIRECTION

FOR EACH WALL, USE THE "CALCULATED" OR "ACCIDENTAL" TORSIONAL MOMENT WHICH PRODUCES THE HIGHEST COMBINED SHEAR. IN THIS CASE, THE TORSIONAL SHEAR WILL ALWAYS BE ADDITIVE FOR WALLS 1 & 3 AND NEGATIVE FOR WALLS 5 & 7.

TORSIONAL MOMENT:

CALCULATED $M_T = V_x(e_x) = 402\,(15.7') = 6311$ ft-k

ACCIDENTAL $M_T = V_x(e_{max}) = V_x(e_x + .05 \times 192') = 402\,(25.3') = 10171$ ft-k

$M_T = V_x(e_{min}) = V_x(e_x - .05 \times 192') = 402\,(6.1') = 2452$ ft-k

EAST-WEST DIRECTION

USE THE "ACCIDENTAL" TORSIONAL MOMENT (W/EITHER SIGN ±).

$\pm M_T = V_x(.05 \times 192') = 402\,(9.6') = 3859$ ft-k

US Army Corps of Engineers

Figure E-2. Building with a box system—continued.

EQ-I : DISTRIBUTION OF SEISMIC FORCES FROM 2ND FLOOR TO WALLS BELOW

TOTAL SHEAR BELOW 2ND FLR. DIAPHRAGM $F_{x(NS)}$ = 402k
$F_{x(EW)}$ = 402k

TORSIONAL MOMENT $M_{T(NS)}$ SEE SHEET 8
$M_{T(EW)}$ = 3859 ft-k

EQ-I	WALL	DIRECT SHEAR			TORSIONAL SHEAR				DIRECT SHEAR + TORSION
		W,t	R	DIRECT SHEAR	d	Rd^2	GOVERNING M_T	$\frac{Rd^2}{\Sigma Rd^2} \cdot \frac{M_T}{d}$	
N-S	1		27.0	61.8	111.28	334347	10171	35.4	97.2
	3		44.9	102.8	47.7	102161	10171	25.2	128.0
	5		44.9	102.8	16.3	11929	2452	-2.1	100.7
	7		58.8	134.6	79.88	375192	2452	-13.3	121.3
			175.6	402.0					447.2
	A		35.6	0	23.58	19794	10171	9.9	9.9 *
	C		35.6	0	23.58	19794	10171	9.9	9.9 *
			71.2			863217			
E-W	1		27.0	0	111.28	334347	3859	13.4	13.4 *
	3		44.9	0	47.7	102161	"	9.6	9.6 *
	5		44.9	0	16.3	11929	"	3.3	3.3 *
	7		58.8	0	79.88	375192	"	21.0	21.0 *
			175.6						
	A		35.6	201.0	23.58	19794	"	3.8	204.8
	C		35.6	201.0	23.58	19794	"	3.8	204.8
			71.2	402.0		863217			409.6

* THESE VALUES ARE NOT CRITICAL, BUT ARE SHOWN HERE FOR CLARITY.

US Army Corps of Engineers

Example E-2 9 of 23 Box System

Figure E-2. Building with a box system—continued.

EQ-I: DISTRIBUTION OF SEISMIC SHEARS AND OVERTURNING MOMENTS

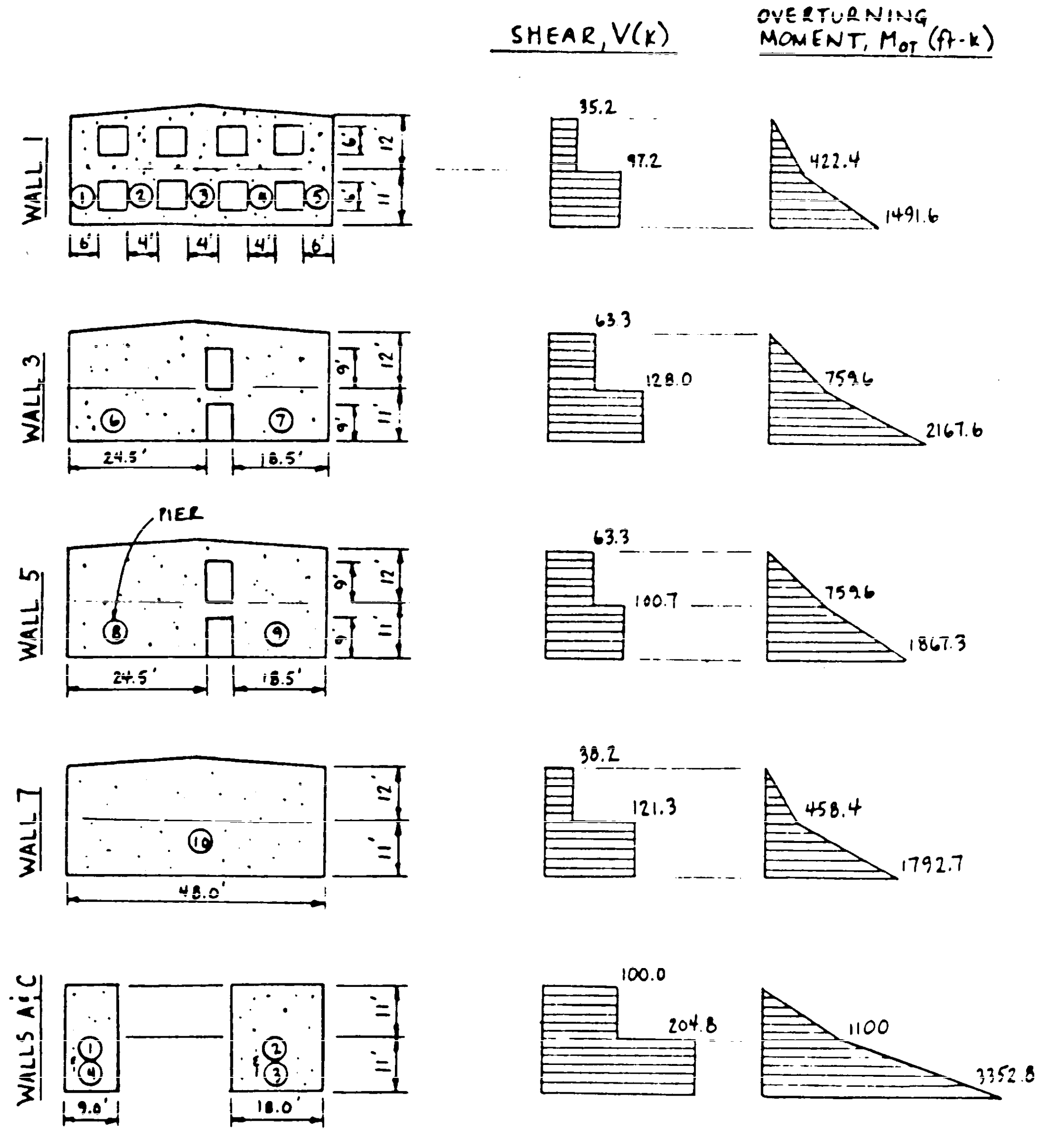

US Army Corps of Engineers

Example E-2 10 of 23 Box System

Figure E-2. Building with a box system—continued.

MOMENT CAPACITY - 1ST STORY WALLS, M_c

$M_c = M_u = \varphi f_y A_s (d - \frac{a}{2})/12$ WHERE $\phi = .9$ FLEXURE

$f_y = 40$ ksi

$d = L - 2''$ COVER

$a = A_s f_y / .85 f'_c b$

WALL	TIER	L, in.	A_s^*, in²	a, in	$d-\frac{a}{2}$, in	M_c, ft-k
1	1	72	.61	.72	69.6	127.4
	2	48	.61	.72	45.6	83.4
	3	48	.61	.72	45.6	83.4
	4	48	.61	.72	45.6	83.4
	5	72	.61	.72	69.6	127.4
	BASE	576	1.2	1.41	572.8	2062.
3,5	6	294	2.0	2.35	290.	1740.
	7	222	1.58	1.85	219.	1030.
7	8	576	2.0	2.35	572.	3431.
A, C	1	108	2.0	2.35	104.	624.
	2	216	3.0	2.53	212.	1905.
	3	216	3.0	2.53	212.	1905.
	4	108	2.0	2.35	104.	624.

*DATA FROM DESIGN MANUAL EXAMPLE A-1.

US Army Corps of Engineers

Example E-2 11 of 23 Box System

Figure E–2. Building with a box system—continued.

EQ-I : CHECK DEMAND/CAPACITY RATIOS FOR PIERS IN 1ST STORY WALLS

SHEAR : $v_{DEMAND} = v_D = V/\phi A_c$ $\quad v_{CAPACITY} = v_C^{\dagger} = 2\sqrt{f'_c} + \rho f_y = 226$ psi

MOMENT: $M_{DEMAND} = M_D = \left(\frac{R}{\Sigma R} M_{OT}\right)$ OR $V\left(\frac{h}{2}\right)$ FOR PIERS $\quad M_{CAPACITY} = M_C = \phi f_y A_s (d - \frac{a}{2})/12$, $f_y = 40$ ksi

EQ-I	WALL	PIER	R* (k/in)	V (k)	A_c* (in²)	v_D (psi)	M_D (k-ft)	A_s* (in²)	M_c (k-ft)	v_D/v_c	M_D/M_c
N-S	1	1	11.1	30.2	720	49	91	.61	127	.22	.72
		2	4.5	12.3	480	30	37	.61	83	.13	.45
		3	4.5	12.3	480	30	37	.61	83	.13	.45
		4	4.5	12.3	480	30	37	.61	83	.13	.45
		5	11.1	30.2	720	49	91	.61	127	.22	.72
			35.7	97.2							
	1	BASE	27.0	97.2	5760	20	1492	1.2	2062	.09	.72
	3	6	27.0	77.0	2940	31	1303	2.0	1740	.14	.75
		7	17.9	51.0	2220	27	864	1.57	1030	.12	.84
			44.9	128.0			2167				
	5	8	27.0	60.6	2940	24	1123	2.0	1740	.11	.65
		9	17.9	40.1	2220	21	744	1.57	1030	.09	.72
			44.9	100.7			1867				
	7	10	58.8	121.3	5760	25	1793	2.0	3431	.11	.52
E-W	A,C	1	4.5	25.9	1080	28	424	2.0	624	.12	.68
		2	13.3	76.5	2160	42	1252	3.0	1905	.19	.66
		3	13.3	76.5	2160	42	1252	3.0	1905	.19	.66
		4	4.5	25.9	1080	28	424	2.0	624	.12	.68
			35.6	204.8			3352				

* DATA FROM DESIGN MANUAL EXAMPLE A-1.
† FROM EXAMPLE A-1 : $f'_c = 4$ ksi, $f_y = 40$ ksi, $\rho = .0025$

US Army Corps of Engineers

Example E-2 12 of 23 Box System

Figure E-2. Building with a box system—continued.

EQ-I : CHECK WALL 3, PIER 7 INCLUDING DEAD LOAD EFFECTS

THE PREVIOUS CALCULATIONS FOR DEMAND MOMENT WERE BASED ON EARTHQUAKE DEMAND ONLY, IGNORING THE DEAD LOADS. FOR WALLS WHICH ARE HIGHLY STRESSED DUE TO THE EARTHQUAKE LOADING, AN ADDITIONAL CHECK CAN BE MADE TO INCLUDE THE DEAD LOAD. FOR THE BEARING WALLS IN THIS EXAMPLE, THIS RESULTS IN A SUBSTANTIAL REDUCTION IN THE DEMAND TO CAPACITY RATIO. (THIS CALCULATION IS INCLUDED HERE FOR ILLUSTRATION ONLY SINCE THE WALLS IN THIS EXAMPLE ARE NOT OVERSTRESSED).

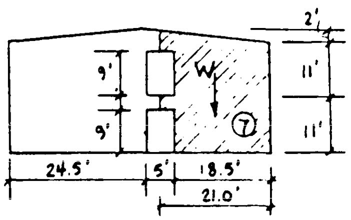

WALL 3

DEAD LOAD ON RIGHT PIER

ROOF	.0245 ksf × 32' × 21'	= 16.5
WALL	.125 ksf × 12' × 21	= 31.5
OPENING	−(.125) ksf × 2.5' × 9	= −2.8
		45.2 k
2ND FLOOR	.073 × 32' × 21'	= 49.06
WALL	.125 × 11' × 21'	= 28.88
OPENING	−(.125) × 2.5' × 9'	= −2.8
		75.1
		Σ 120.3

· ELASTIC CAPACITY (EQ. 4-6, 4-7)

$EC \geq 1.2D + 1.0L + 1.0E$ (COMPRESSION SIDE)

$EC \geq .8D + 1.0E$ (TENSION SIDE - MUST CHECK)

· PIER #7 (M_c FOR .8D)

$P = .8D = .8(120.3) = 96.2\,k$

$T = A_s f_y = 1.57(40) = 62.8\,k$

$C = T + P = 159.0\,k$

$a = \dfrac{C}{.85 f'_c b} = \dfrac{159.0}{.85(4)(10)} = 4.68''$

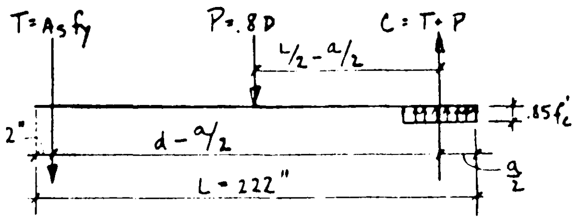

$M_c = \phi\left[T(d - a/2) + P(L/2 - a/2)\right] = .9\left[62.8(217.7'') + 96.2(108.7'')\right]/12 = 1810\ k\text{-}ft$

DEMAND/CAPACITY RATIO $M_D/M_c = 864/1810 = .48 < .84$

US Army Corps of Engineers

Figure E-2. Building with a box system—continued.

CHECK DEFLECTIONS & PERIOD FOR LONGITUDINAL WALLS A & C

CONSIDER EACH PIER AS AN INDEPENDENT CANTILEVER AND COMPUTE THE DEFLECTIONS USING VIRTUAL WORK. ASSUME THE SHEAR IS DISTRIBUTED TO THE INDIVIDUAL PIERS IN ACCORDANCE WITH THEIR RELATIVE RIGIDITIES.

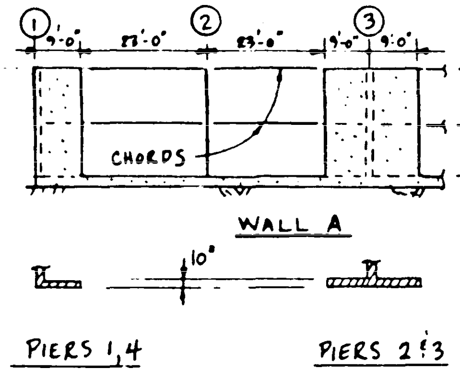

E = 3600 KSI = 518,400
G = .4E

PROPERTIES

PIERS 1 & 4 : FOR CORNER PIER USE $I = 1.5(bd^3/12)$, $A_v = bd$
$I = 1.5(10/12)(9)^3/12 = 75.94\ ft.^4$
$A_v = (10/12)(9) = 7.5\ ft^2$

PIERS 2 & 3 : RECTANGULAR PIER $I = (bd^3/12)$, $A_v = 5/6 bd$
$I = (10/12)(18)^3/12 = 405\ ft^4$
$A_v = 5/6(10/12)(18) = 12.5\ ft^2$

RELATIVE RIGIDITIES

$\Delta = Ph^3/3EI + Ph/A_v G = h^3/3I + h/.4A_v$

PIER 1 : $\Delta = (22)^3/3(75.94) + 22/.4(7.5) = 54.07$ $\quad R = \frac{1}{\Delta} = .0185$
PIER 2 : $\Delta = (22)^3/3(405) + 22/.4(12.5) = 13.16$ $\quad R = \frac{1}{\Delta} = .0760$
$\Sigma R = .1889$

US Army Corps of Engineers

Figure E–2. Building with a box system—continued.

DEFLECTIONS (CONTINUED)

SHEAR DISTRIBUTION & OVERTURNING MOMENT

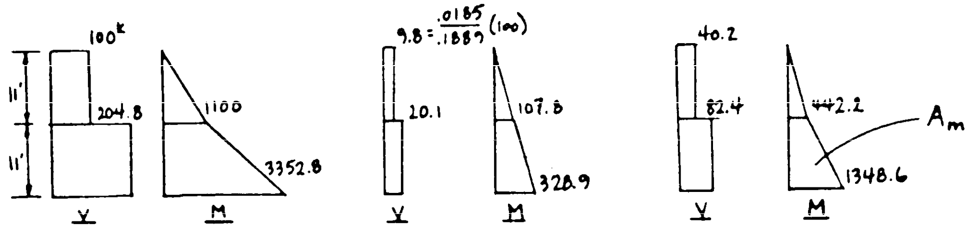

WALL A (SHEET 10) PIERS 1 & 4 PIERS 2 & 3

• VIRTUAL STRUCTURE FOR DISPLACEMENTS @ ROOF AND 2ND FLOOR

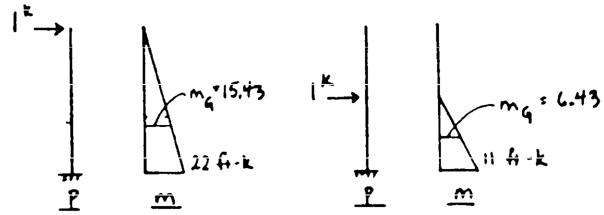

DEFLECTION OF PIERS 1 & 4

• BENDING DEFLECTION PIERS 1 & 4

$$EI\Delta = \int_0^L m M dx = A_m m_G$$

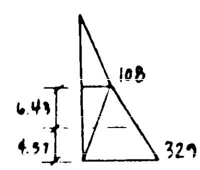

FOR Δ_{2ND} $A_m = \frac{1}{2}(11)(108) + \frac{1}{2}(11)(329) = 2404$

$$C.G. = \frac{\left[\frac{2}{3}(11)(594) + \frac{11}{3}(1810)\right]}{2404} = 4.57'$$

$$m_G = 11 \text{ ft-k} \left(\frac{6.43}{11}\right) = 6.43$$

$$\Delta_{2ND} = A_m m_G / EI = 2404(6.43)12^3 / 518400(75.94)$$

$$= \underline{.0047''}$$

US Army Corps of Engineers

Example E-2	15 of 23	Box System

Figure E-2. Building with a box system—continued.

DEFLECTIONS (CONTINUED)

FOR Δ_{ROOF} $A_m = 2404 + \frac{1}{2}(11)(108) = 2998$

$C.G. = \frac{[4.57'(2404) + \frac{2}{3}(11)(594)]}{2998} = 6.57'$

$\cdot m_G = 22 \text{ ft-k } (15.43/22) = 15.43$

$\Delta_{ROOF} = A_m m_G / EI = 2998(15.43)(12'')/518400(75.94)$
$= \underline{.0141''}$

• SHEAR DEFLECTION PIERS 1 & 4

$\Delta = 1.2Ph/AG = Ph/A_vG = Ph/A_v(.4E)$

$\Delta_{2ND} = 20.1(11)(12'')/7.5(.4)(518400) = \underline{.0017''}$

$\Delta_{ROOF} = \Delta_{2ND} + 9.8(11)(12)/7.5(.4)(518400)$
$= .00171 + .000832 = \underline{.0025''}$

• TOTAL DEFLECTION PIERS 1 & 4

$\Delta_{2ND} = .0047 + .0017 = \underline{.0064''} = .39\,\Delta_{ROOF}$

$\Delta_{ROOF} = .0141 + .0025 = \underline{.0166''}$

US Army Corps of Engineers

Example E-2	16 of 23	Box System

Figure E–2. Building with a box system—continued.

DEFLECTIONS (CONTINUED)

DEFLECTION OF PIERS 2 & 3

BENDING DEFLECTION $EI\Delta = \int mM\,dx = A_m m_G$

FOR Δ_{2ND} $A_m = {}^{11}/_2(442) + {}^{11}/_2(1349) = 9851$

$C.G. = \dfrac{[{}^2/_3(11)(2431) + {}^{11}/_3(7420)]}{9851} = 4.57'$

$m_G = 11\,({}^{6.43}/_{11}) = 6.43$

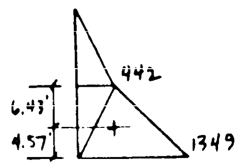

$\Delta_{2ND} = A_m m_G / EI = 9851(6.43)(12)/518400(405)$
$= \underline{.0036''}$

FOR Δ_{ROOF} $A_m = 9851 + {}^{11}/_2(442) = 12282$

$C.G. = \dfrac{[4.57(9851) + {}^4/_3(11)(2431)]}{12282} = 6.57'$

$m_G = 22\,({}^{15.43}/_{22}) = 15.43$

$\Delta_{ROOF} = A_m m_G / EI = 12282(15.43)(12)/518400(405)$
$= \underline{.0108''}$

- SHEAR DEFLECTION PIERS 2 & 3

$\Delta_{2ND} = Ph/A_v(.4E) = 82.4(11)(12'')/12.5(.4)(518400) = \underline{.0042''}$

$\Delta_{ROOF} = \Delta_{2ND} + 40.2(11)(12)/12.5(.4)(518400) = .0042 + .00205 = \underline{.0062''}$

- TOTAL DEFLECTION PIERS 2 & 3

$\Delta_{2ND} = .0036 + .0042 = \underline{.0078''} = .46\,\Delta_{ROOF}$

$\Delta_{ROOF} = .0108 + .0062 = \underline{.0170''}$

US Army Corps of Engineers

Example E-2	17 of 23	Box System

Figure E-2. Building with a box system—continued.

PERIOD OF LONGITUDINAL WALLS A & C

- PIERS 1, 2, 3 & 4 ARE CONNECTED BY CHORD MEMBERS AT THE ROOF AND 2ND FLOOR LEVELS WHICH CONSTRAIN THE PIERS TO DEFLECT TOGETHER. THUS, THE AVERAGE DEFLECTION OF THE 4 PIERS IS USED TO COMPUTE THE PERIOD OF THE WALL.

$$\Delta_{2ND} = \frac{2}{4}(.0064 + .0078) = \underline{.0071"} = .42\,\Delta_{ROOF}$$

$$\Delta_{ROOF} = \frac{2}{4}(.0166 + .0170) = \underline{.0168"}$$

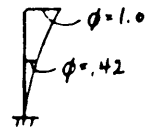

- LONGITUDINAL PERIOD (E-W)

$$T = 2\pi\sqrt{\frac{\Sigma(W_x\,\delta_x^2)}{g\,\Sigma(F_x\,\delta_x)}}$$

$$= 2\pi\sqrt{\frac{534(.0168)^2 + 1080(.0071)^2}{386.4(200(.0168) + 209.6(.0071))}} = \underline{\underline{.066\text{ SEC}}}$$

COMPARISON OF CALCULATED VALUES WITH INITIAL ASSUMPTIONS

LONGITUDINAL (E-W) DIRECTION

ASSUMED T = .079 SEC (SHEET 5)

CALCULATED T = .066 SEC

	W_x	m_x	ASSUMED ϕ_{x1}	ASSUMED F_{x1}	CALCULATED ϕ_{x1}	CALCULATED $m_x\phi_{x1}$	CALCULATED $m_x\phi_{x1}^2$	CALCULATED PF_{x1}	CALCULATED a_{x1}	CALCULATED F_{x1}
2	534	16.6	1.0	200.	1.0	16.6	16.6	1.364	.382	204
1	1080	33.5	.5	202.	.42	14.1	5.9	.573	.160	174
Σ	1614	50.1		402.		30.7	22.5			378

THE 2ND STORY SHEAR AND BASE SHEAR ARE LOWER, AND THE ROOF SHEAR IS ONLY 2% HIGHER THAN THE VALUES ASSUMED INITIALLY. THUS, THE INITIAL ASSUMPTIONS WERE ADEQUATE FOR THE EQ-I ANALYSIS.

US Army Corps of Engineers

Example E-2 18 of 23 Box System

Figure E–2. Building with a box system—continued.

EQ-I COMMENTARY

- THE RATIOS OF THE ELASTIC DEMAND TO THE CAPACITY ARE LESS THAN ONE FOR ALL OF THE WALL ELEMENTS. THUS, THE SHEAR WALLS ARE ADEQUATE FOR AN EARTHQUAKE WITH THE CHARACTERISTICS OF EQ-I APPLIED IN EITHER THE TRANSVERSE OR THE LONGITUDINAL DIRECTION.

- ALTHOUGH THE EFFECTS OF TORSION INCREASE THE LOADS ON WALL 1 BY MORE THAN 50%, (i.e. $V_1 = 35^k$ WHICH IS 36% OF THE TOTAL SHEAR FROM SHEET 9), THE RESULTING FORCES ARE SUBSTANTIALLY LESS THAN THE YIELD CAPACITY.

- CONSIDERATION OF THE DEAD LOAD IN THE CALCULATIONS FOR DEMAND MOMENT, M_r, WOULD REDUCE THE MOMENT DEMAND/CAPACITY RATIOS FOR THE BEARING WALLS IN THIS EXAMPLE, THUS ADDITIONAL SEISMIC CAPACITY IS AVAILABLE.

- THE DEFLECTION CALCULATIONS INDICATE THAT THE MODE SHAPES WHICH WERE ASSUMED INITIALLY ARE REASONABLY ACCURATE, THUS THE ASSUMED STRAIGHT LINE MODE SHAPES WILL ALSO BE USED FOR THE EQ-II ANALYSIS.

- THE CALCULATED E-W PERIOD OF 0.066 SECONDS IS CLOSE TO THE ASSUMED PERIOD OF 0.079 SECONDS. SINCE THE FIRST MODE SPECTRAL ACCELERATION IS CONSTANT FOR ALL PERIODS LESS THAN T = 0.9 SEC. (SEE SHEET 4), VARIATIONS IN THE CALCULATED PERIOD WILL NOT AFFECT THE EQ-I ANALYSIS.

Figure E-2. Building with a box system—continued.

EQ - II

SPECTRAL ACCELERATION FOR FIRST MODE, S_{a_1}

ASSUME PERIOD HAS LENGTHENED BY $\sqrt{1.25}$, WHERE 1.25 REPRESENTS THE INELASTIC SHEAR DEMAND RATIO FROM TABLE 4-2 FOR CONCRETE WALLS IN AN ESSENTIAL FACILITY.

TRANSVERSE (N-S) $T = \sqrt{1.25}\,(.17) = 0.19$ SEC
LONGITUDINAL (E-W) $T = \sqrt{1.25}\,(.079) = 0.088$ SEC

$S_{a_1} = .56g$ FROM EQ-II SPECTRUM FOR BOTH E-W & N-S

MODE SHAPES, ϕ_{x1}

ASSUME $\begin{Bmatrix} \phi_{21} \\ \phi_{11} \end{Bmatrix} = \begin{Bmatrix} 1.0 \\ .5 \end{Bmatrix}$

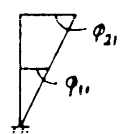

FIRST MODE BASE SHEAR, V_1

LEVEL	w_x, k	m_x, $\frac{k\text{-}sec^2}{ft}$	ϕ_{x1}	$m_x\phi_{x1}$	$m_x\phi_{x1}^2$	PF_{x1}	a_{x1}, g	F_{x1}, k	V_{x1}, k
2	534	16.6	1.0	16.6	16.6	1.336	.748	400.0	400.0
1	1080	33.5	.5	16.8	8.4	.668	.374	404.0	804.0
Σ	1614	50.1		33.4	25.0			804.0	

$$\alpha_1 = \frac{(33.4)^2}{(50.1)(25.0)} = .891$$

$C_{b1} = \alpha_1 S_{a_1} = .891\,(.56) = .498$ MODAL BASE SHEAR COEFFICIENT

$V_1 = \alpha_1 S_{a_1} W = C_{b1} W = \underline{804.0\ k}$ MODAL BASE SHEAR, EQ-II

US Army Corps of Engineers

Figure E–2. Building with a box system—continued.

EQ-II

THE DEMANDS OF EQ-II ARE TWICE THOSE OF EQ-I ($S_{a(EQ-II)} = 0.56g$, $S_{a(EQ-I)} = 0.28g$). THEREFORE, ALL OF THE RATIOS OF v_D/v_C AND M_D/M_C ARE DOUBLED (SEE SHEET 12 OF 23). THE SHEAR INELASTIC DEMAND RATIOS ARE ALL LESS THAN 1.0 (FOR EXAMPLE - WALL 1, PIER 1 : $v_D/v_C = 2 \times .22 = .44 < 1.0$). SOME MOMENT DEMAND RATIOS ARE GREATER THAN 1.0 (FOR EXAMPLE - WALL 3, PIER 7 : $M_D/M_C = 2 \times .84 = 1.68 > 1.0$). HOWEVER WHEN DEAD LOAD EFFECTS ARE INCLUDED (SEE SHEET 13), THE INELASTIC DEMAND RATIOS ARE SIGNIFICANTLY REDUCED ($2 \times .48 = .84 < 1.0$). THUS, THE STRUCTURE REMAINS ESSENTIALLY ELASTIC FOR EQ-II FORCES.

NOTE : IF WALL 1 HAD INELASTIC DEMAND RATIOS SIGNIFICANTLY GREATER THAN 1.0 (i.e. $2 \times .72 = 1.44$) AND WALL 7 DID NOT (i.e. $2 \times .52 = 1.04$), WALL 1 WOULD YIELD AND THUS HAVE REDUCED STIFFNESS, THE C.R. OF THE BUILDING WOULD SHIFT TOWARDS WALL 7 (SEE SHEET 8) RESULTING IN A LARGER ECCENTRICITY, e_x. THIS TYPE OF CONDITION COULD LEAD TO TORSIONAL INSTABILITY. A CHECK FOR THIS CONDITION IS ILLUSTRATED ON THE FOLLOWING PAGE.

US Army Corps of Engineers

Example E-3	21 of 23	Box System

Figure E–2. Building with a box system—continued.

TORSION CHECK (SEE PARA. 4-4c(5)(b), 5-5a(4)(d), 5-4i)

- ASSUME :
  - WALL 1 STIFFNESS REDUCED BY 1.5
  - WALL 3 STIFFNESS REDUCED BY 1.5
  - ECCENTRICITY, e_x, INCREASES FROM 15.7′ TO 29.0′

TORSIONAL MOMENT: (SEE SHEET 8)

CALCULATED $M_T = V_x e_x = 804\,(29')$ = 23316 k-ft

ACCIDENTAL $M_T = V_x e_{max} = 804\,(29'+9.6')$ = 31034 k-ft

$M_T = V_x e_{min} = 804\,(29'-9.6')$ = 15598 k-ft

	DIRECT SHEAR		TORSIONAL SHEAR				DIRECT + TORSION		
WALL	R	V_D	d	Rd^2	$V_T^{(1)}$	$V_T^{(2)}$	$V_D+V_T^{(1)}$	$V_D+V_T^{(2)}$	2*EQ-I(3)
1	18.0	95	125	281250	75	100	170	195	194
3	30.0	159	61	111630	61	82	220	241	256
5	44.9	238	-3	404	-4	-3	234	235	201
7	58.8	312	-67	263953	-132	-88	180	224	243
	151.7	804					804		
A	35.6	0	23.6	19794					
C	35.6	0	23.6	19794					
				696825					

(1) BASED ON CALCULATED TORSIONAL MOMENT M_T = 23316.
(2) BASED ON GOVERNING ACCIDENTAL M_T = 31034 OR M_T = 15598.
(3) EQ-I VALUES FROM SHEET 9 (EQ-II = 2*EQ-I).

COMMENT. THE CASE SHOWN HERE ASSUMES THAT WALLS 1 & 3 HAVE REDUCED STIFFNESS DUE TO CRACKING AND THUS ATTRACT A SMALLER PROPORTION OF THE DIRECT SHEAR THAN IN THE ELASTIC ANALYSIS. THE SHIFT IN THE C.R. RESULTS IN A LONGER MOMENT ARM, d, THUS THEY ATTRACT MORE TORSIONAL SHEAR. A COMPARISON OF THE COMBINED SHEARS FOR THE ELASTIC CASE OR ASSUMED INELASTIC CASE (2 RIGHTHAND COLUMNS) SHOWS NO SUBSTANTIAL CHANGE, THEREFORE INELASTIC TORSION IS NOT CRITICAL.

US Army Corps of Engineers

Example E-2 22 of 23 Box System

Figure E-2. Building with a box system—continued.

EQ-II : COMMENTARY

- THE RATIO OF THE SPECTRAL ACCELERATIONS FOR EQ-II TO EQ-I IS .56/.28 = 2.0 IN THIS EXAMPLE. THE DETAILS OF THE EQ-II ANALYSIS ARE NOT SHOWN HERE SINCE ALL OF EQ-I RESULTS ($V, M_T, M_{OT}, {}^{v_D}/v_c, \Delta$, etc.) ARE INCREASED BY A FACTOR OF 2.0, AND THE CALCULATED PERIOD IS INCREASED BY $\sqrt{2.0}$. FOR EXAMPLE, PIER 7 OF WALL 3 WOULD HAVE A SHEAR OF $2 \times 51 = 102^k$, A MOMENT OF 1728 ft-k, AND INELASTIC DEMAND RATIOS OF .24 AND 1.68 FOR SHEAR AND BENDING, RESPECTIVELY.
- THE WALLS ON LINES 1 & 3 WILL YIELD BEFORE THE WALLS ON LINES 5 & 7, BUT THE EFFECTS OF INELASTIC TORSION WERE INVESTIGATED AND FOUND TO BE INSIGNIFICANT.
- TABLE 4-2 SHOWS THAT INELASTIC DEMAND RATIOS FOR CONCRETE WALLS IN AN ESSENTIAL FACILITY ARE NOT TO EXCEED 1.25 IN SHEAR OR 1.5 IN FLEXURE. THE RESULTS FOR EQ-II ARE SHOWN BELOW.

	LOCATION OF MAX.		INELASTIC DEMAND RATIOS	
	WALL	PIER	ACTUAL MAX.	ALLOWED MAX
SHEAR	1	1,5	0.44	1.25
FLEXURE	3	7	1.68*	2.0

*ACTUALLY LESS THAN 1.0 WHEN DEAD LOAD EFFECTS ARE INCLUDED.

THUS, THE SHEAR WALLS ARE ALSO ADEQUATE FOR EQ-II APPLIED IN EITHER THE TRANSVERSE OR LONGITUDINAL DIRECTION.

US Army Corps of Engineers

Figure E-2. Building with a box system—continued.

DESIGN EXAMPLE: E-3

BUILDING WITH STEEL MOMENT-RESISTING SPACE FRAMES AND STEEL BRACED FRAMES:

Description of Structure. A 3-story hospital building with transverse ductile moment-resisting frames and longitudinal braced frames in structural steel, using nonstructural exterior curtain walls of flexible insulated metal panels. In addition, there are a series of interior vertical load-carrying column and girder bents. The structural concept is illustrated in the Basic Design Manual, design example A-3.

Initial Trial Structure. The building in design example A-3 of the Basic Design Manual was designed for a base shear (V = ZIKCSW) of 0.08W in the transverse direction and 0.14W in the longitudinal direction. In order to utilize the same structure in this example, the following conditions are assumed:

	Transverse	Longitudinal
Seismic Zone 3	Z = 3/4	Z = 3/4
Hospital building	I = 1.5	I = 1.5
Ductile frame/braced frame	K = 0.67	K = 1.0
Soil period	T_s = 1.0 sec	T_s = 1.0 sec
Building period	T = 0.69 sec	F = 0.3 sec
	CS = 0.116	CS = 0.140
	ZIKCS = 0.087	ZIKCS = 0.157

The above base shears (0.087W and 0.157W) are reasonably close to the base shears of the building in design example A-3 of the Basic Design Manual so that building will be used for the initial trial design.

Seismic Design Criteria. The building is to be designed in accordance with the dynamic analysis procedures of this manual. The following conditions apply:

Building classification: Essential facility
Ground motion spectra: ATC 3-06 spectra with $A_a = A_v = 0.30$
Soil profile coefficient: Type S_2

US Army Corps of Engineers

Figure E-3. Building with steel moment-resisting frames and steel braced frames.

Design Procedure. The site response spectra are developed in accordance with the procedure described in chapter 3. The governing equations and spectra for EQ-I and EQ-II, shown on sheets 3 and 4, include the effects of site severity, soil type, and structural damping. The structure of Basic Design Manual design example A-3 is assumed to be the initial trial design (para 5-3a). The EQ-I design spectrum is compared to the static base shear coefficients ZICS as follows:

	T, period (estimate)	$S_a(g)$	ZICS	Ratio $S_a \div$ ZICS
Transverse	0.69 sec	0.35	0.130	2.7
Longitudinal	0.3 sec	0.41	0.157	2.6

These ratios of S_a to ZICS are greater than 2. This is an indication that the structure may have to be modified for the higher force level. Because the ratio is less than 3, it has been decided to continue with the procedure without modifying the structure at this time.

The example building is a steel frame structure with lateral forces resisted by ductile frames in the transverse direction and braced frames in the longitudinal direction. The metal deck roof system forms a flexible diaphragm while the metal deck with concrete fill forms rigid diaphragms at the second- and third-floor levels. The procedure used to distribute the forces is discussed on sheet 5.

An outline of the procedures for the transverse direction and the longitudinal direction are given below:

US Army Corps of Engineers

Example E-3 2 of 34 Steel Frames

Figure E-3. Building with steel moment-resisting frames and steel braced frames—continued.

DETERMINATION OF SITE RESPONSE SPECTRA

SITE SEVERITY

SEE FIGURES 3-40 TO 3-43 AND TABLE 3-4

	ATC 3-06	EQ-I	EQ-II
A_a A_v	0.30g 0.30g	0.14g 0.14g	0.35g 0.35g

SOIL PROFILE COEFFICIENT, S_i

ASSUME SOIL PROFILE TYPE S_2

FROM TABLE 3-6, $S_i = 1.2$

DAMPING ADJUSTMENT FACTORS

DAMPING FROM TABLE 4-1, DAMPING FACTORS FROM TABLE 3-7

	DAMPING	DAMPING FACTOR
EQ-I EQ-II	3% 7%	1.17 0.90

GOVERNING EQUATIONS (EQ. 3-27, 3-28)

$$\text{EQ-I}: \quad S_a = 1.17\,(1.22) A_v S_i / T = 1.17(1.22)(.14)(1.2)/T$$
$$= .2398/T \leq 1.17(2.5)A_a = .41$$

$$\text{EQ-II}: \quad S_a = .9\,(1.22) A_v S_i / T = .9(1.22)(.35)(1.2)/T$$
$$= .4612/T \leq .9(2.5)A_a = .79$$

$$\text{EQ-II}_{MAX} / \text{EQ-I}_{MAX} = 1.93$$

US Army Corps of Engineers

Figure E-3. Building with steel moment-resisting frames and steel braced frames—continued.

DESIGN RESPONSE SPECTRA FOR EQ-I AND EQ-II

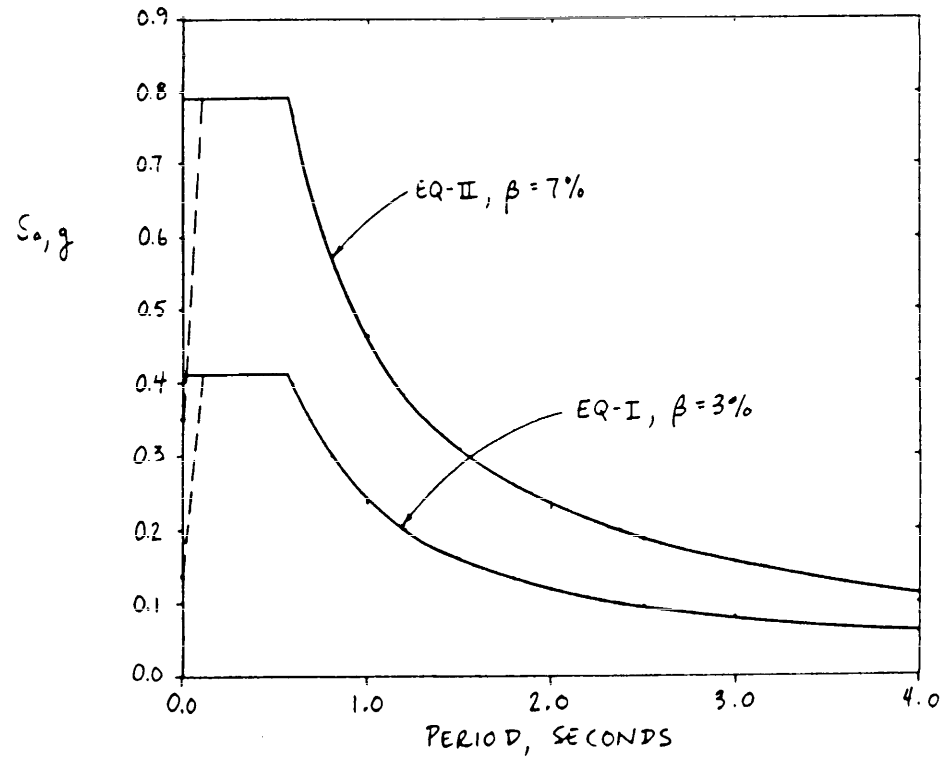

EQ	β		PERIOD							
			0.0	.586	.80	1.0	1.5	2.0	3.0	4.0
EQ-I	3%	S_a, g	.14	.41	.300	.240	.160	.120	.080	.060
EQ-II	7%	S_a, g	.35	.79	.576	.461	.307	.231	.154	.115
		S_d^*, in	0	2.66	3.61	4.51	6.76	9.04	13.57	18.01

*SPECTRAL DISPLACEMENT $S_d = S_a (T/2\pi)^2 g$

US Army Corps of Engineers

Example E-3 4 of 34 Steel Frames

Figure E-3. Building with steel moment-resisting frames and steel braced frames—continued.

DISTRIBUTION OF FORCES FOR DYNAMIC ANALYSIS

THE DISTRIBUTION OF FORCES TO THE FRAMES WHICH WAS DEVELOPED FOR THE STATIC ANALYSES IS SHOWN ON PAGE 11 OF 34 OF EXAMPLE A-3 IN THE DESIGN MANUAL. IT IS ASSUMED THAT THE TRANSVERSE FRAMES ON LINES 1, 4 AND 7 ARE IDENTICAL, AS ARE THE TWO LONGITUDINAL FRAMES ON LINES A AND C. FORCES AT THE ROOF ARE DISTRIBUTED BY TRIBUTARY AREAS, BECAUSE OF A FLEXIBLE DIAPHRAGM, AND BY RELATIVE RIGIDITIES AT THE 2ND AND 3RD FLOORS. WHILE THERE IS NO "CALCULATED" TORSION IN THE BUILDING, AN "ACCIDENTAL" TORSIONAL SHEAR IS DISTRIBUTED TO FRAMES 1, 7, A, AND C.

FOR THE DYNAMIC ANALYSES, COMPUTER MODELS WERE DEVELOPED FOR FRAME 4, THE MOST HEAVILY LOADED OF THE THREE TRANSVERSE FRAMES, AND FRAME A, REPRESENTATIVE OF THE TWO LONGITUDINAL FRAMES. THE PROPERTIES OF THE FRAME 4 MODEL ARE SHOWN ON PAGE 17 OF 34 (EX. A-3). ONE HALF THE ROOF MASS AND ONE THIRD OF THE MASS AT EACH FLOOR ARE CARRIED BY FRAME 4 IN THE TRANSVERSE DIRECTION, CONSISTENT WITH THE DISTRIBUTION DISCUSSED ABOVE. FOR THE LONGITUDINAL ANALYSES, ONE HALF THE BUILDING MASS IS TAKEN BY FRAME A AT EACH LEVEL. THE SHEARS RESULTING FROM THE EQ-I AND EQ-II MODAL ANALYSES WILL BE INCREASED BY 18% ($.59F_L / .50F_L$) IN ORDER TO ACCOUNT FOR THE TORSIONAL SHEAR AT THE 2ND AND 3RD FLOORS.

US Army Corps of Engineers

Example E-3	5 of 34	Steel Frames

Figure E-3. Building with steel moment-resisting frames and steel braced frames—continued.

TRANSVERSE (N-S) DIRECTION : FRAME 4 - DMRSF

MODES SHAPES (ϕ_{xm}) AND PERIODS (T_m) FROM COMPUTER ANALYSIS OF FRAME 4, MASS CALCULATED FROM W/g.

LEVEL	MASS ($\frac{k\text{-}sec^2}{ft.}$)	MODE 1			MODE 2			MODE 3		
		ϕ_{x1}	$m_x\phi_{x1}$	$m_x\phi_{x1}^2$	ϕ_{x2}	$m_x\phi_{x2}$	$m_x\phi_{x2}^2$	ϕ_{x3}	$m_x\phi_{x3}$	$m_x\phi_{x3}^2$
R	5.81	.3320	1.929	.640	.2384	1.385	.330	.0713	.4143	.030
3	7.32	.2044	1.496	.306	-.2201	-1.611	.355	-.2154	-1.577	.340
2	7.32	.0860	.630	.054	-.2075	-1.519	.315	.2936	2.149	.631
Σ	20.45		4.055	1.000**		-1.745	1.000		.9863	1.001
PF_{Rm}^* (Eq. 4-1)		$\frac{\Sigma m\phi}{\Sigma m\phi^2}\cdot\phi_{R1}$ = 1.346			-.416			.070		
PF_{3m}		.829			.384			-.212		
PF_{2m}		.349			.362			.289		
α_m (Eq. 4-2)		$\frac{(\Sigma m\phi)^2}{\Sigma m(\Sigma m\phi^2)}$ = .8040			.149			.048		
T_m, sec.		.964			.356			.182		

*AS A CHECK, NOTE THAT $\sum_{m=1}^{3} PF_{xm} = 1.0$ AND $\sum_{m=1}^{3} \alpha_m = 1.0$.

**THE COMPUTER PROGRAM NORMALIZES THE RESULTS SO THAT $\Sigma m\phi^2 = 1.0$.

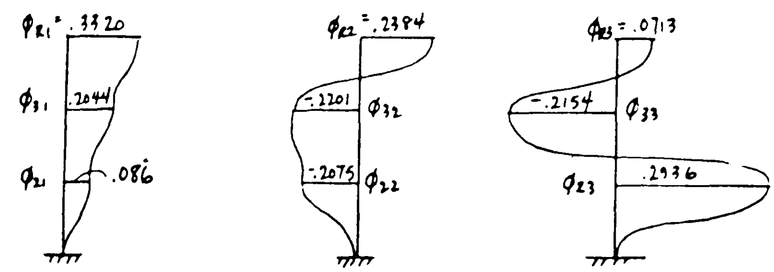

MODE 1 MODE 2 MODE 3

US Army Corps of Engineers

Figure E-3. Building with steel moment-resisting frames and steel braced frames—continued.

TRANSVERSE (N-S) DIRECTION : SPECTRAL ACCELERATIONS, S_{am}
MODAL BASE SHEARS, V_m

EQ		MODE 1	MODE 2	MODE 3
EQ-I (β=3%)	T_m, sec (SHEET 6) S_{am}, g (SHEET 4) $C_{bm} = \alpha_m S_{am}$ $V_m = C_{bm} W = C_{bm}(\Sigma m g)$ (EQ. 4-4)	.964 .251 .202 132.7 k	.356 .41 .061 40.2 k	.182 .41 .020 13.0 k
EQ-II (β=7%)	$T_m \sqrt{1.25}$*, sec S_{am}, g (SHEET 4) $C_{bm} = \alpha_m S_{am}$ $V_m = C_{bm} W$	1.078 .428 .344 226.5 k	.398 .79 .118 77.5 k	.204 .79 .038 25.0 k

* NOTE : FOR THE EQ-II ANALYSIS, AS A ROUGH APPROXIMATION, ASSUME THE PERIOD HAS LENGTHENED BY $\sqrt{X}$, WHERE X REPRESENTS THE INELASTIC DEMAND RATIO FOR THE CRITICAL ELEMENTS IN THE FRAME AS SHOWN IN TABLE 4-2. IN THIS EXAMPLE, X = 1.25 FOR COLUMNS IN A STEEL DMRSF IN A CRITICAL AND ESSENTIAL FACILITY. THE COMPUTER MODEL USED FOR THE EQ-II ANALYSIS HAS A REDUCED ELASTIC MODULUS IN ORDER TO OBTAIN THE LONGER PERIOD ($E_{EQ-II} = E_{EQ-I} / X$).

US Army Corps of Engineers

Example E-3 7 of 34 Steel Frames

Figure E-3. Building with steel moment-resisting frames and steel braced frames—continued.

MODAL ANALYSIS: TRANSVERSE (N-S) DIRECTION - FRAME 4

		LEVEL	PF_{xm}	$\frac{m_x \phi_{xm}}{\Sigma m_x \phi_{xm}}$	F_{xm} (k)	V_{xm} (k)	ΔOTM_{xm} (ft-k)	OTM_{xm} (ft-k)	$a_{xm} = \frac{F_{xm}}{W_x}$	δ_{xm} (in)	Δ_{xm} (in)
MODE 1	EQ-I	R	1.346	.476	63.2	63.2	772	0	.337	3.065	1.182
		3	.829	.369	48.9	112.1	1233	772	.208	1.892	1.101
		2	.349	.155	20.6	132.7	1416	2005	.087	.791	.791
				1.000				3421			
	EQ-II	R			107.8	107.8	1316	0	.576	6.551	2.525
		3			83.6	191.4	2105	1316	.354	4.026	2.331
		2			35.1	226.5	2417	3421	.149	1.695	1.695
								5838			
MODE 2	EQ-I	R	-.416	-.793	-31.9	-31.9	-389	0	-.171	-.212	.407
		3	.384	.923	37.1	5.2	57	-389	.157	.195	.011
		2	.362	.870	35.0	40.2	429	-332	.148	.184	.184
				1.000				97			
	EQ-II	R			-61.4	-61.4	-750	0	-.329	-.612	1.176
		3			71.5	10.1	111	-751	.303	.564	.032
		2			67.4	77.5	827	-639	.286	.532	.532
								188			
MODE 3	EQ-I	R	.070	.420	5.5	5.5	67	0	.029	.0094	.037
		3	-.212	-1.599	-20.8	-15.3	-168	67	-.087	-.028	.066
		2	.289	2.179	28.3	13.0	139	-101	.118	.038	.038
				1.000				38			
	EQ-II	R			10.5	10.5	128	0	.055	.027	.108
		3			-40.0	-29.5	-324	128	-.167	-.081	.191
		2			54.5	25.0	267	-196	.228	.110	.110
								70			
SRSS	EQ-I	R			71.0	71.0	867	0	.379	3.072	1.251
		3			64.8	113.3	1246	867	.275	1.893	1.094
		2			49.5	139.3	1486	2035	.208	.812	.813
								3423			
	EQ-II	R			124.5	124.5	1520	0	.666	6.580	2.788
		3			117.1	193.9	2133	1520	.495	4.066	2.339
		2			93.5	240.7	2568	3653	.395	1.780	1.780
								6221			

US Army Corps of Engineers

Example E-3 8 of 34 Steel Frames

Figure E-3. Building with steel moment-resisting frames and steel braced frames—continued.

MODAL ANALYSIS - INFLUENCE OF HIGHER MODES

HIGHER MODES OF RESPONSE BECOME INCREASINGLY IMPORTANT AS A BUILDING GETS TALLER OR MORE IRREGULAR. FOR THIS REGULAR 3-STORY STRUCTURE, THE FIRST MODE DOMINATES THE LATERAL RESPONSE. A COMPARISON OF THE MODAL STORY SHEARS AND THE SRSS STORY SHEARS IS SHOWN BELOW. FOR EXAMPLE, IF ONLY THE 1ST MODE SHEARS HAD BEEN USED FOR ANALYSIS, THIS REPRESENTS 89% OF THE SRSS SHEAR AT THE ROOF, 99% AT THE 3RD FLOOR AND 95% AT THE 2ND FLOOR. WHILE THE 2ND MODE SHEAR AT THE ROOF IS 50% OF THE 1ST MODE SHEAR, WHEN COMBINED ON AN SRSS BASIS THE 1ST MODE ACCOUNTS FOR 79% OF THE SRSS RESPONSE WITH 20% FOR THE 2ND MODE AND 0.6% FOR THE 3RD MODE. THESE PERCENTAGES ARE 91%, 8% AND 1% AT THE BASE.

STORY SHEARS - EQ-I

		MODE 1			MODE 2		MODE 3	
LEVEL	V_{SRSS}	V_1	V_1/V_{SRSS}	$(V_1/V_{SRSS})^2$	V_2	$(V_2/V_{SRSS})^2$	V_3	$(V_3/V_{SRSS})^2$
R	71.0	63.2	.89	.79	-31.9	.202	5.5	.006
3	113.3	112.1	.989	.98	5.2	.002	-15.3	.018
2	139.3	132.7	.953	.91	40.2	.083	13.0	.009

THE EFFECTIVE MODAL WEIGHT FACTOR, α_m, ALSO SHOWS THE RELATIVE IMPORTANCE OF EACH MODE. IN THIS EXAMPLE, ($\alpha_1=.804$, $\alpha_2=.149$, $\alpha_3=.048$), 80.4% OF THE BUILDING MASS PARTICIPATES IN THE 1ST MODE, 14.9% IN THE 2ND MODE AND 4.8% IN THE 3RD MODE.

US Army Corps of Engineers

Figure E-3. Building with steel moment-resisting frames and steel braced frames—continued.

EQ-I ELEMENT FORCES : TRANSVERSE (N-S) DIRECTION - FRAME 4

- DL & LL RESULTS FROM DESIGN MANUAL EXAMPLE A-3, SHEET 18 OF 34.
- SEISMIC RESULTS FROM COMPUTER ANALYSIS.
- ALL END MOMENTS AND SHEARS GIVEN AT FACE OF SUPPORT.
- UNITS ARE K, K-ft.

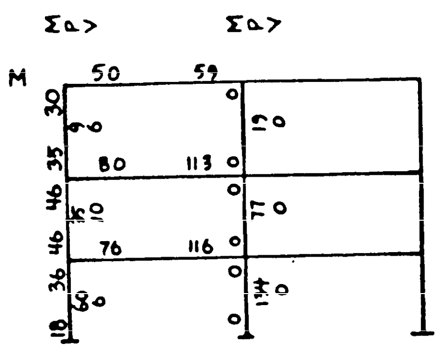

DEAD LOAD

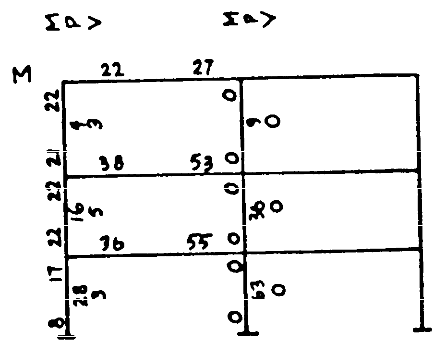

LIVE LOAD

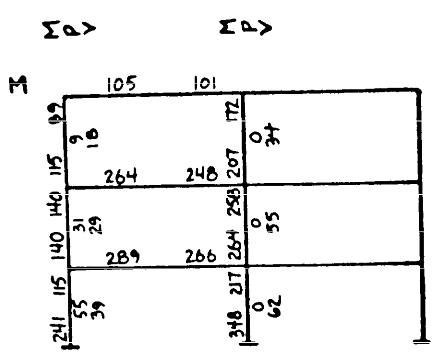

SEISMIC - EQ-I SRSS

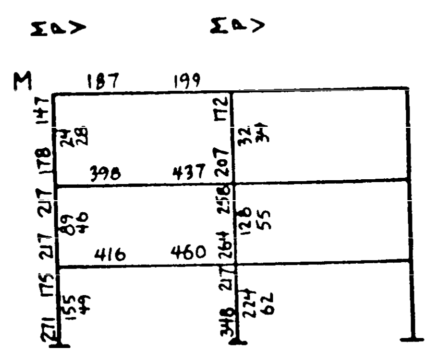

TOTAL = 1.2D + 1.0L + 1.0E (Eq. 4-6)

US Army Corps of Engineers

Figure E–3. Building with steel moment-resisting frames and steel braced frames—continued.

EQ-II ELEMENT FORCES : TRANSVERSE (N-S) DIRECTION - FRAME 4

- DL & LL RESULTS FROM DESIGN MANUAL EXAMPLE A-3, SHEET 18 OF 34.
- SEISMIC RESULTS FROM COMPUTER ANALYSIS.
- ALL END MOMENTS AND SHEARS GIVEN AT FACE OF SUPPORT.
- UNITS ARE K, K-ft.

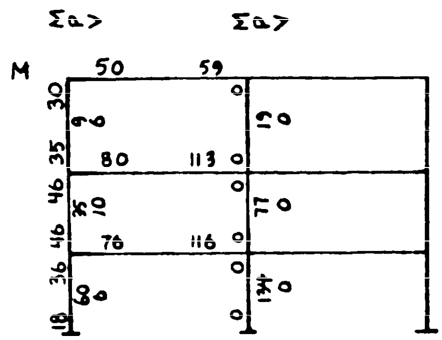

DEAD LOAD

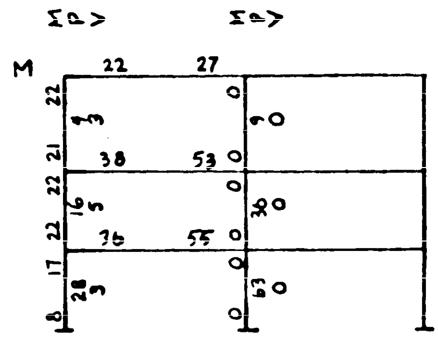

LIVE LOAD

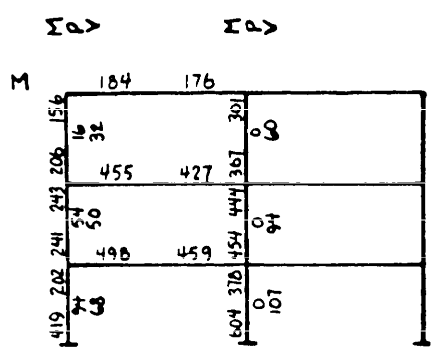

SEISMIC - EQ-II SRSS

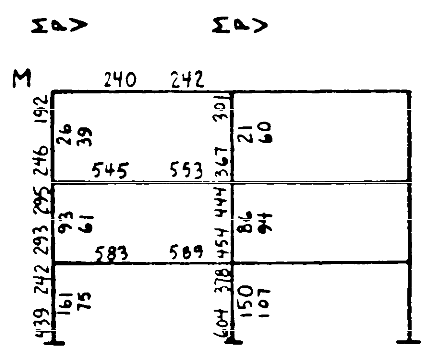

TOTAL = 1.0D + .25L + 1.0E (Eq. 4-9)

US Army Corps of Engineers

Figure E–3. Building with steel moment-resisting frames and steel braced frames—continued.

CHECK ELEMENT STRESSES

FOR EQ-I USE 1.7 * ALLOWABLE STRESSES (SEE AISC, 8^{TH} EDITION, SECTION 1.5) OR USE STRENGTH DESIGN CRITERIA. COMPARE DEMAND FORCES TO CAPACITY FORCES AND REVIEW FOR ELASTIC, OR NEARLY ELASTIC BEHAVIOR (SEE para. 4-3e(1)). FOR THE DMRSF IN THE TRANSVERSE DIRECTION, 20% OF THE BEAMS AND 10% OF THE COLUMNS AT ANY STORY ARE ALLOWED TO EXCEED THE FLEXURAL STRENGTH REQUIREMENTS BY UP TO 25%. FOR THE BRACED FRAMES IN THE LONGITUDINAL DIRECTION (K=1.0), 20% OF THE BEAMS AND 10% OF THE COLUMNS AT ANY STORY ARE ALLOWED TO EXCEED THE FLEXURAL STRENGTH REQUIREMENTS BY UP TO 10%. NO OVERSTRESS IS ALLOWED FOR THE K-BRACES.

FOR EQ-II COMPARE DEMAND FORCES TO THE PLASTIC MEMBER CAPACITIES IN ORDER TO COMPUTE THE INELASTIC DEMAND RATIOS. SEE FIGURE 4-1 FOR STEEL BEAMS AND FIGURE 4-2 FOR STEEL COLUMNS. THE ALLOWABLE DUCTILITIES OR INELASTIC DEMAND RATIOS ARE SHOWN IN TABLE 4-2. FOR THE TRANSVERSE DMRSF, THE ALLOWABLE RATIOS ARE 2.0 FOR BEAMS AND 1.25 FOR COLUMNS (EXCEPT P/P_{cr} MUST BE LESS THAN 1.0). FOR THE BRACED FRAMES, THE ALLOWABLE RATIOS ARE 1.5 FOR BEAMS, 1.25 FOR COLUMNS, AND 1.0 FOR K-BRACES.

US Army Corps of Engineers

Example E-3 12 of 34 Steel Frames

Figure E-3. Building with steel moment-resisting frames and steel braced frames—continued.

ELEMENT STRESSES - FRAME 4 (DMRSF)

BEAM ELEMENTS : EQ-I $EC \geq 1.2D + 1.0L + 1.0E$ (EQ. 4-6)
EQ-II $UC \geq 1.0D + .25L + 1.0E$ (EQ. 4-9)

LEVEL	SIZE	Z_x (in^3)	EQ-I M_D (k-ft)	EQ-I M_C* (k-ft)	EQ-I M_D/M_C	EQ-II M_D (k-ft)	EQ-II M_C* (k-ft)	EQ-II M_D/M_C	IDR**
ROOF	W14×30	47.3	199	142	1.40	242	142	1.70	2.0
3	W18×55	112	437	336	1.30	553	336	1.65	2.0
2	W18×60	123	460	369	1.25	589	369	1.60	2.0

*USE $M_C = M_{px} = Z_x F_y$, $F_y = 36$ ksi
** INELASTIC DEMAND RATIO FROM TABLE 4-2

COMMENT
- FOR EQ-I, THE RATIO OF MOMENT DEMAND TO MOMENT CAPACITY IS LIMITED TO 1.0 FOR MOST ELEMENTS BUT IS ALLOWED TO REACH UP TO 1.25 FOR A LIMITED NUMBER OF ELEMENTS IN ACCORDANCE WITH THE "NEARLY ELASTIC" CRITERIA (SEE PARA. 4-3e(1)(a)). THESE LIMITS HAVE BEEN EXCEEDED FOR EQ-I.

US Army Corps of Engineers

Example E-3 13 of 34 Steel Frames

Figure E-3. Building with steel moment-resisting frames and steel braced frames—continued.

ELEMENT STRESSES - FRAME 4 (CONT'NUED)

STEEL COLUMNS 1ST STORY @ BASE (SEE DESIGN MANUAL EXAMPLE A-3) SHEET 21 OF 34)

EQ-I $EC \geq 1.2D + 1.0L + 1.0E$

SIZE	A (in^2)	S_x (in^3)	EQ - I P_D (k)	M_D (k-ft)	f_a (ksi)	f_{bx} (ksi)	F_a (ksi)	F_{bx} (ksi)	F'_{ex} (ksi)	** EQ1.6-1a	** EQ.1.6-1b
W14x48	14.1	70.3	155	271	11.0	46.3	17.2	24	361	0.84	1.43
W14x61	17.9	92.2	224	348	12.5	45.3	18.4	24	377	0.85	1.45

** MODIFIED UNIAXIAL INTERACTION EQUATIONS USING $1.7F_{allow}$

EQ1.6-1a $\dfrac{f_a}{1.7F_a} + \dfrac{C_{mx} f_{bx}}{\left(1 - \dfrac{f_a}{1.7F'_{ex}}\right) 1.7F_{bx}} \leq 1.0$, EQ1.6-1b $\dfrac{f_a}{1.7(.6F_y)} + \dfrac{f_{bx}}{1.7F_{bx}} \leq 1.0$

EQ-II $UC \geq 1.0D + .25L + 1.0E$

SIZE	A (in^2)	Z_x (in^3)	EQ- II P_D (k)	M_D (k-ft)	M_D (k-in)	$P_y = AF_y$ (k)	$P_{cr} = 1.7AF_a$ (k)	$M_{px} = Z_x F_y$ (k-in)	M_{pcx} (k-in)	$\dfrac{M_x}{M_{pcx}}$ †	IDR (TABLE 4-2)
W14x48	14.1	78.4	161	439	5268	507.6	412.3	2822	2333	2.26	1.25
W14x61	17.9	102	150	604	7248	644.4	559.9	3672	3324	2.18	1.25

† SEE FIGURE 4-2, $M_x / M_{cpx} < \mu$ (μ = IDR)

US Army Corps of Engineers

Example E-3	14 of 34	Steel Frames

Figure E–3. Building with steel moment-resisting frames and steel braced frames—continued.

CHECK INTERSTORY DRIFT

ALLOWABLE DRIFT FOR ESSENTIAL FACILITIES:
.005 * STORY HEIGHT FOR EQ-I (par. 4-3(c)(7)(a))
.010 * STORY HEIGHT FOR EQ-II (par. 4-4(c)(2)(a))

TRANSVERSE (N-S) DIRECTION - FRAME 4

LEVEL	STORY HT. h, in	EQ - I		EQ - II	
		Δ_{sess}, in*	.005h	Δ_{sess}, in*	.010h
ROOF	147	1.251	.733	2.788	1.465
3	132	1.094	.660	2.339	1.320
2	128	.813	.640	1.780	1.280

* Δ_{srss} VALUES FROM SHEET 8.

• THE ALLOWABLE DRIFT LIMITS ARE EXCEEDED AT EVERY LEVEL OF FRAME 4 FOR BOTH EQ-I AND EQ-II.

US Army Corps of Engineers

Example E-3 15 of 34 Steel Frames

Figure E-3. Building with steel moment-resisting frames and steel braced frames—continued.

FRAME 4 (DMRSF) - COMMENTARY

EQ-I THE ELASTIC ANALYSIS OF FRAME 4 FOR EQ-I SHOWS THAT THE FIRST FLOOR COLUMNS AND ALL OF THE BEAMS ARE OVERSTRESSED, AND THE ALLOWABLE DRIFT LIMITS HAVE BEEN EXCEEDED. THE FRAME HAS EXCEEDED THE "NEARLY ELASTIC" CRITERIA SINCE THE OVERSTRESS RATIOS FOR BOTH BEAMS AND COLUMNS ARE GREATER THAN THE 1.25 ALLOWED FOR DUCTILE FRAMING SYSTEMS.

FRAME 4 INCLUDES 1/3 OF THE SEISMIC RESISTING ELEMENTS IN THE TRANSVERSE DIRECTION, AND WAS INITIALLY SELECTED FOR ANALYSIS BECAUSE IT CARRIES MORE LOAD THAN EITHER OF THE END FRAMES. A SIMILAR ANALYSIS FOR FRAMES 1 & 7 MIGHT RESULT IN LOWER STRESS RATIOS FOR THESE FRAMES BUT THE BUILDING AS A WHOLE STILL WOULD NOT MEET THE "NEARLY ELASTIC" CRITERIA.

EQ-II - METHOD 1 THE EQ-II ANALYSIS FOLLOWED THE ELASTIC PROCEDURE DESCRIBED AS METHOD 1 IN PARAGRAPH 4-4c. THE INELASTIC DEMAND RATIOS FOR THE FIRST FLOOR COLUMNS ARE GREATER THAN THE 1.25 WHICH IS ALLOWED, AND THE DRIFT LIMITS HAVE BEEN EXCEEDED.

EQ-II - METHOD 2 WHILE FRAME 4 DOES NOT HAVE SUFFICIENT CAPACITY TO RESIST EITHER EQ-I OR EQ-II, A FURTHER CHECK WAS PERFORMED TO SHOW AN EXAMPLE OF METHOD 2 DESCRIBED IN PARAGRAPH 4-4d. THIS IS SHOWN ON THE FOLLOWING PAGES.

US Army Corps of Engineers

Example E-3 | 16 of 34 | Steel Frames

Figure E-3. Building with steel moment-resisting frames and steel braced frames—continued.

METHOD 2: CAPACITY SPECTRUM METHOD FOR TRANSVERSE DIRECTION RESPONSE TO EQ-II
REFER TO PARA 4-4d AND PARA 5-5b.

DETERMINE ELASTIC CAPACITY RATIO TO EQ-I.
USE EQ-II LOAD FACTORS. (PARA 5-5b(3)(a)-(d)

BEAM ELEMENTS: REFER TO SHEETS 10 AND 13

LEVEL	SIZE	EC	D	.25L	NET*	E_I	ECR
ROOF	W 14×30	142	59	7	76	101	0.75
3RD	W 18×55	336	113	13	210	248	0.85
2ND	W 18×60	369	116	14	239	266	0.90

* NET EARTHQUAKE CAPACITY = EC - D - .25L (eq 5-7)
E_I = EQ-I DEMANDS
ECR = ELASTIC CAPACITY RATIO = NET*/E_I

INDICATES FIRST YIELD AT 0.75 EQ-I - BUT CHECK THE COLUMNS

COLUMN ELEMENTS: REFER TO SHEETS 10 AND 14

LEVEL	SIZE	0.75 EQ-I P_D	0.75 EQ-I M_D	f_a	f_b	EQ 1.6-1b SHT 14	
BASE	W 14×48	108	201	7.7	34.3	1.13	YIELD AT BASE PRIOR TO BMS.
BASE	W 14×61	150	261	8.4	34.0	1.06	
BASE$^\Delta$	W 14×48	26	162	1.2	27.6	0.77	

P_D AND M_D = D + 0.25L + 0.75(EQ-I)
Δ SEISMIC FORCES OPPOSITE DIRECTION TO GRAVITY.

FIRST YIELD: $\frac{0.75}{1.13}$ × EQ-I = 0.66 TIMES EQ-I

(REFER TO SHEET 7)

	MODE 1	MODE 2	MODE 3	SRSS
BASE SHEAR COEF, C_B, EQ-I	0.202	0.061	0.020	0.212
YIELD AT 0.66 × EQ-I	0.133	0.040	0.013	0.140

CAPACITY CURVE DATA: YIELD SRSS, C_B = 0.14
1st MODE, C_B = 0.13

USE 1ST MODE VALUES TO PLOT CURVE. SEE SHEET 18, 19, 20

US Army Corps of Engineers

Example E-3 17 of 34 Steel Frames

Figure E-3. Building with steel moment-resisting frames and steel braced frames—continued.

It has been determined that the seismic base shear coefficient (in terms of first mode values) could reach a value of 0.13 before any yielding would occur in the structural frame. For seismic forces applied towards the north (towards the right on sheet 19), the base of the north (right) column and the center column will yield in flexure (the column bases were assumed fixed). The south (left) column does not yield because both the dead and live load stresses are counter-balancing some of the lateral load stresses. At a base shear coefficient of 0.13, the spectral acceleration is 0.161g, the spectral displacement is 1.43 inches, the roof displacement is 1.93 inches, and the period is 0.97 second (refer to sheet 20).

A new mathematical model is constructed that allows the base of two columns to yield in flexure. A nominal lateral force is applied. The relative distribution of beam moments will vary from the distribution of beam moments shown on sheet 10 for seismic forces. New values for periods, mode shapes, and participation factors are calculated. The forces are proportionally adjusted until a number of additional structural elements begin to yield (±5% of calculated yield capacity). At an additional equivalent base shear coefficient of 0.06, yielding occurs at the base of the third (left) column, the tops of the other two first-story columns, the top and bottom of the second-story center column, and the north end of the first- and second-story beams (Model 3 on sheet 19). The period of this revised model is 1.14 seconds and the roof displacement is 1.10 inches for the base shear of 0.06. When the results of this model are superimposed on the initial model, the following results are obtained: base shear is 0.19 (0.13 + 0.06), spectral acceleration is 0.224g, spectral displacement is 2.27 inches, the roof displacement is 3.02 inches, and the effective period is 1.02 seconds. These results are summarized on sheet 20.

The mathematical model is revised again to allow the newly formed hinges to yield. These hinges were given sectional properties roughly equal to 5% of their fully elastic value. An additional set of periods, mode shapes, and participation factors are calculated. New increments of force are applied until additional hinges form and a mechanism forms at the first floor (see model 4 on sheet 19). The period for this last increment of displacement is 2.29 seconds, the base shear coefficient is 0.04, and the roof displacement is 2.69 sec-inches. When these results are superimposed on the previous results, the following values were obtained: base shear is 0.23, spectral acceleration is 0.257g, spectral displacement is 4.45 inches, roof displacement is 5.71 inches, and the effective period of vibration is 1.33 seconds (refer to sheet 20).

US Army Corps of Engineers

Example E-3 | 18 of 34 | Steel Frames

Figure E-3. Building with steel moment-resisting frames and steel braced frames—continued.

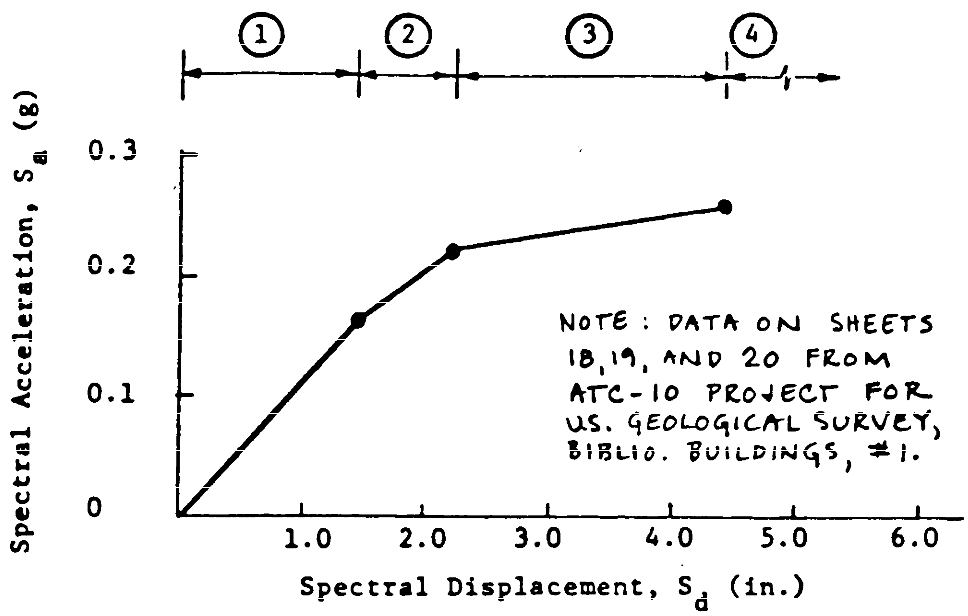

CAPACITY CURVE

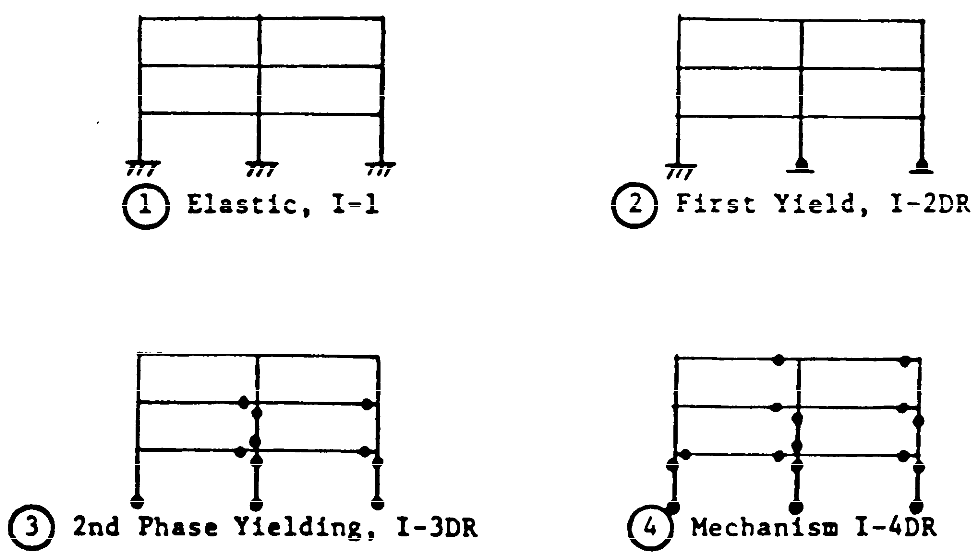

MODELS

METHOD 2 MODELS AND CAPACITIES

US Army Corps of Engineers

Example E-3	19 of 34	Steel Frames

Figure E-3. Building with steel moment-resisting frames and steel braced frames—continued.

DEFLECTED SHAPES (INCHES)

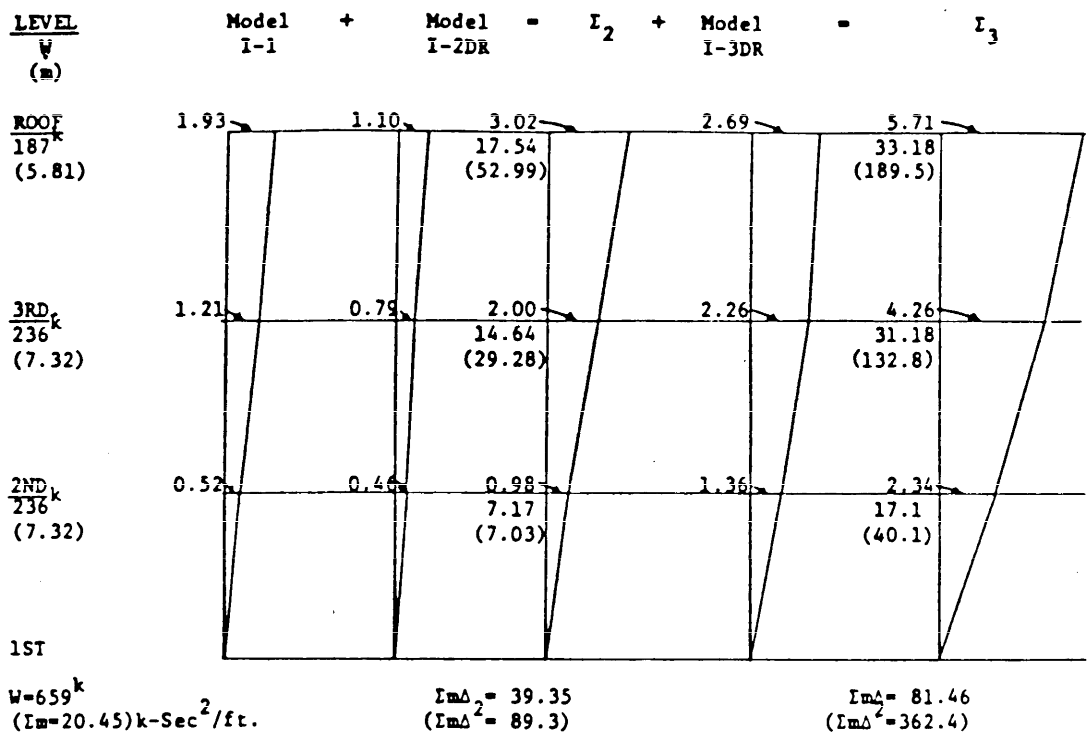

	Model I-1	Model I-2DR	Σ_2	Model I-3DR	Σ_3
Δ_T(in)	1.93	1.10	3.02	2.69	5.71
T(sec)	0.97	1.14		2.29	
C_B	0.13	0.06	0.19	0.04	0.23
C_B/S_a	0.805	0.897	0.848	0.934	0.895
S_a	0.161g		0.224g		0.257g
Δ_T/S_d	1.345	1.298	1.331	1.219	1.283
S_d(in)	1.43		2.27		4.45
$T=2\pi\sqrt{\frac{S_d}{S_a g}}$	0.95		1.02 sec.		1.33 sec.

CAPACITY SUMMARY

US Army Corps of Engineers

Example E-3 | 20 of 34 | Steel Frames

Figure E-3. Building with steel moment-resisting frames and steel braced frames—continued.

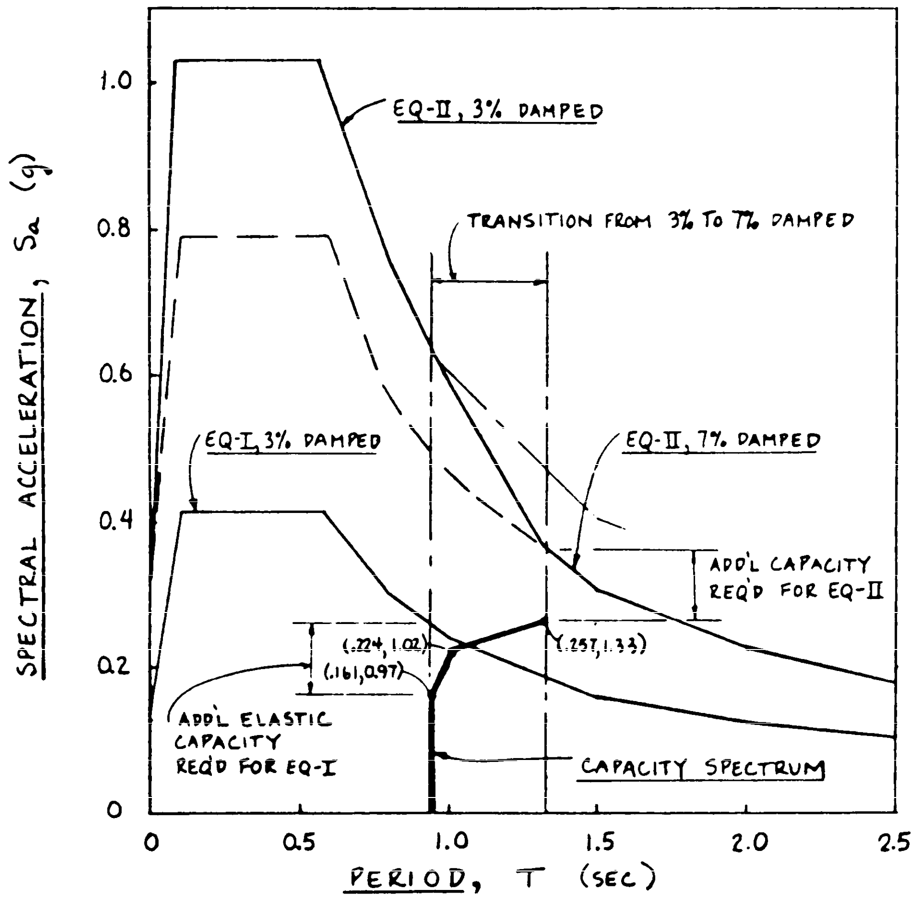

REFER TO SHEET 20 FOR CAPACITY SPECTRUM VALUES
SHEET 4 FOR RESPONSE SPECTRA

CAPACITY SPECTRUM METHOD

US Army Corps of Engineers

Example E-3 21 of 34 Steel Frames

Figure E–3. Building with steel moment-resisting frames and steel braced frames—continued.

METHOD 2 (CONTINUED)

SUMMARY

1. THE STRUCTURE YIELDS AT EQ-I.

2. THE FIRST YIELD OCCURS AT 0.66 EQ-I; THEREFORE IT DOES NOT HAVE THE CAPACITY TO SATISFY THE NEARLY ELASTIC CRITERIA.

3. THE CAPACITY SPECTRUM DOES NOT CROSS THE EQ-II DEMAND RESPONSE SPECTRUM (SHEET 21); THEREFORE THE STRUCTURE DOES NOT SATISFY THE EQ-II CRITERIA. REFER TO PARAGRAPH 5-5b(2)(g) AND TO FIGURE 5-6.

US Army Corps of Engineers

Example E-3	22 of 34	Steel Frames

Figure E-3. Building with steel moment-resisting frames and steel braced frames—continued.

FRAME 4 (DMRSF) - MODIFICATIONS

THE TRANSVERSE FRAMES MUST BE MODIFIED IN ORDER TO INCREASE THEIR CAPACITY TO RESIST SEISMIC LOADING. THREE POSSIBLE MODIFICATION SCHEMES ARE DISCUSSED BELOW.

- THE BUILDING ACTUALLY CONTAINS 7 TRANSVERSE FRAMES, ONLY 3 OF WHICH HAVE BEEN DETAILED AS DUCTILE MOMENT RESISTING FRAMES. BY CHANGING THE CONNECTION DETAILS FOR THE 4 INTERMEDIATE FRAMES, ALL 7 FRAMES MAY BE USED TO RESIST THE LATERAL LOADS.

- THE MEMBER SIZES FOR BEAMS AND COLUMNS IN FRAMES 1, 4 AND 7 CAN BE INCREASED TO IMPROVE THEIR LATERAL RESISTANCE. FOR EXAMPLE, THE ROOF BEAM HAS A DEMAND MOMENT $M_D = 199$ k-ft. A SECTION WITH SUFFICIENT PLASTIC CAPACITY MUST HAVE A PLASTIC SECTION MODULUS $Z_x = 199(12)/36 = 66.3$ in^3. A W14×43 ($Z_x = 69.6$) OR A W18×35 ($Z_x = 66.5$) WOULD BE ADEQUATE. AFTER THE MEMBERS HAVE BEEN RESIZED, THE ANALYSES FOR EQ-I AND EQ-II SHOULD BE REPEATED. INCREASING THE STIFFNESS OF THE FRAME MAY RESULT IN A HIGHER 1ST MODE SPECTRAL ACCELERATION AND A HIGHER DESIGN BASE SHEAR.

- THE TRANSVERSE FRAMES CAN BE STRENGTHENED WITH THE ADDITION OF A BRACED FRAME SYSTEM. THIS WILL STIFFEN THE STRUCTURE AND INCREASE THE SEISMIC FORCES SO THAT THE EQ-I AND EQ-II ANALYSES MUST BE REPEATED. SEE THE FOLLOWING SECTION FOR AN EXAMPLE OF A BRACED FRAME ANALYSIS.

US Army Corps of Engineers

Example E-3	23 of 34	Steel Frames

Figure E–3. Building with steel moment-resisting frames and steel braced frames—continued.

LONGITUDINAL (E-W) DIRECTION: FRAME A - BRACED FRAME

MODE SHAPES (ϕ_{xm}) AND PERIODS (T_m) FROM COMPUTER ANALYSIS OF FRAME A, MASS CALCULATED FROM W/g.

LEVEL	MASS ($\frac{k \cdot sec^2}{ft.}$)	MODE 1			MODE 2			MODE 3		
		ϕ_{x1}	$m_x\phi_{x1}$	$m_x\phi_{x1}^2$	ϕ_{x2}	$m_x\phi_{x2}$	$m_x\phi_{x2}^2$	ϕ_{x3}	$m_x\phi_{x3}$	$m_x\phi_{x3}^2$
R	5.82	.2523	1.468	.370	.2489	1.449	.361	.2149	1.251	.269
3	10.98	.2095	2.300	.482	-.0262	-.288	.008	-.2156	-2.367	.510
2	10.98	.1159	1.273	.147	-.2399	-2.634	.632	.1417	1.556	.220
Σ	27.78		5.041	.999		-1.473	1.001		.440	.999
PF^*_{Rm} (Eq. 4-1)	$\frac{\Sigma m\phi}{\Sigma m\phi^2}\phi_{R1}$ =	1.273			-.366			.095		
PF_{3m}		1.057			.039			-.095		
PF_{2m}		.585			.353			.062		
α_m (Eq. 4-2)	$\frac{(\Sigma m\phi)^2}{\Sigma m(\Sigma m\phi^2)}$ =	.916			.078			.007		
T_m, sec		.299			.112			.079		

* AS A CHECK, NOTE THAT $\sum_{m=1}^{3} PF_{Rm} = 1.0$ AND $\sum_{m=1}^{3} \alpha_m = 1.0$.

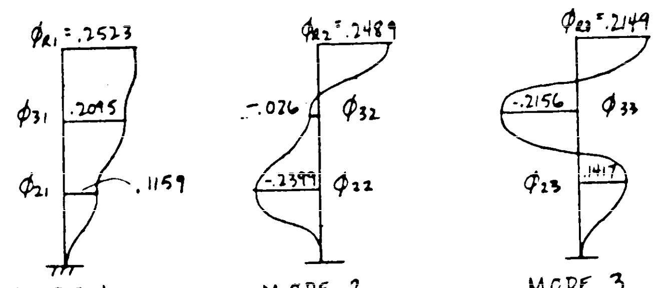

MODE 1 MODE 2 MODE 3

US Army Corps of Engineers

Figure E-3. Building with steel moment-resisting frames and steel braced frames—continued.

LONGITUDINAL (E-W) DIRECTION: SPECTRAL ACCELERATIONS, S_{am}
MODAL BASE SHEARS, V_m

EQ		MODE 1	MODE 2	MODE 3
EQ-I (β=3%)	T_m, sec (SHEET 24)	.299	.112	.079
	S_{am}, g (SHEET 4)	.41	.41	.41
	$C_{bm}=\alpha_m S_{am}$	.376	.032	.003
	$V_m=C_{bm}W$ (Eq. 4-4)	335.6 k	28.6 k	2.55 k
EQ-II (β=7%)	$T_m\sqrt{1.0}^{*}$, sec	.299	.112	.079
	S_{am}, g	.79	.79	.79
	$C_{bm}=\alpha_m S_{am}$	.724	.062	.006
	$V_m'=C_{bm}W$	646.6k	55.1 k	4.91 k

*NOTE: AS SHOWN IN TABLE 4-2, THE INELASTIC DEMAND RATIO FOR K-BRACES IN A CRITICAL, ESSENTIAL FACILITY IS 1.0. THUS, THE LONGITUDINAL PERIOD IS THE SAME FOR BOTH EQ-I AND EQ-II AND THE SAME COMPUTER MODEL WAS USED FOR BOTH ANALYSES.

US Army Corps of Engineers

Figure E-3. Building with steel moment-resisting frames and steel braced frames—continued.

MODAL ANALYSIS: LONGITUDINAL (E-W) DIRECTION - FRAME A

MODE		LEVEL	PF_{xm}	$\frac{m_x \phi_{xm}}{\Sigma m_x \phi_{xm}}$	F_{xm} (k)	V_{xm} (k)	ΔOTM_{xm} (ft-k)	OTM_{xm} (ft-k)	$a_{xm} = \frac{F_{xm}}{W_x}$	δ_{xm} (in.)	Δ_{xm} (in)
MODE 1	EQ-I	R	1.273	.291	97.7	97.7	1075	0	.522	.456	.078
		3	1.057	.456	153.2	250.9	2760	1075	.433	.378	.169
		2	.585	.253	-84.7	335.6	3692	3835	.240	.209	.209
				1.000				7526			
	EQ-II	R			188.3	188.3	2071	0	1.005	.878	.150
		3			295.0	483.3	5316	2071	.834	.728	.324
		2			163.3	646.6	7113	7388	.462	.404	.404
								14500			
MODE 2	EQ-I	R	-.366	-.984	-28.2	-28.2	-310	0	-.150	-.018	.020
		3	.039	.196	5.6	-22.6	-249	-310	.016	.002	.016
		2	.353	1.788	51.2	28.6	315	-559	.145	.018	.018
				1.000				-244			
	EQ-II	R			-54.3	-54.3	-597	0	-.290	-.036	.040
		3			10.8	-43.5	-479	-597	.030	.004	.030
		2			98.6	55.1	606	-1076	.279	.034	.034
								-470			
MODE 3	EQ-I	R	.095	2.843	7.26	7.26	80	0	.039	.0024	.005
		3	-.095	-5.380	-13.74	-6.48	-71	80	-.039	-.0024	.004
		2	.062	3.537	9.03	2.55	28	9	.026	.0016	.002
								37			
	EQ-II	R			14.0	14.0	154	0	.075	.0046	.009
		3			-26.5	-12.5	-138	154	-.075	-.0046	.008
		2			17.41	4.91	54	17	.049	.0030	.003
								71			
SRSS	EQ-I	R			102.0	102.0	1078	0	.544	.456	.081
		3			153.9	251.9	2772	1078	.435	.378	.170
		2			99.4	336.8	3706	3876	.281	.210	.210
								7530			
	EQ-II	R			196.5	196.5	2161	0	1.048	.878	.156
		3			296.4	485.5	5339	2161	.838	.729	.325
		2			191.6	649.0	7139	7466	.542	.405	.405
								14508			

US Army Corps of Engineers

Example E-3	26 of 34	Steel Frames

Figure E-3. Building with steel moment-resisting frames and steel braced frames—continued.

EQ-I ELEMENT FORCES : LONGITUDINAL (E-W) - FRAME A

SEE NOTES ON SHEET 10.

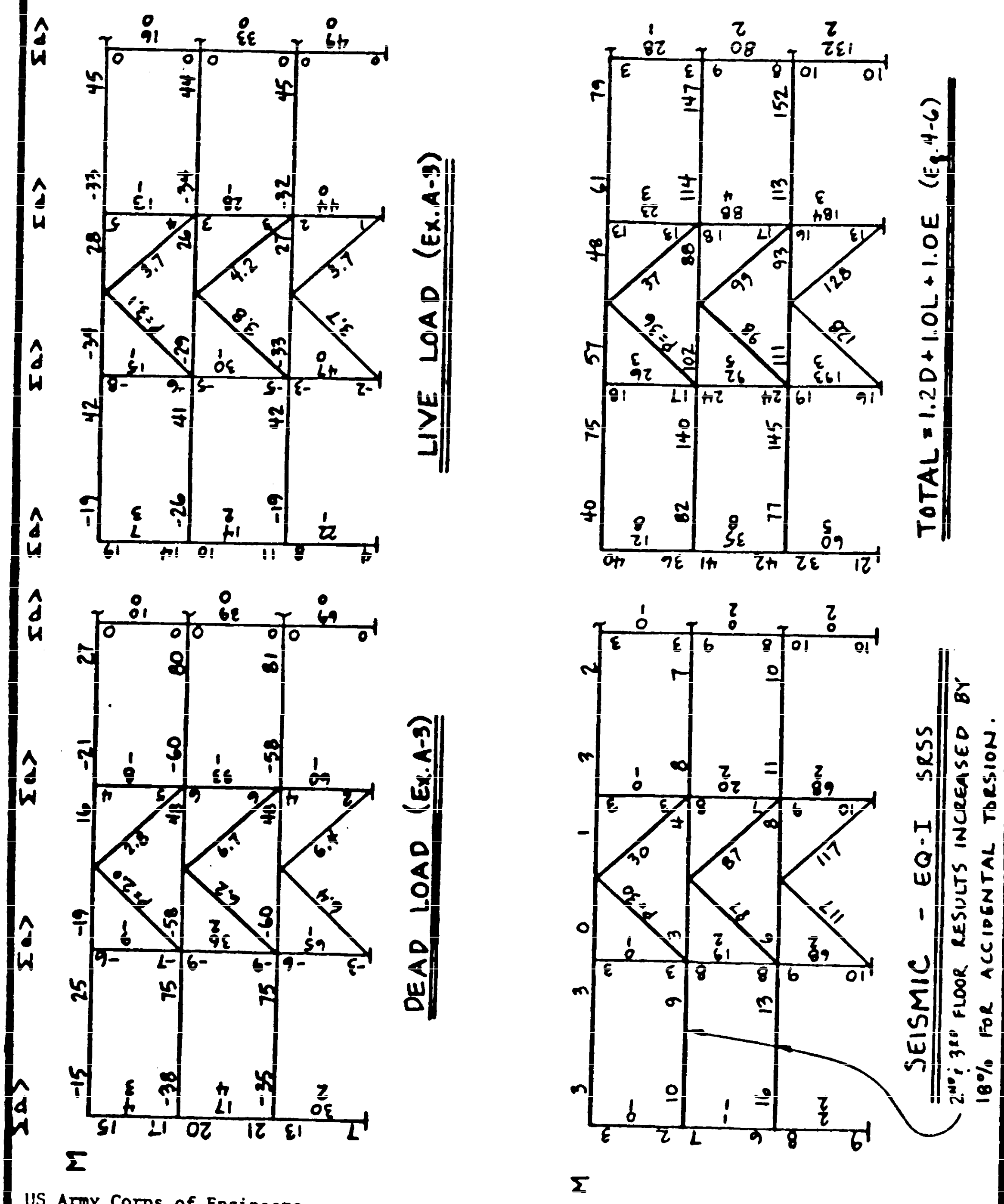

US Army Corps of Engineers

Example E-3 27 of 34 Steel Frames

Figure E-3. Building with steel moment-resisting frames and steel braced frames—continued.

EQ-II ELEMENT FORCES : LONGITUDINAL (E-W) - FRAME A

SEE NOTES ON SHEET 10.

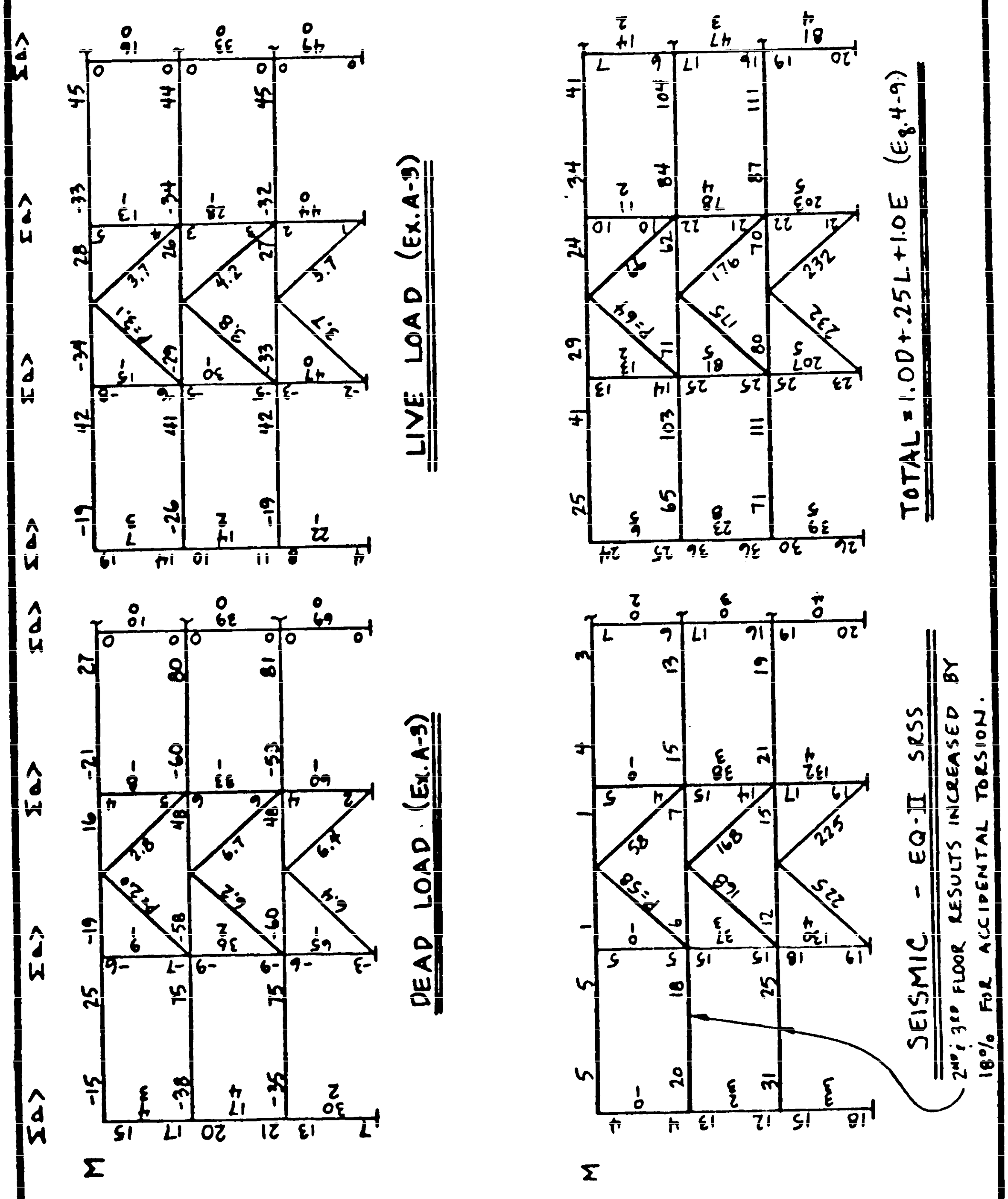

US Army Corps of Engineers

Example E-3 28 of 34 Steel Frames

Figure E-3. Building with steel moment-resisting frames and steel braced frames—continued.

ELEMENT STRESSES – FRAME A (BRACED FRAME)

• K-BRACES 1ST STORY ($F_y = 46$ ksi)

STEEL TUBE	A (in²)	r (in)	$\frac{kL}{r}$	F_a	$P_{cr} = 1.7AF_a$ (k)	EQ-I P_D (k)	EQ-I $\frac{P_D}{P_{cr}}$	EQ-II P_D (k)	EQ-II $\frac{P_D}{P_{cr}}$	IDR*
5×5×1/4	4.59	1.92	121.4	10.13	79.1	128	1.62 ×	232	2.93 ×	1.0

• BEAM ELEMENTS IN UNBRACED BAYS

LEVEL	SIZE	Z_x (in³)	EQ-I M_D (k-ft)	EQ-I M_C (k-ft)	EQ-I $\frac{M_D}{M_C}$	EQ-II M_D (k-ft)	EQ-II M_C (k-ft)	EQ-II $\frac{M_D}{M_C}$	IDR*
ROOF	W14×30	47.3	79	142	.56	42	142	.30	1.5
2	W18×40	78.4	152	235	.65	111	235	.47	1.5

*INELASTIC DEMAND RATIO FROM TABLE 4-2.

US Army Corps of Engineers

Figure E–3. Building with steel moment-resisting frames and steel braced frames—continued.

ELEMENT STRESSES - FRAME A (CONTINUED)

• BEAM ELEMENTS IN BRACED BAYS (CHECK INTERACTION EQUATIONS, SAME AS FOR COLUMNS) L=16'

EQ-I $EC \geq 1.2D + 1.0L + 1.0E$

SIZE	A (in²)	Sx (in³)	EQ-I P_D (k)	M_D (k-ft)	f_a (ksi)	f_{bx} (ksi)	F_a (ksi)	F_{bx} (ksi)	F'_{ex} (ksi)	* EQ1.6-1a	* EQ 1.6-1b
W14×30	8.85	42.0	29.7	57	3.36	16.3	19.7	24.0	133	.34	.49
W18×40	11.8	68.4	105.5	111	8.94	19.5	20.2	19.1	211	.64	.84

* MODIFIED INTERACTION EQUATIONS - SEE FRAME 4, SHEET 14.

EQ-II $UC \geq 1.0D + .25L + 1.0E$

SIZE	A (in²)	Zx (in³)	EQ-II P_D (k)	M_D (k-ft)	M_D (k-in)	P_y (k)	P_{cr} (k)	M_{px} (k-in)	M_{pcx} (k-in)	$\frac{M_x}{M_{pcx}}$ †	IDR (TABLE 4-2)
W14×30	8.85	47.3	52.7	29	348	318.6	2964	1703	1677	.21	1.5
W18×40	11.8	78.4	191.1	80	960	424.8	405.2	2822	1832	.52	1.5

† SEE FIGURE 4-2, $M_x/M_{pcx} \leq \mu$ ... (μ = IDR)

US Army Corps of Engineers

Figure E-3. Building with steel moment-resisting frames and steel braced frames—continued.

ELEMENT STRESSES - FRAME A (CONTINUED)

• STEEL COLUMNS 1ST STORY @ BASE

$\boxed{EQ-I}$ EC ≥ 1.2D + 1.0L + 1.0E

SIZE	A (in²)	S_y (in³)	EQ-I: P_0 (k)	M_0 (k-ft)	f_a (ksi)	f_{by} (ksi)	F_a (ksi)	F_{by} (ksi)	F'_{ey} (ksi)	EQ1.6-1a *	EQ1.6-1b *
W14×43	12.6	11.3	193	16	15.3	17.0	17.1	27	37.6	.72	.79
W14×48	14.1	12.8	132	10	9.36	9.38	17.2	27	38.5	.42	.46

*MODIFIED UNIAXIAL INTERACTION EQUATIONS - SEE FRAME 4, SHEET 14.

$\boxed{EQ-II}$ UC ≥ 1.0D + .25L + 1.0E

SIZE	A (in²)	Z_y (in³)	EQ-II: P_0 (k)	M_0 (k-ft)	M_0 (k-in)	P_y (k)	P_{cr} (k)	M_{py} (k-in)	M_{pcy} (k-in)	M_y / M_{pcy} †	IDR (TABLE 4-2)
W14×43	12.6	17.3	207	23.	276	453.6	366.3	623	587	.47	1.5
W14×48	14.1	19.6	81	20	240	507.6	412.3	766	819	.29	1.5

† SEE FIGURE 4-2, $M_y/M_{pcy} \le \mu$. (μ = IDR)

US Army Corps of Engineers

Example E-3 31 of 34 Steel Frames

Figure E-3. Building with steel moment-resisting frames and steel braced frames—continued.

CHECK INTERSTORY DRIFT

ALLOWABLE DRIFT FOR ESSENTIAL FACILITIES:
.005h FOR EQ-I
.010h FOR EQ-II

LONGITUDINAL (E-W) DIRECTION - FRAME A

LEVEL	STORY HT. h, in	EQ-I		EQ-II	
		*Δ_{SESS}, in	.005h	*Δ_{SESS}, in	.010h
ROOF	132	.081	.66	.156	1.32
3	132	.201	.66	.384	1.32
2	132	.248	.66	.478	1.32

* Δ_{SESS} FROM PREVIOUS CALCULATIONS ON SHEET 26 SCALED BY 1.18 AT THE 2ND & 3RD FLOORS TO ACCOUNT FOR ACCIDENTAL TORSION.

US Army Corps of Engineers

Figure E–3. Building with steel moment-resisting frames and steel braced frames—continued.

FRAME A - COMMENTARY

EQ-I THE ELASTIC ANALYSIS INDICATES THAT THE BRACES IN THE FIRST STORY ARE OVERSTRESSED BY 62%, ALTHOUGH THE BEAMS AND COLUMNS AT THIS LEVEL ARE NOT OVERSTRESSED. THE FRAME HAS EXCEEDED THE 10% OVERSTRESS ALLOWED FOR SOME MEMBERS AT EACH STORY AND THEREFORE DOES NOT MEET THE "NEARLY ELASTIC" CRITERIA FOR A K=1.00 FRAME.

EQ-II NO OVERSTRESS IS ALLOWED FOR K-BRACE ELEMENTS IN AN ESSENTIAL FACILITY SINCE THIS TYPE OF STRUCTURAL SYSTEM HAS LITTLE RESERVE CAPACITY ONCE THE COMPRESSION BRACES HAVE BUCKLED. THE FIRST STORY BRACES ARE OVERSTRESSED BY 193% FOR EQ-II ALTHOUGH ALL OF THE OTHER ELEMENT STRESSES ARE WITHIN ALLOWABLE LIMITS.

CONCLUSION SINCE THE FRAME DOES NOT MEET THE REQUIREMENTS OF EITHER EQ-I OR EQ-II, THE BRACING SYSTEM MUST BE MODIFIED.

US Army Corps of Engineers

Example E-3 | 33 of 34 | Steel Frames

Figure E-3. Building with steel moment-resisting frames and steel braced frames—continued.

FRAME A - MODIFICATIONS

THE LONGITUDINAL FRAMES REQUIRE MODIFICATION IN ORDER TO INCREASE THEIR SEISMIC RESISTANCE. THE K-BRACES AND BEAMS IN THE BRACED BAYS OF THE LOWER TWO STORIES ARE OVERSTRESSED FOR EQ-I. IN ADDITION TO INCREASING THE MEMBER SIZES FOR THE ELEMENTS WHICH ARE OVERSTRESSED, IT IS ALSO ADVANTAGEOUS TO CHANGE THE GEOMETRY OF THE BRACES IN THIS FRAME. TABLE 4-2 SHOWS AN INELASTIC DEMAND RATIO OF 1.0 FOR K-BRACES IN AN ESSENTIAL FACILITY, BUT 1.25 FOR DIAGONAL BRACES. THUS, REVERSING THE ORIENTATION OF THE K-BRACE IN THE 2ND STORY WOULD RESULT IN A DIAGONAL BRACING SCHEME FOR THE LOWER FLOORS WHERE THE BRACES ARE OVERSTRESSED. THESE DIAGONAL BRACES MUST BE SIZED TO REMAIN ELASTIC FOR EQ-I BUT ARE ALLOWED 25% OVERSTRESS FOR EQ-II.

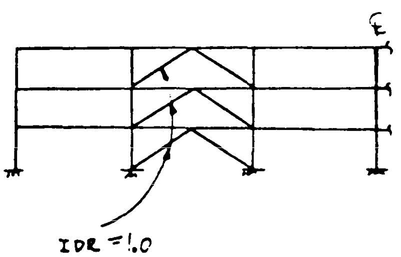

FRAME A

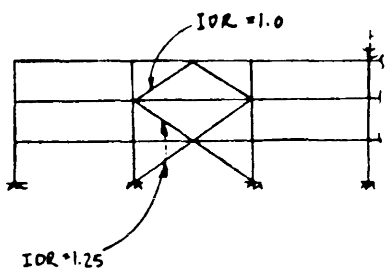

MODIFIED FRAME A

US Army Corps of Engineers

Figure E-3. Building with steel moment-resisting frames and steel braced frames—continued.

DESIGN EXAMPLE: E-4

SEVEN-STORY DUCTILE CONCRETE FRAME BUILDING:

Purpose. This example is presented in order to illustrate the modal analysis of a multistory building and the procedure for checking the ductility of beams and columns in a reinforced concrete frame.

Description of Structure. Design example E-4 is based upon a building with the same characteristics as the one that was used for design example E-1 and for the examples given in paragraph 2-5c of this manual. The building is a 7-story, reinforced concrete moment-resisting space frame building as shown on sheet 2. The computer program TABS was used to model the structure for the seismic analyses. The section properties for the model were based on gross concrete sections and the properties for the spandrel beams around the perimeter were increased by 50% to approximate the influence of the slab.

Modal Analysis. The transverse modal analysis of the structure is shown in example E-1. The site response spectra for EQ-I and EQ-II were provided by the soils engineer. The spectrum for EQ-I was based on 5% structural damping and a soil profile similar to type S_2. The EQ-I spectrum has a peak ground acceleration of 0.20g and a maximum spectral acceleration of 0.50g. The seismic analyses included three modes of vibration from which the SRSS responses were determined.

Ductility Check. One beam and one column section were selected from the sixth-floor level of frame B in order to illustrate the ductility check procedure. The properties of these sections and appropriate dead load, live load, and seismic analysis results are shown on sheets 5 and 6. The beam ductility check is presented on sheets 6-8 and the column ductility check is on sheets 9-12.

US Army Corps of Engineers

Example E-4 1 of 12 Concrete Frame

Figure E-4. Seven-story ductile concrete frame building.

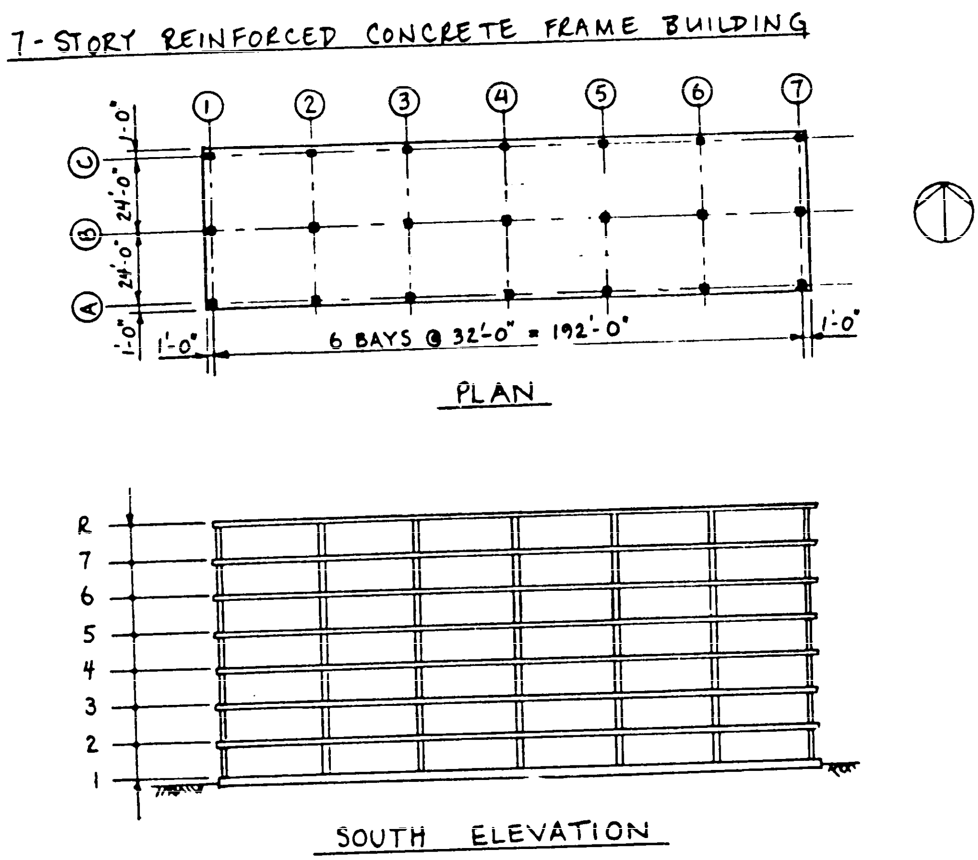

US Army Corps of Engineers

Example E-4	2 of 12	Concrete Frame

Figure E-4. Seven-story ductile concrete frame building—continued.

MODAL ANALYSIS - INFLUENCE OF HIGHER MODES (SEE PARA. 5-4a(3))

HIGHER MODES OF RESPONSE BECOME MORE IMPORTANT IN THE RESPONSE OF THE UPPER STORIES OF A MULTI-STORY BUILDING. A COMPARISON OF THE MODAL STORY SHEARS AND THE SRSS STORY SHEARS IS SHOWN BELOW.

STORY SHEARS, EQ-I

LEVEL	V_{SRSS}	MODE 1			MODE 2		MODE 3	
		V_1*	V_1/V_{SRSS}	$(V_1/V_{SRSS})^2$	V_2*	$(V_2/V_{SRSS})^2$	V_3*	$(V_3/V_{SRSS})^2$
R	629	508	.81	.65	-330	.275	170	.073
7	1139	1002	.88	.774	-518	.207	160	.020
6	1529	1445	.95	.893	-499	.107	-6	—
5	1846	1816	.98	.968	-283	.024	-169	.008
4	2106	2098	.996	.992	46	—	-175	.007
3	2312	2283	.987	.975	365	.025	-19	—
2	2498	2408	.964	.929	632	.064	200	.006

*MODAL SHEARS FROM DESIGN EXAMPLE E-1, SHEETS 4,5 & 6.

THUS, FOR THIS REGULAR 7-STORY CONCRETE FRAME BUILDING, THE 2ND AND 3RD MODES CONTRIBUTE VERY LITTLE TO THE STORY SHEARS AT FLOORS 2-5. FOR FLOORS 6,7,&R, THESE HIGHER MODES CONTRIBUTE 11%, 23%, AND 35% RESPECTIVELY, WHEN THE MODAL FORCES ARE COMBINED ON AN SRSS BASIS.

THE SRSS RESULTS FROM THE 3-MODE ANALYSIS WILL BE USED TO CHECK THE BEAM AND COLUMN IN THE REMAINDER OF THIS EXAMPLE.

US Army Corps of Engineers

Example E-4 3 of 12 Concrete Frame

Figure E-4. Seven-story ductile concrete frame building—continued.

ELEMENT PROPERTIES

FOR THIS EXAMPLE, ONE BEAM AND ONE COLUMN WILL BE CHECKED FOR EQ-I AND EQ-II LOADING IN ORDER TO SHOW THE PROCEDURE. THE PROPERTIES OF THE SELECTED ELEMENTS ARE SHOWN BELOW FOR THE INITIAL TRIAL DESIGN.

BEAM FRAME (B) FLOOR 6 FROM (1) TO (2)

CLEAR SPAN $\ell' = 30.0'$

$f_y = 60$, $f'_c = 4$

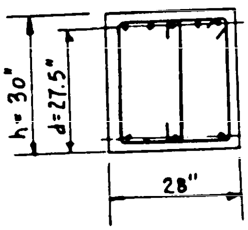

	END (1)	MIDSPAN	END (2)
TOP BARS	5-#9		6-#9
BOTTOM BARS	3-#9	4-#9	3-#9

COLUMN LINE B-2 BETWEEN 5TH & 6TH FLOORS

CLEAR STORY HEIGHT $L_u = 9.5'$

$f_y = 60$, $f'_c = 4$

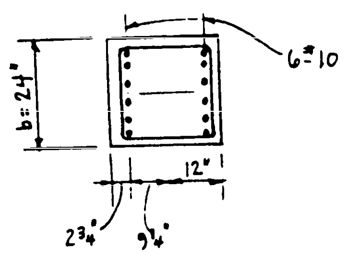

$A_s = A_s' = 7.62\ in^2$

$d = 21\frac{1}{4}''$

$\gamma = 18\frac{1}{2}/24 = 0.77$

US Army Corps of Engineers

Figure E-4. Seven-story ductile concrete frame building—continued.

ELEMENT FORCES (UNITS: k, ft.)

THE RESULTS FROM THE DEAD LOAD, LIVE LOAD AND SEISMIC ANALYSES (NOT INCLUDED) ARE SHOWN BELOW FOR THE SELECTED ELEMENTS IN FRAME B AT THE 6TH FLOOR LEVEL. END MOMENTS AND SHEARS ARE GIVEN FOR THE FACE OF SUPPORT.

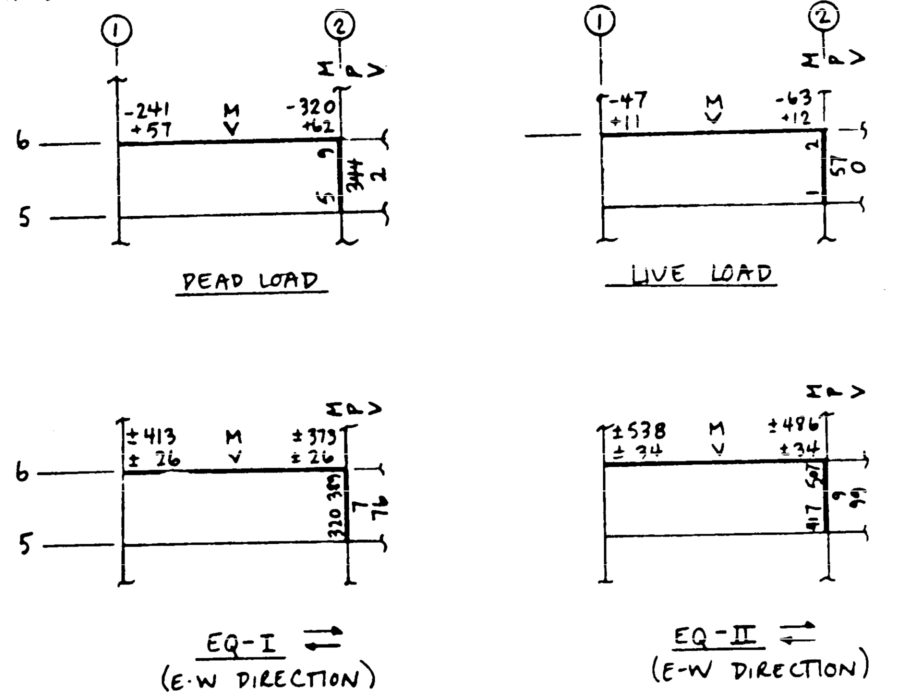

US Army Corps of Engineers

Figure E-4. Seven-story ductile concrete frame building—continued.

BEAM FORCES AND LOAD COMBINATIONS (UNITS: k, ft.)

FRAME (B) FLOOR 6 FROM (1) TO (2)

	END @ 1		SPAN	END @ 2	
	M	V	M	M	V
DEAD LOAD (1.0D)	-241	+57	164	-320	+62
LIVE LOAD (1.0L)	-47	+11	31	-63	+12
EQ-I					
SEISMIC (1.0E)	±413	±26	-	±373	±26
1.2D+1.0L+1.0E →	+77	+53	+228	$\boxed{-820}$	+112
1.2D+1.0L+1.0E ←	$\boxed{-749}$	+105	+228	-74	+60
.8D + 1.0E →	+220	+20	+131	-629	+76
.8D + 1.0E ←	-606	+72	+131	+117	+24
EQ-II					
SEISMIC (1.0E)	±538	±34	-	±486	±34
1.0D+.25L+1.0E →	+285	+26	+172	$\boxed{-822}$	+99
1.0D+.25L+1.0E ←	$\boxed{-791}$	+94	+172	+150	+31

US Army Corps of Engineers

Example E-4 6 of 12 Concrete Frame

Figure E-4. Seven-story ductile concrete frame building—continued.

DUCTILITY CHECK FOR BEAM

THE RATIO OF DEMAND MOMENT TO ULTIMATE MOMENT CAPACITY FOR THE BEAM IS CHECKED AS FOLLOWS:

EQ-I $M_D/M_u < 1.0$

EQ-II $M_D/M_u < 2.5$ (TABLE 4-2)

ULTIMATE MOMENT CAPACITY $M_u \equiv M_c$

$M_u = \phi f_y A_s (d - a/2)/12$ where $\phi = .9$

$f_y = 60$, $f'_c = 4$

$a = A_s f_y / .85 f'_c b$

	END ①	MIDSPAN	END ②
NEGATIVE MOMENT $-M_u$			
TOP BARS	5-#9		6-#9
A_s, in²	5.0		6.0
a, in	3.15		3.78
$-M_u$, k-ft	$\boxed{583}$		$\boxed{691}$
POSITIVE MOMENT $+M_u$			
BOTTOM BARS	3-#9	4-#9	3-#9
A_s, in²	3.0	4.0	3.0
a, in	1.89	2.52	1.89
$+M_u$, k-ft.	$\boxed{358}$	$\boxed{472}$	$\boxed{358}$

US Army Corps of Engineers

Example E-4 7 of 12 Concrete Frame

Figure E-4. Seven-story ductile concrete frame building—continued.

DUCTILITY CHECK (CONTINUED) - DEMAND RATIOS

EQ		TOP BARS			BOTTOM BARS			IDR*
		M_D	M_C	$\frac{M_D}{M_C}$	M_D	M_C	$\frac{M_D}{M_C}$	
EQ-I	END ①	749	583	1.28	220	358	.61	1.0
	SPAN	-	-	-	228	472	.48	1.0
	END ②	820	691	1.19	117	358	.33	1.0
EQ-II	END ①	791	583	1.36	285	358	.80	2.0
	SPAN	-	-	-	172	472	.36	2.0
	END ②	822	691	1.19	150	358	.42	2.0

*INELASTIC DEMAND RATIO FOR EQ-II FROM TABLE 4-2.

COMMENT

- FOR EQ-I THE DEMAND MOMENTS HAVE EXCEEDED THE NEGATIVE BENDING CAPACITIES AT BOTH ENDS OF THE BEAM. IF THE TOP STEEL IS INCREASED TO 7-#9 AT BOTH ENDS, THE MOMENT CAPACITY WOULD INCREASE TO 797 K-ft. AND THE DEMAND RATIOS WOULD DECREASE TO .94 AT END ①, AND 1.03 AT END ②. THE CRITERIA FOR "NEARLY ELASTIC" BEHAVIOR (SEE PARA. 4-3e(1)(a)) ALLOW SOME OVERSTRESS, BUT ALL OF THE OTHER BEAMS AT THIS LEVEL MUST BE CHECKED IN ORDER TO DETERMINE WHETHER THE OVERSTRESS AT END ② IS WITHIN ALLOWABLE LIMITS (i.e. 20% OF ALL BEAMS AT THIS FLOOR ARE ALLOWED UP TO 25% OVERSTRESS).

- FOR EQ-II THE DEMAND RATIOS ARE WITHIN THE ALLOWABLE INELASTIC DEMAND CRITERIA IN TABLE 4-2, BUT THE BUILDING AS A WHOLE MUST BE CHECKED FOR MECHANISMS AND UNSYMMETRICAL YIELDING (SEE PARA. 4-4c(5)).

US Army Corps of Engineers

Example E-4	8 of 12	Concrete Frame

Figure E-4. Seven-story ductile concrete frame building—continued.

COLUMN FORCES AND LOAD COMBINATIONS (UNITS: k, ft.)

COLUMN B-2 BETWEEN 5TH & 6TH FLOORS
E-W EARTHQUAKE

	P	Mx TOP	Mx BOTTOM	My* TOP	My* BOTTOM
DEAD LOAD (1.0D)	344	-9	-5	-9	-5
LIVE LOAD (1.0L)	57	-2	-1	-2	-1
EQ-I					
SEISMIC (1.0E)	±7	±389	±320	±78	±64
1.2D+1.0L+1.0E →	463	$\boxed{-402}$	-327	$\boxed{-91}$	-71
1.2D+1.0L+1.0E ←	$\boxed{477}$	376	313	65	57
.8D+1.0E →	268	-396	-324	-85	-68
.8D+1.0E ←	282	382	316	71	60
EQ-II					
SEISMIC (1.0E)	±9	±507	±417	±101	±83
1.0D+.25L+1.0E →	349	$\boxed{-517}$	-422	$\boxed{-111}$	-88
1.0D+.25L+1.0E ←	$\boxed{367}$	498	412	92	78

* IN A REGULAR FRAME BUILDING, AN EARTHQUAKE APPLIED IN THE PLANE OF A GIVEN FRAME WOULD PRODUCE A VERY SMALL OUT-OF-PLANE MOMENT IN AN INTERIOR COLUMN. FOR THE PURPOSE OF ILLUSTRATING A BIAXIAL CHECK, THE SEISMIC MOMENT M_y IS TAKEN AS 20% OF M_x. AN ADDITIONAL BIAXIAL CHECK MUST BE PERFORMED FOR THIS COLUMN FOR LOADS DUE TO A N-S EARTHQUAKE (NOT SHOWN).

US Army Corps of Engineers

Example E-4 9 of 12 Concrete Frame

Figure E-4. Seven-story ductile concrete frame building—continued.

DUCTILITY CHECK FOR CONCRETE COLUMNS

THE BIAXIAL CAPACITY OF COLUMN B-2 WILL BE CHECKED FOR LOADS RESULTING FROM AN EARTHQUAKE APPLIED IN THE E-W DIRECTION. FIGURE 4-3 PRESENTS THE EQUATIONS REQUIRED FOR A BIAXIAL DUCTILITY CHECK OF A CONCRETE COLUMN. TABLE 4-2 LISTS AN INELASTIC DEMAND RATIO OF 1.25 FOR COLUMNS IN A CONCRETE DMRSF IN AN ESSENTIAL BUILDING.

COLUMN B-2 IS IN COMPRESSION FOR ALL LOAD COMBINATIONS FOR BOTH EQ-I AND EQ-II.

∴ MUST CHECK $\frac{M_X}{M_{UX}}\left(\frac{1-\beta}{\beta}\right) + \frac{M_Y}{M_{UY}} \le \mu_{ALLOW}$

$$\frac{M_X}{M_{UX}} + \frac{M_Y}{M_{UY}}\left(\frac{1-\beta}{\beta}\right) \le \mu_{ALLOW}$$

where $\mu_{ALLOW} = 1.0$ FOR EQ-I
$= 1.25$ FOR EQ-II (TABLE 4-2)

M_{UX}, M_{UY} = UNIAXIAL ULTIMATE MOMENT CAPACITIES FROM INTERACTION DIAGRAMS

FIND M_{UX}, M_{UY} - UNIAXIAL ULTIMATE MOMENT CAPACITIES

USE INTERACTION DIAGRAMS FROM ACI SP17A-78

FIND $\frac{P_u}{A_g}$: $\frac{477}{24 \times 24} = .83$ FOR EQ-I , $\frac{367}{24 \times 24} = .64$ FOR EQ-II

US Army Corps of Engineers

Example E-4	10 of 12	Concrete Frame

Figure E–4. Seven-story ductile concrete frame building—continued.

DUCTILITY CHECK - COLUMN B-2 (CONTINUED)

FOR THIS COLUMN $f'_c = 4$ ksi
$f_y = 60$ ksi
$\gamma = 0.77$
$\rho = 15.24/24 \times 24 = .0264$
$M_{ux} = \phi M_{nx} = \left(\frac{\phi M_{nx}}{A_g \times h}\right) \times A_g \times h$, k-ft.

	EQ-I	EQ-II	ACI DIAGRAM
$\phi P_n / A_g$	.83	.64	
$\phi M_{nx}/A_g h$ $M_{ux} = \phi M_{nx}$	.67 772	.64 737	E4-60.75
$\phi M_{ny}/A_g h$ $M_{uy} = \phi M_{ny}$	.48 553	.47 541	L4-60.75

FIND β (SEE PCA BULLETIN 20, "BIAXIAL AND UNIAXIAL CAPACITY OF RECTANGULAR COLUMNS", OR ACI SP17A(78) - COLUMNS 11)

$q = \rho f_y / f'_c = .0264 (60/4) = .397 \sim .4$

$P_o = (.85 + q) f'_c bt = (.85 + .397) 4 \times 24 \times 24 = 2873$ k

$P_u/P_o = 477/2873 = .17$ FOR EQ-I
$367/2873 = .13$ FOR EQ-II

$\beta = .61$ FOR EQ-I
$= .62$ FOR EQ-II
INTERPOLATE FROM PCA TABLE 5

US Army Corps of Engineers

Example E-4 11 of 12 Concrete Frame

Figure E-4. Seven-story ductile concrete frame building—continued.

DUCTILITY CHECK - COLUMN B-2 (CONTINUED)

AXIAL COMPRESSION + BIAXIAL BENDING :

$$\frac{M_X}{M_{UX}}\left(\frac{1-\beta}{\beta}\right) + \frac{M_Y}{M_{UY}} = \frac{402}{772}\left(\frac{1-.61}{.61}\right) + \frac{91}{553} = .50 < 1.0 \quad \text{EQ-I}$$

$$\frac{517}{737}\left(\frac{1-.62}{.62}\right) + \frac{111}{541} = .64 < 1.25 \quad \text{EQ-II}$$

$$\frac{M_X}{M_{UX}} + \frac{M_Y}{M_{UY}}\left(\frac{1-\beta}{\beta}\right) = \frac{402}{772} + \frac{91}{553}\left(\frac{1-.61}{.61}\right) = .63 < 1.0 \quad \text{EQ-I}$$

$$\frac{517}{737} + \frac{111}{541}\left(\frac{1-.62}{.62}\right) = .83 < 1.25 \quad \text{EQ-II}$$

COMMENT

THIS COLUMN IS ADEQUATE FOR EQ-I AND EQ-II APPLIED IN THE E-W DIRECTION. AN ADDITIONAL CHECK SHOULD BE PERFORMED FOR BIAXIAL BENDING WHEN THE EARTHQUAKE IS APPLIED IN THE N-S DIRECTION.

US Army Corps of Engineers

Example E-4 | 12 of 12 | Concrete Frame

Figure E-4. Seven-story ductile concrete frame building—continued.

APPENDIX F
DESIGN EXAMPLES—EQUIPMENT IN BUILDINGS

F–1. Purpose and scope.

The design examples in this appendix are to illustrate principles, factors, and concepts described in chapter 6 of this manual for the anchorage or bracing of mechanical or electrical equipment in buildings.

F–2. Design examples.

The following design examples are representative of typical mechanical or electrical equipment supported on the roof or on a floor of any building. The various examples illustrate the procedures for the analysis and design of both rigid and flexibly mounted equipment.

Table F–1. Design Examples—Equipment in Buildings.

Fig. No.	*Example No. and Description*
F–1	F–1 Cooling tower in building: presents analysis for a rigidly mounted cooling tower in a multi-story building.
F–2	F–2 Unit heater—flexible brace: analysis of a unit heater not rigidly braced.
F–3	F–3 Unit heater—rigid support: demonstrates the reduction of the lateral seismic load by rigidly bracing the unit heater of design example F–2.
F–4	F–4 Tank on a building: demonstrates the seismic analysis of a storage tank on a building. Emphasis is placed on the period determination.

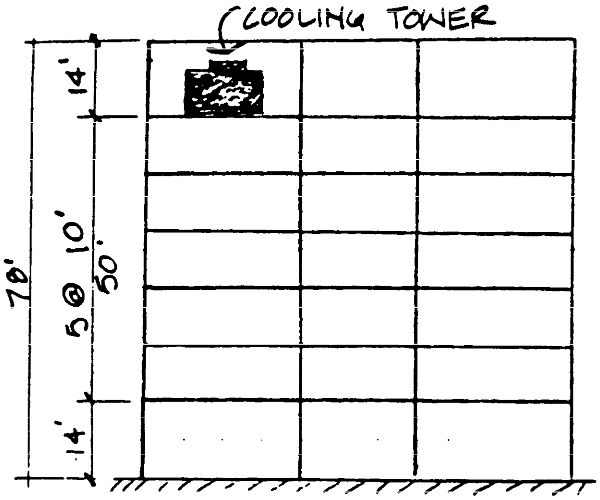

GIVEN:

WT. OF COOLING TOWER = 20.0 KIPS
WT. TYPICAL FLOOR = 1460 KIPS
CONSIDER TOWER RIGIDLY MOUNTED

EQ-I PER FIG. 2-8, 5% DAMPED BUILDING RESPONSE PER FIG. 2-10

EQ-II IS 2x FIG. 2-8, 10% DAMPED BUILDING PERIODS ARE 40% LONGER THAN EQ-I.
BUILDING ELASTIC CAPACITY RATIO = 1.7

REQUIRED:

FIND SEISMIC DESIGN FORCES FOR EQ-I AND EQ-II TO BE APPLIED AT C.G. OF COOLING TOWER

SOLUTION:

1. EQ-I

FROM FIG. 2-10, MODAL STORY ACCELERATIONS FOR 7^{TH} FLOOR:

	1ST MODE	2ND MODE	3RD MODE	SRSS
a_{xm}	.338	.129	-.007	.362 g

SINCE TOWER IS RIGIDLY CONNECTED,

$$F_p = (a_x)_{MAX} W_p \qquad \text{(EQ. 6-5)}$$

$$F_p = .362\,g \times 20.0^{\text{KIPS}}$$

$$\underline{F_p = 7.24^{\text{KIPS}} \text{ FOR EQ-I}}$$

US Army Corps of Engineers

Design Example F-1	1 of 2	Cooling Tower in Building

Figure F-1. Cooling tower in building.

2. EQ · II

a) IF ELASTIC CAPACITY OF BUILDING EXCEEDS EQ-II DEMAND, ELASTIC RESPONSE TO EQ-II GOVERNS DESIGN.

$S_a = 2 \times S_{a\,EQ-I}$

$\therefore \quad F_p = 2 \times .362 \times 20.0^K$

$= \underline{14.52^K}$

b) IF ELASTIC CAPACITY RATIO = 1.7, 2 CONDITIONS RESULT

CONDITION 1: $a_{xm} = .362 \times 1.7 = .615\,g$

CONDITION 2: FIND NEW ACCELERATIONS BASED ON 10% DAMPING AND PERIODS INCREASED 40%

	1ST MODE	2ND MODE	3RD MODE	SRSS
T	1.23 s	.403 sec	.233 s	
$2 \times S_a$	.326	.76	.76	
a_{xm}*	.399	.196	.011	.445

*FOR a_{XM} ASSUME PROPORTIONAL TO EQ-I ACCELERATIONS

$$a_{XM\,II} = a_{XM\,I}\left(\frac{S_{a\,EQ-II}}{S_{a\,EQ-I}}\right)$$

FOR MODE 1,

$$a_{XM} = .338\left(\frac{.326}{.276}\right) = 0.399$$

$0.615 > 445 \quad \therefore$ CONDITION 1 GOVERNS

$F_p = 0.615 \times 20^K = \underline{12.3^K \text{ FOR EQ-II}}$

US Army Corps of Engineers

Design Example F-1 2 of 2 Cooling Tower in Building

Figure F-1. Cooling tower in building—continued.

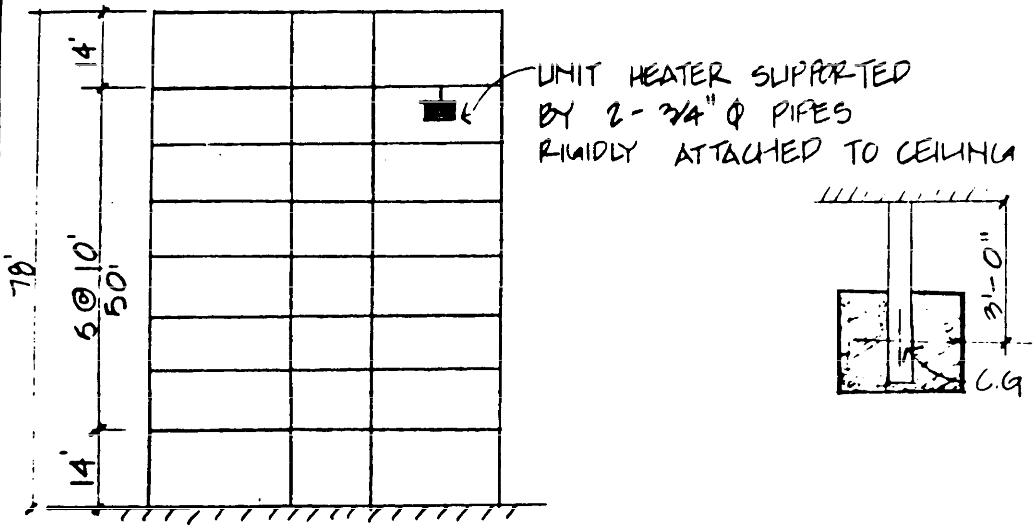

GIVEN: NEGLECT EFFECTS OF ROTATION OF UNIT HEATER.
W_p = WT. OF UNIT HEATER = 350 LB.
EQ-I PER FIG 2-8, 5% DAMPED
BUILDING RESPONSE PER FIG. 2-10
EQ-II IS 2x FIG. 2-8, 10% DAMPED, BUILDING PERIODS ARE 40% LONGER THAN EQ-I.

REQUIRED: FIND SEISMIC DESIGN FORCES FOR EQ-I AND EQ-II TO BE APPLIED AT C.G. OF HEATER.

SOLUTION:

FIND T_a FOR HEATER

$$K = 2\left\{\frac{3(30,000)(0.037)}{36^3}\right\} = .142 \text{ K/IN}$$

$$T_a = 0.32\sqrt{\frac{W_p}{K}} = 0.32\sqrt{\frac{.35}{.142}} = \underline{0.50 \text{ SEC}}$$

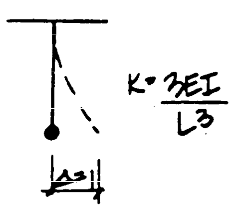

$T_a > .05$ ∴ QUALIFY AS FLEXIBLE (PARA. 6.3e (1))

US Army Corps of Engineers

Design Example F-2   1 of 5   Unit Heater - Flexible Brace

Figure F-2. Unit heater—flexible brace.

1. EQ-I

USING FIGS 2-10 AND 6-1,

MODE 1 $T_M = .88$ SEC, $a_{xM} = .338$

T_a/T	0	.5	.8	1.2	2	3
M.F.	1	1	7.5	7.5	1	1
T_a*	0	.44	.704	1.06	1.76	2.64
Sp_{fa}**	.338	.338	2.535	2.535	.338	.338

MODE 2 $T_M = .288$, $a_{xM} = .129$

T_a/T	0	.5	.8	1.2	2	3
M.F.	1	1	7.5	7.5	1	1
T_a*	0	.144	.230	.346	.576	.864
Sp_{fa}**	.129	.129	.968	.968	.129	.129

* $T_a = T_n \left(T_a/T\right)$ (EQ 6-3)

** $Sp_{fa} = a_{xm}(M.F.)$ (EQ 6-4)

LOWER LIMIT = $a_{x\,MAX}$ (PARA. 6.3 c (2)(b))

$$a_{x\,MAX} = \sqrt{.338^2 + .129^2} = .362$$

US Army Corps of Engineers

Design Example F-2 2 of 5 Unit Heater - Flexible Brace

Figure F-2. Unit heater—flexible brace—continued.

7TH FLOOR RESPONSE SPECTRUM (EQ-I)

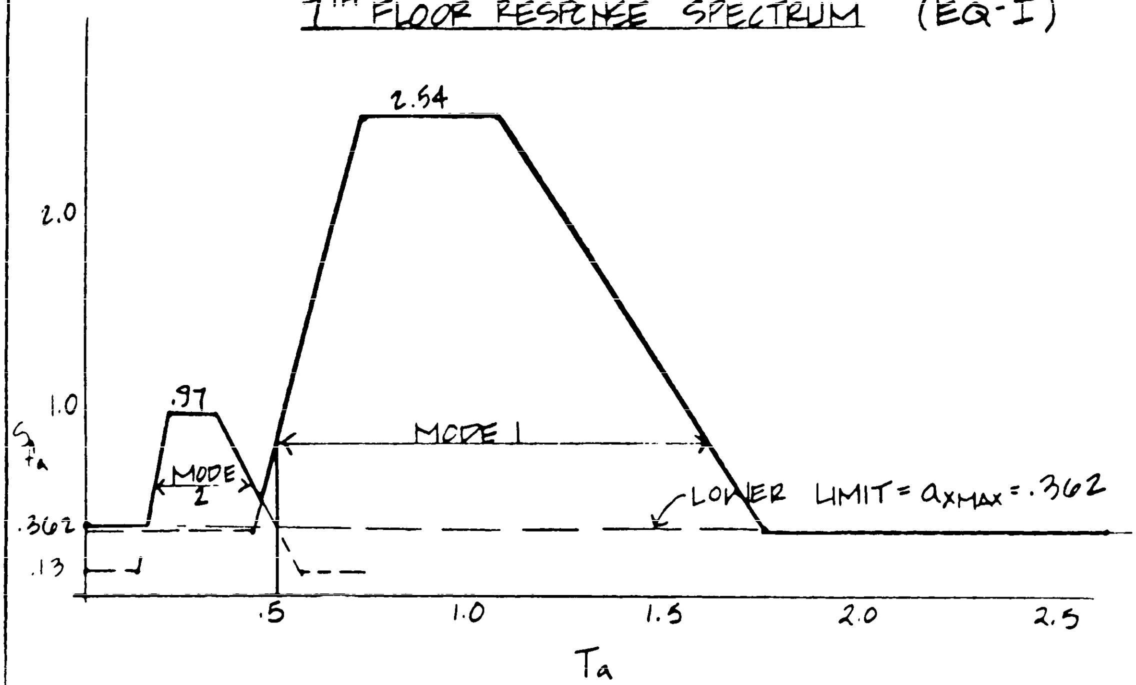

FROM GRAPH, FIND S_{fa} FOR $T_a = .5$

INTERPOLATE:

$$(2.54-.34)\frac{.5-.44}{.704-.44}+.34 = .84$$

FOR FLEXIBLY MOUNTED EQUIPMENT,

$F_p = S_{fax} W_p$ (EQ 6-6)

$= .84 \times 350^{LB}$

$F_p = 294$ LBS FOR EQ I

US Army Corps of Engineers

Design Example F-2	3 of 5	Unit Heater - Flexible Brace

Figure F–2. Unit heater—flexible brace—continued.

2. EQ-II

CONSIDER 2 CONDITIONS, MAXIMUM S_{fa} GOVERNS

CONDITION 1

GIVEN:

ELASTIC CAPACITY RATIO = 1.7

$S_{fa} = 1.7 \times .84 = \underline{1.43}$

CONDITION 2

DRAW POST-YIELD RESPONSE SPECTRUM BASED ON 10% DAMPING, 40% PERIOD INCREASE AND 2 x FIG 2-8 VALUES (SEE F-1)

USE FIG. 6-3.

MODE 1 $T_M = 1.23$, $a_{xm} = .399$

T_a/T_M	0	.5	.7	1.5	2
M.F.	1.0	1.0	5.0	5.0	1.0
T_a	0	.615	.86	1.85	2.46
S_{fa}	.399	.399	2.0	2.0	.399

MODE 2 $T_M = .403$, $a_{xm} = .196$

T_a/T_M	0	.5	.7	1.5	2
M.F.	1.0	1.0	5.0	5.0	1.0
T_a	0	.202	.282	.605	.806
S_{fa}	.196	.196	.98	.98	.196

LOWER LIMIT: $a_{x\,MAX} = \sqrt{.399^2 + .196^2} = .444$

US Army Corps of Engineers

Design Example F-2 4 of 5 Unit Heater - Flexible Brace

Figure F-2. Unit heater—flexible brace—continued.

7TH FLOOR RESPONSE SPECTRUM (EQ-II)

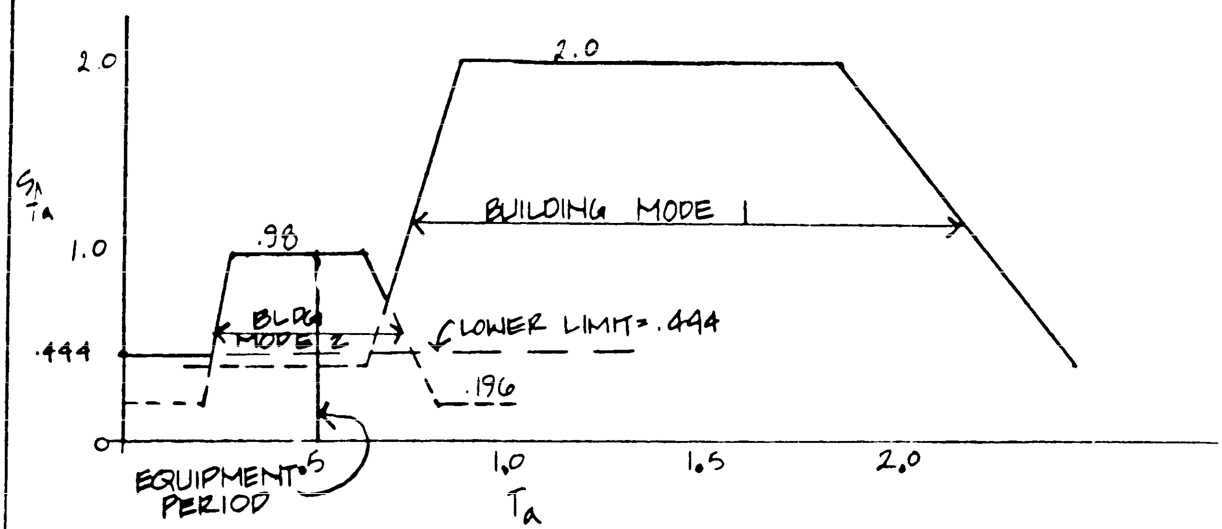

FROM GRAPH, FIND S_{fa} FOR $T_a = .5$

$\underline{S_{fa}} = .98$

SINCE $1.43 > .98$, <u>CONDITION 1 GOVERNS</u>

$F_p = S_{fax} W_p$ (EQ 6-6)

$= 1.43 \times 350^{LB}$

$= 501$ LBS FOR EQ II

US Army Corps of Engineers

Design Example F-2	5 of 5	Unit Heater - Flexible Brace

Figure F–2. Unit heater—flexible brace—continued.

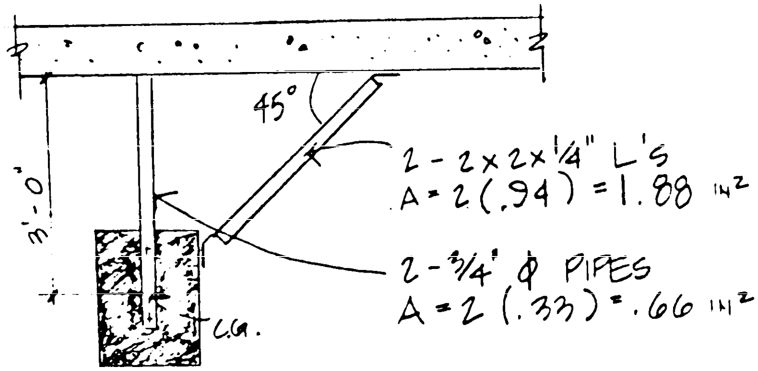

DETAIL OF UNIT HEATER

GIVEN: USE DATA GIVEN IN DESIGN EX. F-2
DIAGONAL BRACE ADDED TO STIFFEN SUPPORT

REQUIRED: FIND DESIGN SEISMIC FORCE

SOLUTION:

FIND T_a FOR RIGIDITY CHECK:

APPROXIMATE ANGLE CONNECTIONS BY PINS. ASSUME ALL LATERAL FORCE IS RESISTED BY BRACING ANGLES. USE ENERGY METHOD TO CALC. K_2

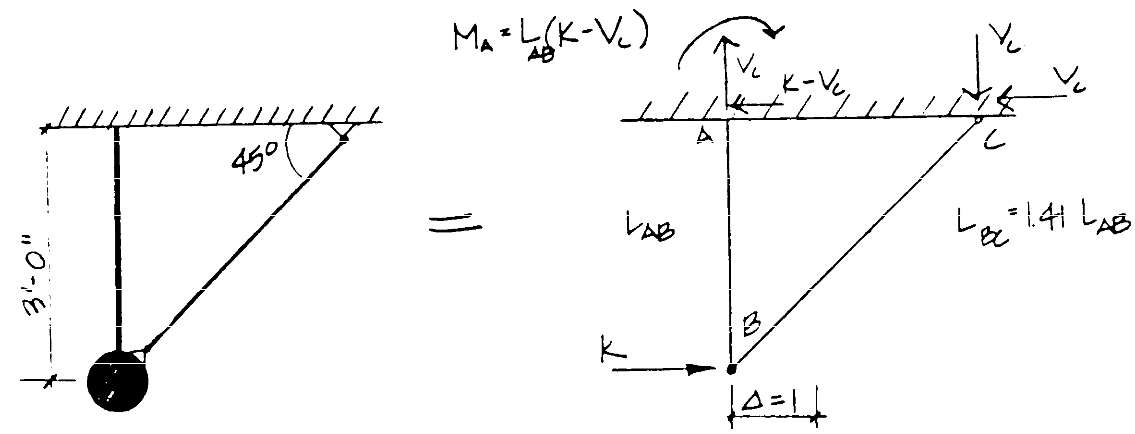

US Army Corps of Engineers

Design Example F-3	1 of 2	Unit Heater - Rigid Support

Figure F-3. Unit heater—rigid support.

ASSUME $K - V_c \doteq 0$: THIS ASSUMES ALL OF THE HORIZONTAL FORCE K IS RESISTED BY THE DIAGONAL.

$$\Sigma W_{EXTERNAL} = \Sigma W_{INTERNAL}$$

$$K\left(\frac{\Delta}{2}\right) = \frac{K^2 L_{AB}}{2 A_{AB} E} + \frac{(1.41 K)^2 L_{BC}}{2 A_{BC} E}$$

$$1 = K\left(\frac{L_{AB}}{A_{AB} E} + \frac{1.41^3 L_{AB}}{A_{BC} E}\right)$$

$$K = \frac{30 \times 10^6}{\left(\frac{36}{0.66} + \frac{1.41^3 (36)}{1.88}\right)} = 2.78 \times 10^5 \text{ LB/IN}$$

$$T_a = 0.32 \sqrt{\frac{360}{2.78 \times 10^5}} = 0.011 \text{ SEC}$$

$T_a < 0.05$ SEC, THEREFORE SUPPORT IS RIGID (PARA. 6.3e (1))

FIND SEISMIC FORCES - SIMILAR TO F-1

1. EQ-I

$(a_x)_{MAX} = .362$ IN/SEC²

$F_p = a_{xMAX} W_P$

$= .362 \times 360$ LB

$= 126.7$ LB FOR EQ-I

2. EQ-II ELASTIC CAPACITY RATIO = 1.7

CONDITION 1 GOVERNS (SEE F-1)

$a_{xM} = 1.7 \times .362 = .615$ (CONDITION 2, $a_{xMAX} = .444$)

$F_p = a_{xMAX} W_P$

$= .615 \times 360 = 215$ LB FOR EQ-II

US Army Corps of Engineers

Design Example F-3	2 of 2	Unit Heater - Rigid Support

Figure F-3. Unit heater—rigid support—continued.

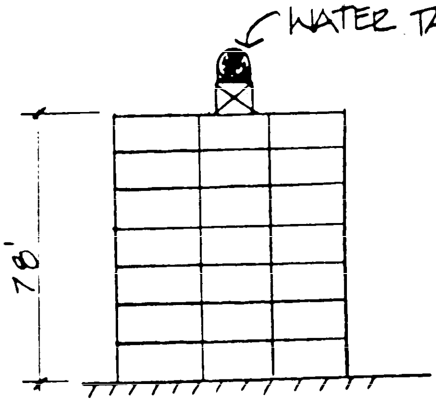

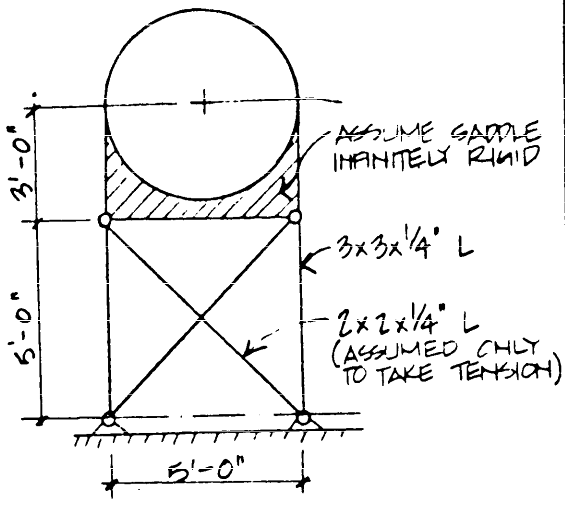

DETAIL OF TANK SUPPORT

GIVEN:

WT OF TANK + WATER = 10.0 K/TRUSS
BUILDING STRUCTURE SAME AS F-1 AND F-2
(SEE FIG. 2-10 FOR BUILDING RESPONSE)
EQ.-I PER FIG. 2-8, 5% DAMPED
EQ-II IS 2 x FIG. 2-8, 10% DAMPED, BUILDING PERIODS 40% LONGER THAN EQ-I.

REQUIRED:

FIND SEISMIC DESIGN FORCES DUE TO EQ-I AND EQ-II.

SOLUTION:

HYDRO-DYNAMIC EFFECTS ARE NEGLECTED EVEN WHEN TANK IS PARTIALLY FULL. CALCULATION OF STIFFNESS OF TANK STRUCTURE: USE ENERGY METHOD TO FIND K.

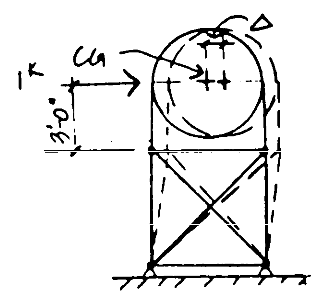

$\Longrightarrow$

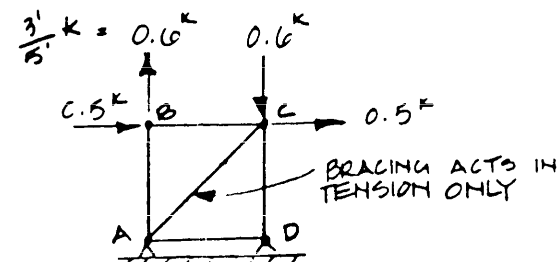

US Army Corps of Engineers

Design Example F-4	1 of 6	Tank on a Building

Figure F-4. Tank on a building.

COMPUTATION OF Δ : $1^{K} \cdot \Delta/2 = \dfrac{\Sigma F^{2}L}{2AE}$

MEMBER	LENGTH	AREA	F	F^2L/A
AB	5.00'	1.44 IN^2	$+.6^K$	1.25
CD	5.00'	1.44	-1.6^K	8.89
CA	7.07'	0.94	+1.414	15.03
				25.17

$$1^{K} \times \left(\frac{\Delta}{2}\right) = \frac{25.17 \frac{K^2\text{-}FT}{IN^2} \times 12\ ^{IN}/_{FT}}{2(30\times 10^{3}\ K/IN^{2})} = 0.5025 \times 10^{-2}\ IN\text{-}K$$

$$\Delta = 1.005 \times 10^{-2}\ IN/K$$

$$K = 1/\Delta = 99.5\ K/IN$$

$$T_a = .32\sqrt{\frac{W}{K}} = .32\sqrt{\frac{10}{99.5}} = .102\ SEC$$

$T_a > .05$ SEC THEREFORE SUPPORT IS NOT RIGID (PARA. 6.3e(1))

DESIGN AS FLEXIBLY MOUNTED

1. EQ-I

USING FIGS. 2-10 AND 6-1,

MODE 1 $T_M = .88$ SEC, $a_{XM} = .360$

T_a/T	0	.5	.8	1.2	2	3
M.F.	1	1	7.5	7.5	1	1
T_a	0	.44	.704	1.06	1.76	2.64
S_{fa}	.360	.360	2.7	2.7	.36	.36

US Army Corps of Engineers

Design Example F-4   2 of 6   Tank on a Building

Figure F–4. Tank on a building—continued.

FROM GRAPH, $S_{f_a} = .91$

$F_P = S_{f_a} \times W_P$ (6-6)

$= .91 \times 10.0^k$

$F_P = 9.1^k$ PER TRUSS FOR EQ-I

2. EQ-II

CONSIDER 2 CONDITIONS, MAX S_{f_a} GOVERNS

CONDITION 1

ELASTIC CAPACITY RATIO = 1.7 (GIVEN)

$S_{f_a} = 1.7 \times .91 = 1.55$

CONDITION 2

DRAW POST-YIELD RESPONSE SPECTRUM
BASED ON 10% DAMPING, 40% PERIOD INCREASE
AND 2x FIG. 2-8 VALUES
ONLY MODES 2 & 3 ARE NECESSARY TO PLOT

FIND a_{xm} FOR EACH MODE:

	1ST MODE	2ND MODE	3RD MODE	SRSS
T	1.23	.403	.23	
$2 \times S_a$	.326	.76	.76	
a_{xm}	.425	.356	.190	.586

$a_{xm\,II} = a_{xm\,I}\left(\frac{S_{a\,EQ-II}}{S_{a\,EQ-I}}\right)$ FOR MODE 1, $a_{xm\,II} = .360\left(\frac{.326}{.276}\right) = .425$

US Army Corps of Engineers

Design Example F-4	4 of 6	Tank on a Building

Figure F-4. Tank on a building—continued.

2ND MODE $T_m = .403$ $a_{xm} = .356$

T_a/T	0	.5	.7	1.5	2
M.F.	1.0	1.0	5.0	5.0	1.0
T_a	0	.202	.282	.605	.806
Sf_a	.356	.356	1.78	1.78	.356

3RD MODE $T_m = .23$ $a_{xm} = .190$

T_a/T	0	.5	.7	1.5	2
M.F	1.0	1.0	5.0	5.0	1.0
T_a	0	.115	.161	.345	.46
Sf_a	.190	.190	.95	.95	.190

$Sf_{a\,MIN} = a_{x\,max}$ = SRSS OF a_x FOR ROOF = .586
(ESTABLISHES LOWER LIMIT)

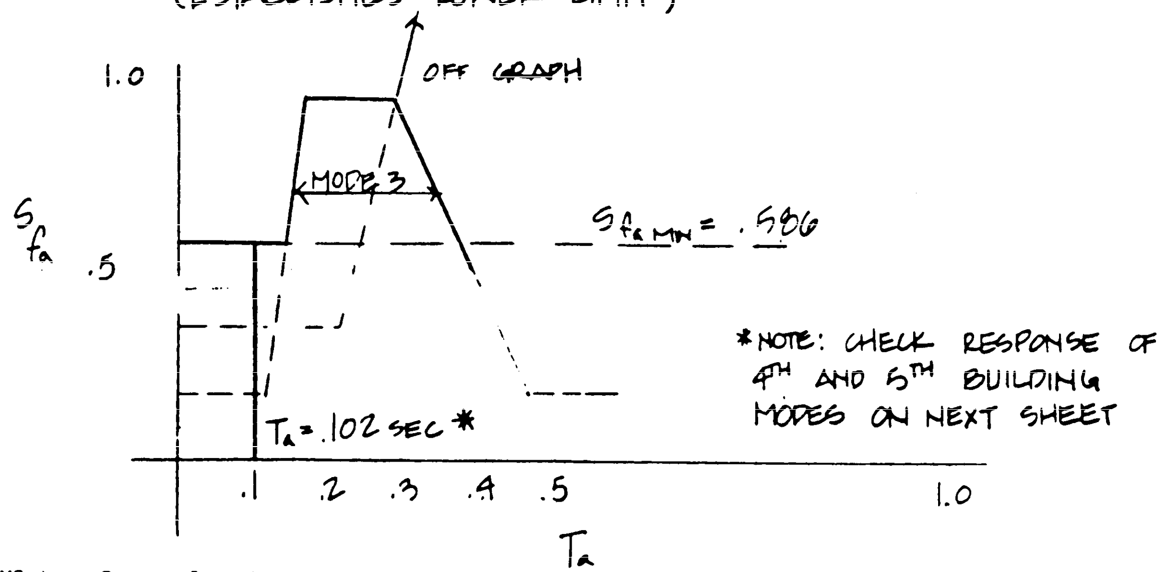

US Army Corps of Engineers

Design Example F-4 5 of 6 Tank on a Building

Figure F–4. Tank on a building—continued.

FROM GRAPH,

$S_{fa} = .586$

SINCE .586 < 1.55, CONDITION 1 GOVERNS

$\therefore \quad F_p = S_{fax} W_p \qquad (6\text{-}6)$

$F_p = 1.55 \times 10^k$ PER TRUSS FOR EQ-II

NOTE FROM SHEET 5 OF 6: CHECK MODES 4 AND 5

GIVEN:

MODE 4 $T_m = 0.106$ FOR EQ-I, $PF_{xm} = 0.11$

MODE 5 $T_m = 0.073$ FOR EQ-I, $PF_{xm} = 0.05$

(SEE EXAMPLE E-1, SHEET 3 OF 7 FOR MODES 1, 2, AND 3)

REQUIRED:

S_{fa} MAXIMUM OF MODES 4 AND 5 FOR EQ-II (I.E., M.F. = 5.0)

MODE 4 $T_m = 1.4 \times 0.106 = 0.15$ SEC

$2 \times S_a$ (10% DAMPED) $= 2 \times 0.38g = 0.76g$ (FIG. 2-8)

$a_{xm} = 0.11 \times 0.76g = 0.08g$ (EQN 6-1)

S_{fa} MAX $= 0.08 \times 5.8 = \underline{0.40g}$ (EQN 6-4)

MODE 5 $T_m = 1.4 \times 0.073 = 0.10$ SEC, $2S_a = 0.76g$

$a_{xm} = 0.05g \times 0.76 = 0.10$ SEC, $S_{fa\,MAX} = \underline{0.20g}$

IN BOTH CASES, MAXIMUM RESPONSE IS LESS THAN SRSS OF $a_x = 0.586$.

THEREFORE, MODES 4 AND 5 DO NOT GOVERN DESIGN

US Army Corps of Engineers

Design Example F-4 | 6 of 6 | Tank on a Building

Figure F-4. Tank on a building—continued.

BIBLIOGRAPHY

Chapter 3

(1) *Aki, K.*, "Generation and Propagation of G Waves from the Niigata Earthquake of June 16, 1964. Part 2. Estimation of Earthquake Moment, Released Energy, and Stress-Strain Drop from the G Wave Spectrum," Bulletin of the Earthquake Research Institute, Tokyo University, Vol. 44, 1966, pp. 73–88.

(2) *Algermissen, S. T., and Perkins, D. M.*, "A Probabilistic Estimate of Maximum Acceleration in Rock in the Contiguous United States," U.S. Geological Survey Open File Report No. 76–416, 1976.

(3) *Algermissen, S. T.*, "Seismic Risk Studies in the United States," Proceedings of the 4th World Conference on Earthquake Engineering, Santiago, Chile, Vol. I, Section A–1, 1969, pp. 14–27.

(4) *Archuleta, R. J., and Frazier, G. A.*, "Three-Dimensional Numerical Simulations of Dynamic Faulting in a Half Space," Bulletin of the Seismological Society of America, Vol. 68, No. 3, 1978, pp. 541–572.

(5) *Barstow, N. L., Brill, K. G., Nuttli, O. W., and Pomeroy, P. W.*, "An Approach to Seismic Zonation for Sitting Nuclear Electric Power Generating Facilities in the Eastern United States." Technical Report NUREG/CR–1577, Nuclear Regulatory Commission, 1981.

(6) *Benjamin, J. R.*, "Probabilistic Models for Seismic Force Design." Journal of the Structural Division, ASCE, ST5, No. 94, 1968, pp. 1175–1196.

(7) *Bernreuter, D. L., Mortgat, C. P., and Wight, L. H.*, "Seismic Hazard Analysis: Site Specific Response Spectra. Sensitivity Results," Nuclear Regulatory Commission Report No. NUREG/CR–1582, Vol. 4, 1981.

(8) *Bollinger, G. A.*, "Reinterpretation of the Intensity Data for the Charleston, S.C., Earthquake," U.S. Geological Survey, Professional Paper 1028, 1977.

(9) *Bollinger, G. A.*, "A Catalog of Southeastern United States Earthquakes 1754 through 1974," Virginia Polytechnic Institute and State University, Blacksburg, Va., Research Division Bulletin 101, 1975.

(10) *Bollinger, G. A.*, "The Giles County, Va., Seismic Zone: Configuration and Hazard Assessment," Proceedings of the Conference on Earthquakes and Earthquake Engineering: Eastern United States, Knoxville, Tenn., Vol. 1, 1981, pp. 277–308.

(11) *Bonilla, M. G., and Buchanan, J. M.*, "Interim Report on Worldwide Historic Surface Faulting," Open File Report, U.S. Geological Survey, 1970.

(12) *Boore, D. M., and Joyner, W.*, "The Influence of Rupture Incoherence on Seismic Directivity," Bulletin of the Seismological Society of America, Vol. 68, No. 2, 1978, pp. 283–300.

(13) *Boore, D. M., Joyner, W. B., Oliver, A. A., and Page, R. A.*, "Estimation of Ground Motion Parameters," United States Geological Survey Circular No. 795, 1978.

(14) *Campbell, K. W.*, "Near-Source Attenuation of Peak Horizontal Attenuation," Bulletin of the Seismological Society of America, Vol. 71, No. 6, 1981, pp. 2039–2070.

(15) *Chung, D. H., and Bernreuter, D. L.*, "On the Regionalization of Ground Motion Attenuation in the Conterminous United States," Second U.S. National Conference on Earthquake Engineering, Stanford, California, 1979, pp. 753–762.

(16) *CIT.*, "Analysis of Strong Motion Earthquake Accelerograms," California Institute of Technology, Earthquake Research Laboratory Reports, Vol. I-IV, 1969–1975.

(17) *Cluff, L. S.*, "Geological Perspectives on Earthquake Hazards and Dam Safety," Seminar Workshop Lecture Notes on New Perspectives on the Safety of Dams, Stanford University, 1978.

(18) *Cornell, C. A.*, "Engineering Seismic Risk Analysis," Bulletin of the Seismological Society of America, Vol. 58, No. 5, 1968, pp. 1583–1606.

(19) *Cornell, C. A., and VanMarcke, E. H.*, "The Major Influences on Seismic Risk," Proceedings of the Fourth World Conference on Earthquake Engineering, Santiago, Chile, Vol. I, Section A–1, 1969, pp. 69–83.

(20) *Cornell, C. A., Banan, H., and Shakal, A. F.*, "Seismic Motion and Response Prediction Alternatives," Journal of Earthquake Engineering and Structural Dynamics, Vol. 7, 1979, pp. 295–315.

(21) *Dalal, J. S.*, "Probabilistic Seismic Exposure and Structural Risk Evaluation," Technical Report No. 169, Department of Civil Engineering, Stanford University, 1973.

(22) *Der-Kiureghian, A., and Ang, A.H-S.*, "A Fault Rupture Model for Seismic Risk Analysis," Bulletin of the Seismological Society of America, Vol. 65, No. 4, 1975, pp. 1023–1027.

(23) *Dong, W. M., Shah, H. C., and Bao, A. B.*, "Use of Maximum Entropy Principal in Earthquake Recurrence Relationships," Final Report to the U.S. Geological Survey, The John A. Blume Earthquake Engineering Center, Stanford University, 1982.

(24) *Geller, R. J., and Kanamori, H.*, "Magnitudes of Great Shallow Earthquakes from 1904 to 1952," Bulletin of the Seismological Society of America, Vol. 67, 1977, pp. 587–598.

(25) *Gupta, I. N., and Nuttli, O. W.*, "Spatial Attenuation of Intensities for Central U.S. Earthquakes," Bulletin of the Seismological Society of America, Vol. 66, No. 3, 1976, pp. 743–751.

(26) *Gutenberg, B., and Richter, C. F.*, "Earthquake Magnitude, Intensity, Energy, and Acceleration," Bulletin of the Seismological Society of America, Vol. 46, 1956.

(27) *Hadely, J. B., and Devine, J. F.*, "Seismotectonic Map of the Eastern United States," U.S. Geological Survey, Report No. MF–620, 1974.

(28) *Haskell, N. A.*, "Total Energy and Energy Spectral Density of Elastic Wave Radiation from Propagating Faults, Part II: Statistical Source Model," Bulletin of the Seismological Society of America, Vol. 56, No. 1, 1966, pp. 125–140.

(29) *Haskell, N. A.*, "Total Energy and Energy Spectral Density of Elastic Wave Radiation from Propagating Faults, Part I," Bulletin of the Seismological Society of America, Vol. 56, No. 1, 1964, pp. 125–140.
(30) *Idriss, I. M.*, "Characteristics of Earthquake Ground Motions," Proceedings of the ASCE Specialty Conference on Earthquake Engineering and Soil Dynamics, Pasadena, California, 1978.
(31) *Joyner, W. B., and Boore, D. M.*, "Peak Horizontal Acceleration and Velocity from Strong Motion Records Including Records from the 1979 Imperial Valley, California, Earthquake," Bulletin of the Seismological Society of America, Vol. 71, No. 6, 1981, pp. 2011–2038.
(32) *Kiremidjian, A. S., and Shah, H. C.*, "Seismic Hazard Mapping of California," Technical Report No. 21, the John A. Blume Earthquake Engineering Center, Stanford University, 1975.
(33) *Kiremidjian, A. S., and Shah, H. C.*, "Probabilistic Site-Dependent Response Spectra," Journal of the Structural Division, Proceedings of the ASCE, Vol. 106, No. ST1, January 1980, pp. 69–86.
(34) *Liu, S. C., and Fagel, L. W.*, "Seismic Risk Analysis-Comparison of Three Different Methods for Seismic Regionalization," Bulletin of the Seismological Society of America, Vol. 65, No. 4, pp. 1023–1027.
(35) *McCann, M. W. Jr.*, "A Bayesian Geophysical Model for Seismic Hazard," Technical Report No. 47, The John A. Blume Earthquake Engineering Center, Stanford University, 1981.
(36) *McGuire, R. K.*, "Effects of Uncertainty in Seismicity on Estimates of Seismic Hazard for the East of the United States," Bulletin of the Seismological Society of America, Vol. 67, No. 3, 1977, pp. 827–848.
(37) *McGuire, R. K.*, "Seismic Structural Response Risk Analysis, Incorporating Peak Response Regressions on Earthquake Magnitude and Distance," Massachusetts Institute of Technology, Department of Civil Engineering, Technical Report No. R74–51, 1974.
(38) *McGuire, R. K., and Barnhard, J. A.*, "Magnitude, Distance and Intensity Data for C.I.T. Strong Motion Records," U.S. Geological Survey, Journal of Research, Vol. 5, No. 4, 1977, pp. 437–443.
(39) *Mertz, H. A., and Cornell, C. A.*, "Seismic Risk Analysis Based on a Quadratic Magnitude-Frequency Law," Bulletin of the Seismological Society of America, Vol. 63, No. 6, 1973, pp. 1999–2006.
(40) *Molinar, P.*, "Earthquake Recurrence Intervals and Plate Tectonics," Bulletin of the Seismological Society of America, Vol. No. 1, 1979, pp. 115–133.
(41) *Mortgat, C. P., and Shah, H. C.*, "A Bayesian Approach to Seismic Hazard Mapping," Technical Report No. 28, The John A. Blume Earthquake Engineering Center, Stanford University, 1978.
(42) *Mortgat, C. P., Zsutty, T. C., Shah, H. C., and Lubetkin, L.*, "A Study of Seismic Risk for Costa Rica," Technical Report No. 25, The John A. Blume Earthquake Engineering Center, Stanford University, 1977.
(43) *Murphy, J. E., and O'Brian, L. J.*, "Analysis of a Worldwide Strong Motion Data Sample to Develop an Improved Correlation Between Peak Acceleration, Seismic Intensity, and Other Physical Parameters," Nuclear Regulatory Commission, Report, No. NUREG–0402, 1978.
(44) *Newmark, N. M., and Hall, W. J.*, "Earthquake Spectra and Design," EERI Monograph Series, 1982.
(45) *Nishioka, T., and Shah, H. C.*, "Application of the Markov Chain on Probability of Earthquake Occurrence," Proceedings of the Japan Society of Civil Engineers, No. 298, June 1980, pp. 137–145.
(46) *Nuttli, O. W., and Zollweg, J. E.*, "The Relationship Between Felt Area and Magnitude for Central United States Earthquakes," Bulletin of the Seismological Society of America, Vol. 64, No. 1, 1974, pp. 73–83.
(47) *Nuttli, O. W.*, "Similarities and Differences Between the Western United States Earthquakes and Their Consequences for Earthquake Engineering," Proceedings of the Conference on Earthquakes and Earthquake Engineering in the Eastern United States, Vol. 1, Knoxville, 1981, pp. 25–51.
(48) *Nuttli, O. W.*, "The Relationship of Sustained Maximum Ground Acceleration and Velocity to Earthquake Intensity and Magnitude," Report No. 16, Miscellaneous Paper S–73–1, U.S. Army Engineer Waterways Experiment Station, 1979.
(49) *Nuttli, O. W.*, "The Mississippi Valley Earthquakes of 1811 and 1812, Intensities, Ground Motion, and Magnitudes," Bulletin of the Seismological Society of America, Vol. 63, 1973, pp. 227–248.
(50) *Patwardham, A. S., Kulkarni, R. B., and Tocher, D.*, "A Semi-Markov Model for Characterizing Recurrence of Great Earthquakes," Bulletin of the Seismological Society of America, Vol. 70, No. 1, 1980, pp. 323–347.
(51) *Savage, J. G.*, "Radiation from a Realistic Model of Faulting," Bulletin of the Seismological Society of America, Vol. 56, No. 2, 1966, pp. 577–592.
(52) *Savy, J. B., Shah, H. C., and Boore, D.*, "Non-Stationary Risk Model with Geophysical Input," Journal of the Structural Division, Proceedings of the ASCE, Vol. 106, No. ST1, January 1980, pp. 145–163.
(53) *Savy, J. B.*, "Determination of Seismic Design Parameters: A Stochastic Approach, Technical Report No. 34, The John A. Blume Earthquake Engineering Center, Stanford University, 1979.
(54) *Schnabel, P. B., and Lysmer, J.*, "SHAKE—A Computer Program for Earthquake Response Analysis of Horizontally Layered Sites," Report No. EERC 72–12, University of California, Berkeley, 1972.
(55) *SEAOC*, "Suggested Procedures for Developing Seismic Ground Motions," Structural Engineers Association of California, 171 Second Street, San Francisco, 1979.
(56) *Seed, H. B., et al*, "Site-Dependent Spectra for Earthquake Resistant Design," Report No. EERC 74–12, University of California, Berkeley, 1974.
(57) *Seed, H. B., et al.* "Characteristics of Rock Motions During Earthquakes," Report No. EERC 68–5, University of California, Berkely, 1968.
(58) *Shah, H. C., Mortgat, C. P., Kiremidjian, A. S., and Zsutty, T. C.*, "A Study of Seismic Risk for Nicaragua, Part I," The John A. Blume Earthquake Enginering Center, Technical Report No. 11, Stanford University, 1975.
(59) *Shah, H. C., Zsutty, T. C., Krawinkler, H., Mortgat, C. P., Kiremidjian, A. S., and Dizon, J. O.*, "A Study of Seismic Risk for Nicaragua, Part II, Commentary," The John A. Blume Earthquake Engineering Center, Technical Report No. 12A, Stanford University, 1976.

(60) *Sieh, K. E.*, "Prehistoric Large Earthquakes Produced by Slip on the San Andreas Fault at Pallet Creek, California," Journal of Geophysics Research, Vol. 83, 1978, pp. 3907–3939.
(61) *Slemmons, D. B.*, "Fault and Earthquake Magnitude," State-of-the-Art for Assessing Earthquake Hazards in the United States, Report No. 6, Miscellaneous Paper S–73–1, U.S. Army Engineer Waterways Experiment Station, 1977.
(62) *Stepp, J. C.*, "Analysis of Completeness of the Earthquake Sample in the Puget Sound Area and its Effect on Statistical Estimates of Earthquake Hazard," Proceedings of the First Microzonation Conference, Seattle, 1974.
(63) *Tera Corporation*, "Seismic Hazard Analysis: Solicitation of Expert Opinion," Nuclear Regulatory Commission Report No, NUREG/CR–1582, Vol. 3, 1980.
(64) *Tera Corporation*, "Seismic Hazard Analysis-Solicitation of Expert Opinion," Nuclear Regulatory Commission, NUREG/CR–1582, Vol. 4, 1980.
(65) *Tera Corporation*, "Seismic Hazard Analysis: Results," Report to Lawrence Livermore National Laboratory, 1981.
(66) *Trifunac, M. D., and Brady, A. G.*, "On the Correlation of Seismic Intensity Scales with the Peaks of Recorded Strong Ground Motion," Bulletin of the Seismological Society of America, Vol. 65, No. 1, 1975, pp. 139–162.
(67) *U.S. Geological Survey Circular No. 898*, "Summary of Workshops Concerning Regional Seismic Source Zones of Parts of the Conterminous United States," Convened by the U.S. Geological Survey, 1979–1980, Golden, Colorado. Edited by Paul C. Thenhaus.
(68) *Vagliente, V. N.*, "Forecasting the Risk Inherent in Earthquake Resistant Design," Ph.D. Dissertation, Department of Civil Engineering, Stanford University, 1973. Also published as Technical Report No. 174, Department of Civil Engineering, Stanford University.
(69) *Wiggins, J. H.*, "Procedure of Determining Acceptable Risk Ground Motion Design Criteria," Technical Report. No. 75–1229, J. H. Wiggins Company, Redondo Beach, California, 1975.
(70) *Woodward Clyde Consultants*, "Offshore Alaska Seismic Exposure Study," in six volumes, prepared for Alaska Subartic Offshore Committee (OASES), 1978.
(71) *Yegian, M. K.*, "Probabilistic Seismic Hazard Analysis," Report No. 17, Miscellaneous Paper S–73–1, U.S. Army Engineer Waterways Experiment Station, 1979.
(72) *Zoback, M. D., et al*, "Major Fault Zone Associated with the Main New Madrid Fault Seismic Trend Shown by Seismic-Reflection Profiling," 51st Annual Meeting, Eastern Section of the Seismological Society of America, 1979.

Chapters 4 and 5

(73) *Applied Technology Council*, "An Investigation of the Correlation Between Earthquake Ground Motion and Building Performance," ATC–10, Palo Alto, California, 1983.
(74) *Blume, J. A., et al*, "Design of Multistory Reinforced Concrete Buildings for Earthquake Motions," Portland Cement Association, Skokie, Illinois, 1961.
(75) *Chopra, Anil, K.*, "Dynamics of Structures—A Primer," Earthquake Engineering Research Institute, Berkeley, California, 1981.
(76) *Freeman, S. A.*, "Prediction of Response of Concrete Buildings to Severe Earthquake Motion," Douglas McHenry International Symposium on Concrete and Concrete Structures, American Concrete Institute, SP–55, Detroit, Michigan, 1978.
(77) *Freeman, S. A., Nicoletti, J. P., and Tyrrell, J. V.*, "Evaluation of Existing Buildings for Seismic Risk—A Case Study of Puget Sound Naval Shipyard, Bremerton, Washington," Proceedings of the U.S. National Conference on Earthquake Engineering—1975, Earthquake Engineering Research Institute, Berkeley, California, 1975.
(78) *Hudson, D. E.*, "Reading and Interpreting Strong Motion Accelerograms," Earthquake Engineering Research Institute, Berkeley, California, 1979.
(79) *Jeing, J. C.*, "Problems in the Use of Root-Sum-Square Solutions for Three-Dimensional Dynamic Analysis of Buildings," Proceedings of the Seventh World Conference on Earthquake Engineering, Istanbul, Turkey, 1980.
(80) *Murphy, L. M., Scientific Coordinator*, "San Fernando, California, Earthquake of February 9, 1971," Effects on Building Structures, Vol. 1, U.S. Department of Commerce, National Oceanic and Atmospheric Administration, Washington, DC, 1973.
(81) *Newmark, N. M., and Hall, W. J.*, "Procedures and Criteria for Earthquake Resistant Design," Buildings Practices for Disaster Mitigation, Building Sciences Series 46, National Bureau of Standards, Washington, DC, 1973.
(82) *Seismology Committee*, "Recommended Lateral Force Requirements and Commentary," Structural Engineers Association of California, San Francisco, California, 1980.
(83) *URS/John A. Blume & Asssociates, Engineers*, "Effects Prediction Guidelines for Structures Subjected to Ground Motion," JAB–99–115, San Francisco, California, 1975.

Appendix C

(84) *Ambraseys, N. N.*, "The Correlation of Intensity with Ground Motions," Advancements in Engineering Seismology in Europe, Trieste, Italy, 1972.

(85) *Chinnery, M. A., and Rodgers D. A.*, "Earthquake Statistics in Southern New England," Earthquake Notes, Vol. XLIV, No. 304, 1973.
(86) *Chopra, A. K.*, "Dynamics of Structures—A Primer," EERI Monograph, 1981.
(87) *Gutenberg, B., and Richter, C. F.*, "Earthquake Magnitude, Intensity, Energy, and Acceleration," Bulletin of the Seismological Society of America, Vol. 46, No. 2, 156, pp. 105–145.
(88) *Gutenberg, B., and Richter, C. F.*, "Earthquake Magnitude, Intensity, Energy, and Acceleration," Bulletin of the Seismological Society of America, Vol. 32, No. 3, 1942, pp. 163–191.

(89) *Hershberger, J.*, "A Comparison of Earthquake Acceleration with Intensity Ratings," Bulletin of the Seismological Society of America, Vol. 46, No. 2, 1956, pp. 317–320.

(90) *Hudson, E. E.*, "Readings and Interpreting Strong Motion Accelerograms," EERI Monograph, 1981.

(91) *Krinitzsky, E. L., and Chang, F. K.*, "Specifying Peak Motions for Design Earthquakes," Report No. 7 in the Series, State-of-the-Art for Assessing Earthquake Hazards in the United States, U.S. Army Engineer Waterways Experiment Station, Miscellaneous Paper S–73–1, 1977.

(92) *Krinitzsky, E. L., and Chang, F. K.*, "Earthquake Intensity and the Selection of Ground Motion for Seismic Design," Report No. 4 in the Series, State-of-the-Art for Assessing Earthquake Hazards in the United States, U.S. Army Engineer Waterways Experiment Station, Miscellaneous Paper S–73–1, 1975.

(93) *Lysmer, J., Udaka, T., Tsai, C. F., and Seed, H. B.*, "FLUSH—A Computer Program for Approximate 3-D Analysis of Soil-Structure Interaction Problems," Report No. EERC 75–30, University of California, Berkeley, 1975.

(94) *McGuire, R. K.*, "FRISK: Computer Program for Seismic Risk Analysis Using Faults at Earthquake Sources," U.S. Geological Survey Open File Report No. 78–1007, 1978.

(95) *Newmark, N. M., and Hall, W. J.*, "Earthquake Spectra and Design," EERI Monograph, 1982.

(96) *Richter, C. F.*, "An Instrumental Earthquake Magnitude Scale," Bulletin of the Seismological Society of America, Vol. 25, No. 1, 1935, pp. 1–32.

(97) *Richter, C. F.*, "Elementary Seismology," W. H. Freeman & Company, San Francisco, 1958.

(98) *Schnabel, P. B., and Lysmer, J.*, "SHAKE—A Computer Program for Earthquake Response Analysis of Horizontally Layered Sites," Report No. EERC 72–12, University of California, Berkeley, 1972.

(99) *Seed, H. B., and Idriss, I. M.*, "Influence of Soil Conditions on Ground Motions During Earthquakes," Journal of Soil Mechanics and Foundation Division, ASCE, Vol. 95, No. SM1, 1969, pp. 99–137.

(100) *Shah, H. C.*, "Earthquake Engineering and Seismic Risk Analysis," Class Notes by the John A. Blume Earthquake Engineering Center, Stanford University, 1979.

(101) *Slemmons, D. B.*, "Faults and Earthquake Magnitude," Report No. 6 in the Series, State-of-the-Art for Assessing Earthquake Hazards in the United States, U.S. Army Engineer Waterways Experiment Station, Miscellaneous Paper S–73–1, 1977.

(102) *Tera Corporation*, "Seismic Hazard Analysis: Solicitation of Expert Opinion," NRC Report No. NUREG/CR–1582, Vol. 3, 1980.

(103) *Trifunac, M. D., and Brady, A. G.*, "On the Correlation of Seismic Intensity Scales with the Peaks of Recorded Strong Motion," Bulletin of the Seismological Society of America, Vol. 65, No. 1, 1975, pp. 139–162.

GLOSSARY
TERMS FOR PROBABILISTIC SEISMIC RISK AND HAZARD ANALYSIS

Acceptable Risk—a probability of social or economic consequences due to earthquakes that is low enough (for example in comparison with other natural or manmade risks) to be judged by appropriate authorities to represent a realistic basis for determining design requirements for engineered structures, or for taking certain social or economic actions.

Active Fault—a fault that on the basis of historical, seismological, or geological evidence has a high probability of producing an earthquake. (Alternate: a fault that may produce an earthquake within a specified exposure time, given the assumptions adopted for a specific seismic-risk analysis.)

Attenuation Law—a description of the behavior of a characteristic of earthquake ground motion as a function of the distance from the source of energy.

B-Value—a parameter indicating the relative frequency of occurrence of earthquakes of different sizes. It is the slope of a straight line indicating absolute or relative frequency (plotted logarithmically) versus earthquake magnitude or meizoseismal Modified Mercalli intensity. (The B-value indicates the slope of the Gutenberg-Richter recurrence relationship.)

Coefficient of Variation—the ratio of standard deviation to the mean.

Damage—any economic loss or destruction caused by earthquakes.

Design Acceleration—a specification of the ground acceleration at a site, terms of a single value such as the peak or rms; used for the earthquake-resistant design of a structure (or as a base for deriving a design spectrum). See "Design Time History."

Design Earthquake—a specification of the seismic ground motion at a site; used for the earthquake-resistant design of a structure.

Design Event, Design Seismic Event—a specification of one or more earthquake source parameters, and of the location of energy release with respect to the site of interest; used for the earthquake-resistant design of a structure.

Design Ground Motion—see "Design Earthquake."

Design Spectrum—a set of curves for design purposes that gives acceleration velocity, or displacement (usually absolute acceleration, relative velocity, and relative displacement of the vibrating mass) as a function of period of vibration and damping.

Design Time History—the variation with time of ground motion (e.g., ground acceleration or velocity or displacement) at a site; used for the earthquake-resistant design of a structure. See "Design Acceleration."

Duration—a qualitative or quantitative description of the length of time during which ground motion at a site shows certain characteristics (perceptibility, violent shaking, etc.).

Earthquake—a sudden motion or vibration in the earth caused by the abrupt release of energy in the earth's lithosphere. The wave motion may range from violent at osme locations to imperceptible at others.

Elements at Risk—population, properties, economic activities, including public services etc., at risk in a given area.

Exceedence Probability—the probability that a specified level of ground motion or specified social or economic consequences of earthquakes, will be exceeded at a site or in a region during a specified exposure time.

Expected—mean, average.

Expected Ground Motion—the mean value of one or more characteristics of ground motion at a site for a single earthquake. (Mean ground motion.)

Exposure—the potential economic loss to all or certain subset of structures as a result of one or more earthquakes in an area. This term usually refers to the insured value of structures carried by one or more insurers. See "Value at Risk."

Exposure Time—the time period of interest for seismic-risk calculations, seismic-hazard calculations, or design of structures. For structures, the exposure time is often chosen to be equal to the design lifetime of the structure.

Geologic Hazard—a geologic process (e.g., landsliding, liquefaction soils, active faulting) that during an earthquake or other natural event may produce effects in structures.

Intensity—a qualitative or quantitative measure of the severity of seismic ground motion at a specific site (e.g., Modified Mercalli intensity, Rossi-Forel intensity, Housner Spectral intensity, Arias intensity, peak acceleration, etc.).

Loss—any adverse economic or social consequence cause by one or more earthquakes.

Maximum—the largest value attained by a variable during a specified exposure time. See "Peak Value."

Maximum Credible
Maximum Expectable
Maximum Expected
Maximum Probable—These terms are used to specify the largest value of a variable, for example, the magnitude of an earthquake, that might reasonably be expected to occur. *These are misleading terms and their use is discouraged.* (The U.S. Geological Survey and some individuals and companies define the maximum credible earthquake as "the largest earthquake that can be reasonably expected to occur." The Bureau of Reclamation, the First Interagency Working Group (Sept. 1978) defined the maximum credible earthquake as "the earthquake that would cause the most severe vibratory ground motion capable of being produced at the site under the current known tectonic framework." It is an event that can be supported by all known geologic and seismologic data. The maximum expectable or expected earthquake is defined by USGS as "the largest earthquake that can be reasonably expected to occur." The maximum probable earthquake is sometimes defined as the worst historic earthquake. Alternatively, it is defined as the 100-year-return-period earthquake, or an earthquake that probabilistic determination of recurrence will take place during the life of the structure.)

Maximum Possible—the largest value possible for a variable. This follows from an explicit assumption that larger values are not possible, or implicitly from assumptions that related variables or functions are limited in range. The maximum possible value may be expressed deterministically or probabilistically.

Mean Recurrence Interval, Average Recurrence Interval—the average time between earthquakes or faulting vents with specific characteristics (e.g., magnitude $\geqslant$ 6) in a specified region or in a specified fault zone.

Mean Return Period—the average time between occurrences of ground motion with specific characteristics (e.g., peak horizontal acceleration $\geqslant$ 0.1 g) at a site. (Equal to the inverse of the annual probability of exceedance.)

Mean Square—expected value of the square of the random variable. (Mean square minus square of the mean gives the variance of random variable.)

Peak Value—the largest value of a time-dependent variable during an earthquake.

Response Spectrum—a set of curves calculated from an earthquake accelerogram that gives values of peak response of a damped linear oscillator, as a function of its period of vibration and damping.

Root Mean Square (rms)—square root of the mean square value of a random variable.

Seismic-Activity Rate—the mean number per unit time of earthquakes with specific characteristics (e.g., magnitude $\geqslant$ 6) originating on a selected fault or in a selected area.

Seismic-Design-Load Effects—the actions (axial forces, shears, or bending moments) and deformations induced in a structural system due to a specified representation (time history, response spectrum, or base shear) or seismic design ground motion.

Seismic-Design Loading—the prescribed representation (time history, response spectrum, or equivalent static base shear) of seismic ground motion to be used for the design of a structure.

Seismic Event—the abrupt release of energy in the earth's lithosphere, causing an earthquake.

Seismic Hazard—any physical phenomenon (e.g., ground shaking, ground failure) associated with an earthquake that may produce adverse effects on human activities.

Seismic Risk—the probability that social or economic consequences of earthquakes will equal or exceed specified values at a site, at several sites, or in an area, during a specified exposure time.

Seismic-Risk Zone—an obsolete term. See "Seismic Zone."

Seismic-Source Zone—an obsolete term. See "Seismogenic Zone" and "Seismotectonic Zone."

Seismic Zone—a generally large area within which seismic-design requirements for structures are constant.

Seismic Zoning, Seismic Zonation—the process of determining seismic hazard at many sites for the purpose of delineating seismic zones.

Seismic Microzone—a generally small area within which seismic-design requirements for structures are uniform. Seismic microzones may show relative ground motion amplification due to local soil conditions without specifying the absolute levels of motion or seismic hazard.

Seismic Microzoning, Seismic Microzonation—the process of determining absolute or relative seismic hazard at many sites, accounting for the effects of geologic and topographic amplification of motion and of soil stability and liquefaction, for the purpose of delineating seismic microzones. Alternatively, microzonation is a process for identifying detailed geological, seismological, hydrological, and geotechnical site characteristics in a specific region and incorporating them into land-use planning and the design of safe structures in order to reduce damage to human life and property resulting from earthquakes.

Seismogenic Zone, Seismogenic Province—a planar representation of a three-dimensional domain in the earth's lithosphere in which earthquakes are inferred to be of similar tectonic origin. A seismogenic zone may represent a fault in the earth's lithosphere. See "Seismotectonic Zone."

Seismogenic Zoning—the process of delineating regions have nearly homogeneous tectonic and geologic character, for the purpose of drawing seismogenic zones. The specific procedures used depend on the assumptions and mathematical models used in the seismic-risk analysis or seismic-hazard analysis.

Seismotectonic Zone, Seismotectonic Providence—a seismogenic zone in which the tectonic processes causing earthquakes have been identified. These zones are usually fault zones.

Source Variable—a variable that describes a physical characteristic (e.g., magnitude, stress drop, seismic moment, displacement) of the source of energy release causing an earthquake.

Standard Deviation—the square root of the variance of a random variable.

Upper Bound—see "Maximum Possible."

Value at Risk—the potential economic loss (whether insured or not) to all or certain subset of structures as a result of one or more earthquakes in an area. See "Exposure."

Variance—the mean squared deviation of a random variable from its average value.

Vulnerability—the degree of loss to a given element at risk, or set of such elements, resulting from an earthquake of a given magnitude or intensity, which is usually expressed on a scale from 0 (no damage) to 10 (total loss).

INDEX

The proponent agency of this publication is the Office of the Chief of Engineers, United States Army. Users are invited to send comments and suggested improvements on DA Form 2028 (Recommended Changes to Publications and Blank Forms) direct to HQDA (DAEN–ECE–D), WASH DC 20314–1000.

By Order of the Secretaries of the Army, the Air Force, and the Navy:

JOHN A. WICKHAM, JR.
General, United States Army
Chief of Staff

Official:

MILDRED E. HEDBERG
Brigadier General, United States Army
The Adjutant General

CHARLES G. GABRIEL
General, USAF
Chief of Staff

Official:

NORMAND G. LEZY
Colonel, USAF
Director of Administration

J. P. JONES, JR
Rear Admiral, CEC, U.S. Navy
Commander, Naval Facilities
Engineering Command

Distribution:
Army: To be distributed in accordance with DA Form 12–34B,
Requirements for Seismic Design for Buildings.
Air Force: F
Navy:

☆U.S. GOVERNMENT PRINTING OFFICE : 1986 O - 180-976 (52158)